

STUDIES ON RHEOLOGICAL PROPERTIES OF POLYMERS

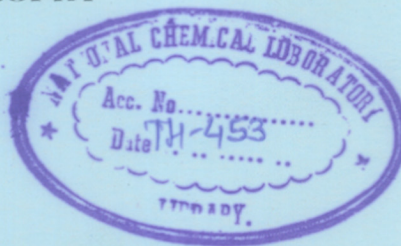
A Thesis

COMPUTERISED

*Submitted to the
University of Poona
for the degree of*

DOCTOR OF PHILOSOPHY

(in chemistry)



BY

VIVEK DATTATRAYA DEUSKAR

M. Sc.

678.01:532.135(043)
DEU

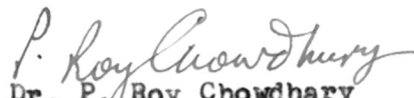
PHYSICAL CHEMISTRY DIVISION
NATIONAL CHEMICAL LABORATORY
PUNE - 411 008 (INDIA)

NOVEMBER 1984

Dedicated to My Parents

COMPUTERISED

Certified that the work incorporated in the thesis 'STUDIES ON RHEOLOGICAL PROPERTIES OF POLYMERS' submitted by Shri Vivek D. Deuskar was carried out by the candidate under my supervision. Such material as has been obtained from other sources has been duly acknowledged in the thesis.


Dr. P. Roy Chowdhary
(Research Guide)

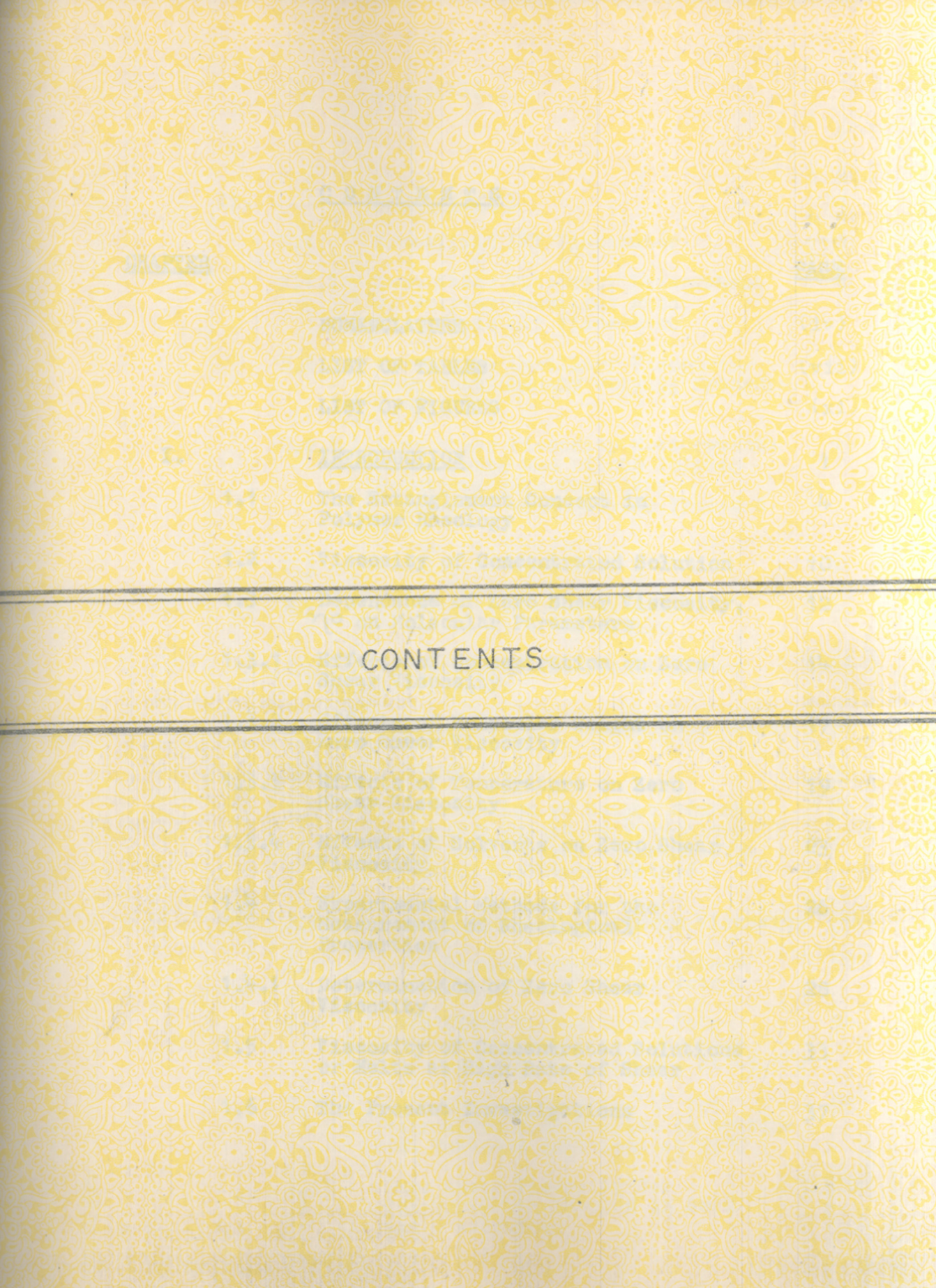
ACKNOWLEDGEMENT

The entire work of this thesis has been carried out under the guidance and encouragement of Dr. P. Roychowdhary, Scientist, Physical Chemistry Division, National Chemical Laboratory, Pune. By appending a customary note of acknowledgement, I will be doing injustice to my research guide, Dr. P. Roychowdhary, who more than richly deserves the gratitude of his students for many years to come.

My sincere thanks are also due to my colleagues, friends and relatives who rendered the help and inspired me at all the stages.

I am grateful to the Director, National Chemical Laboratory, Pune, for kindly permitting me to submit this work in the form of a thesis.

I am also thankful to CSIR, New Delhi, for the monetary support in the form of a research fellowship.



CONTENTS

CONTENTS

CHAPTER		PAGE
	NOMENCLATURE	(iv)
	LIST OF TABLES	(vii)
	LIST OF FIGURES	(xi)
I.	INTRODUCTION	1
1.1	The Entanglement Concept in Polymer Rheology	4
1.2	Viscosity of Concentrated Solution	10
1.3	Dependence of Zero Shear Viscosity, η_0 on Molecular Parameters	12
1.3.1	Effects of Concentration on Zero Shear Viscosity	14
1.3.2	Effect of Molecular Weight on Shear Viscosity	17
1.3.3	Effects of Temperature on Zero Viscosity	19
1.3.4	Effects of Solvents on Zero Shear Viscosity	23
1.4	Experimental Methods for the Measurement of Rheological Properties	26
1.4.1	Determination of Zero Shear Viscosity	28
1.5	Viscosity of Concentrated Solutions or Melts at High Rate of Shear	33
1.6	The Present Investigations	37

(ii)

II	EXPERIMENTAL	41
2.1	Brookfield LVT Viscometer	41
2.1.1	Zero Shear Viscosity Measurement of Polymer Solutions with Brookfield LVT Viscometer	46
2.2	Maron-type Capillary Viscometer with Continuously Varying Pressure Head	50
2.2.1	Zero Shear Viscosity Measurements of Solvents and Dilute Polymer Solutions with Capillary Viscometer with Varying Pressure Head	56
2.3	Density Measurements	61
2.4	Purification of Solvents and Preparation of Solutions	65
2.5	Purification and Fractionation of Polymers	66
2.5.1	Polychloroprene (Denkaprene M-40)	66
2.5.2	Polybutadiene	67
2.6	Determination of Weight Average Molecular Weight of Polychloroprene and Polybutadiene Samples by Light Scattering Method.	70
2.7	Measurement of Intrinsic Viscosity	78
2.8	Relationship between Intrinsic Viscosity and Molecular Weight	90
2.9	Zero Shear Viscosity of Polychloroprene Samples in Benzene and Cyclohexane Solutions at 45.5 ⁰ C	94
2.10	Zero Shear Viscosity, η_0 for Polychloroprene Samples in Benzene and Butanone Solutions at 25 ⁰ C	95
2.11	Zero Shear Viscosity for Polybutadiene Samples in Good and θ solvents.	108

(ii)

III.	DISCUSSION	118
3.1	Dependence of Zero Shear Viscosity on Concentration	118
3.2	Dependence of Zero Shear Viscosity on Molecular Weight	119
3.3	Dependence of Zero Shear Viscosity on Both Concentration and Molecular Weight	128
3.4	Dependence of Zero Shear Viscosity on quality (Good and Θ) of Solvents	132
3.4.1	Relation Between Viscosity Cross Over and Entanglement Composition	141
3.5	Correlation of Viscosity Data	148
3.5.1	Method of Graessley	148
3.5.2	Method of Dreval and coworkers	155
	SUMMARY	173
	REFERENCES	184
	REPRINT	



NOMENCLATURE

NOMENCLATURE

C	-	Concentration
E	-	Apparent activation energy Kcal/mole
F	-	Product of transmittance of the neutral filters which are used
G_0	-	Observed galvanometer deflection at 0° angle
G_θ	-	Observed galvanometer deflection when the photo tube is at an angle θ to the incident beam
h	-	Height of mercury column in manometer tube of radius R_c
h	-	Slit width (light scattering of measurement)
K	-	Boltzmann constant
K	-	Logarithm of shift factor
K	-	Parameter relating to the Rayleigh scattering - concentration ratio to the molecular weight (Chap. II)
K'	-	Huggin's constant
K_M	-	Martin's constant
L	-	Length of the capillary
M	-	Molecular weight
M_e	-	Entanglement molecular weight
\bar{M}_w	-	Weight average molecular weight
n	-	Number of links in the molecular chain (Number of chain atoms)
n^*	-	Effective number of links
η^0	-	Zero shear viscosity
η^0_r	-	Relative viscosity
N	-	Number of entanglement points per molecule

η_{sp}°	- Specific viscosity
$\eta_{sp/c}^{\circ}$	- Reduced specific viscosity
$[\eta]$	- Intrinsic viscosity
dn/dc	- Refractive index gradient
λ	- Wavelength
p	- Number of jumps per second
P	- Pressure drop across the capillary
PB	- Polybutadiene
PC	- Polychloroprene
$P(\theta)$	- Particle scattering factor
π	- Osmotic pressure
Q	- Volume flow through capillary
q	- Number of links between points of entanglements
R_0	- Unperturbed end-to-end distance
R	- Radius of capillary (related to capillary viscometer with continuous varying pressure head)
R	- Gas constant
\bar{R}^2	- Mean square end-to-end distance of polymer molecule
R_{θ}	- Rayleigh ratio at an angle θ to the incident beam
T	- Absolute temperature
T_1	- Terminal relaxation time
T_g	- Glass transition temperature
V_p	- Apparent specific volume of polymer

(vi)

- V_s - Apparent specific volume of solvent
- ζ' - Friction coefficient
- Z - The dissymmetry ratio



LIST OF TABLES

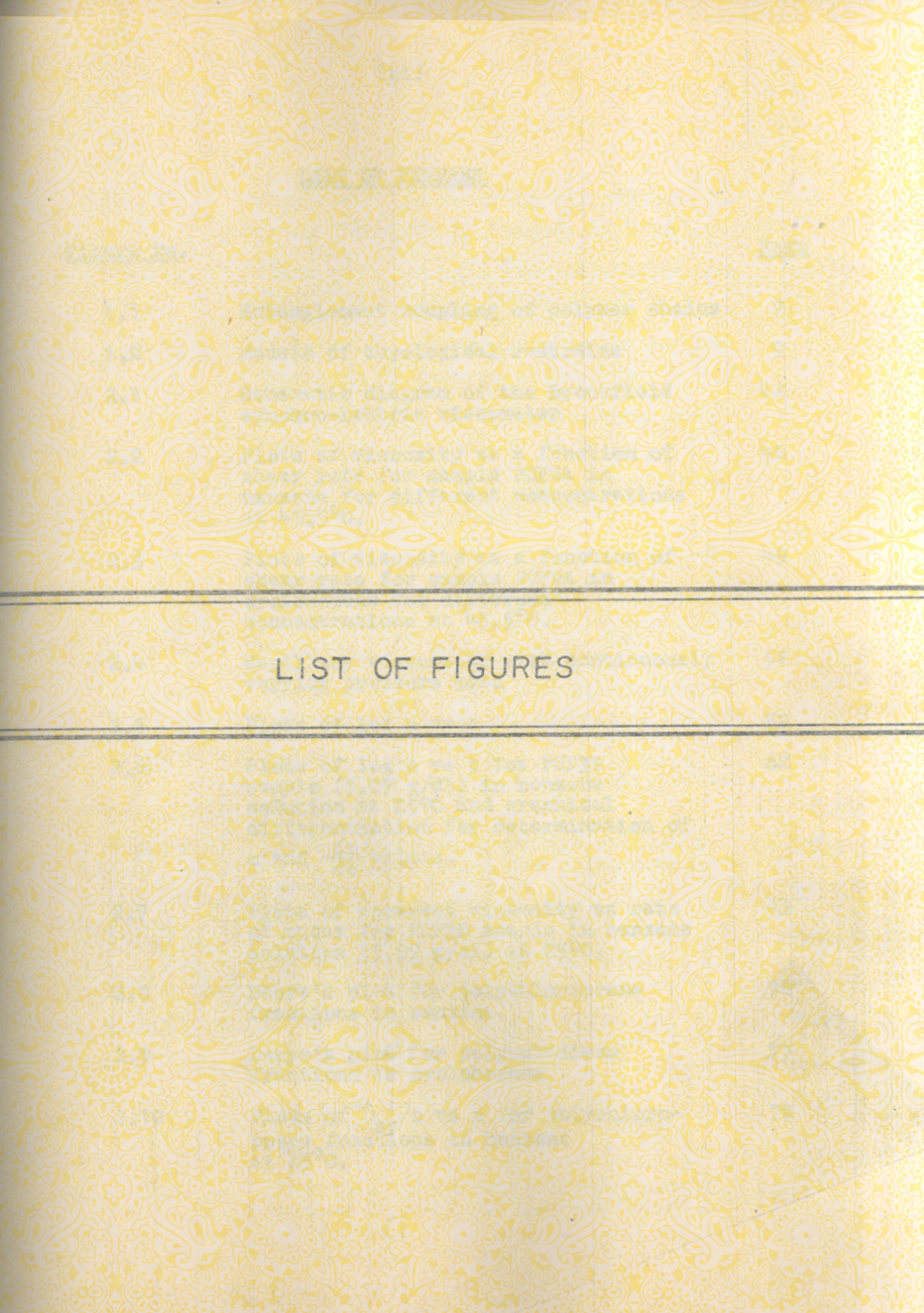
LIST OF TABLES

<u>TABLE NO.</u>		<u>PAGE</u>
2.1	The zero shear viscosity, η^0 and θ temperature for the solvents	59
2.2	The summary of data obtained by the capillary viscometer for PCF3B sample in benzene solution (5.07 gm/dl) at 25°C.	60
2.3	Values of intrinsic viscosity and molecular weight for the polychloroprene samples	68
2.4	Values of intrinsic viscosity and molecular weight for polybutadiene samples.	69
2.5	Summary of results for light scattering measurements of polychloroprene fractions in benzene solution at room temperature ($\sim 25^\circ\text{C}$)	74
2.6	Summary of results for light scattering measurements of polybutadiene fractions in cyclohexane solution at room temperature ($\sim 25^\circ\text{C}$).	75
2.7	Summary of results for intrinsic viscosity measurements in different solvents and temperatures for polychloroprene fractions.	88
2.8	Summary of results for intrinsic viscosity measurements in different solvents and temperatures for polybutadiene fractions.	89
2.9	The values of K and a for polychloroprene and polybutadiene in good and θ solvents.	93
2.10	Summary of results for zero shear viscosity, η^0 measurements for polychloroprene sample PCF1B in benzene solution at 45.5°C.	96

2.11	Summary of results for zero shear viscosity, η^0 measurements for polychloroprene sample PCF1B in cyclohexane solution at 45.5°C.	97
2.12	Summary of results for zero shear viscosity, η^0 measurements for polychloroprene sample PCF2A in benzene at 45.5°C.	98
2.13	Summary of results for zero shear viscosity, η^0 measurements for polychloroprene sample PCF2A in cyclohexane solution at 45.5°C.	99
2.14	Summary of results for zero shear viscosity, η^0 measurements for polychloroprene sample PCF3A in benzene at 45.5°C.	100
2.15	Summary of results for zero shear viscosity, η^0 measurements for polychloroprene sample PCF3A in cyclohexane at 45.5°C.	101
2.16	Summary of results for zero shear viscosity, η^0 measurements for polychloroprene sample PCF2B in benzene solution at 25°C.	102
2.17	Summary of results for zero shear viscosity, η^0 measurements for polychloroprene sample PCF2B in butanone solution at 25°C.	103
2.18	Summary of results for zero shear viscosity, η^0 measurements for polychloroprene sample PCF2C in benzene solution at 25°C.	104
2.19	Summary of results for zero shear viscosity, η^0 measurements for polychloroprene sample PCF2C in butanone solution at 25°C.	105
2.20	Summary of results for zero shear viscosity, η^0 measurements for polychloroprene sample PCF3B in benzene solution at 25°C.	106

2.21	Summary of results for zero shear viscosity, η° measurements for polychloroprene sample PCF3B in butanone solution at 25°C.	107
2.22	Summary of results for zero shear viscosity, η° measurements for polybutadiene sample PB2F1 in benzene solution at 20.5°C.	109
2.23	Summary of results for zero shear viscosity, η° measurements for polybutadiene sample PB2F1 in isobutyl acetate solution at 20.5°C.	110
2.24	Summary of results for zero shear viscosity, η° measurements for polybutadiene sample PB2F1 in dioxane solution at 20.2°C.	111
2.25	Summary of results for zero shear viscosity, η° measurements for polybutadiene sample PB2F2 in benzene solution at 20.5°C.	112
2.26	Summary of results for zero shear viscosity, η° measurements for polybutadiene sample PB2F2 in isobutyl acetate at 20.5°C.	113
2.27	Summary of results for zero shear viscosity, η° measurements for polybutadiene sample PB2F2 in dioxane solution at 20.2°C.	114
2.28	Summary of results for zero shear viscosity, η° measurements for polybutadiene sample PB2F3 in benzene solution at 20.5°C.	115
2.29	Summary of results for zero shear viscosity, η° measurements for polybutadiene sample PB2F3 in isobutyl acetate solution at 20.5°C.	116
2.30	Summary of results for zero shear viscosity, η° measurements for polybutadiene sample PB2F3 in dioxane solution at 20.2°C.	117

3.1	Cross over point concentration and viscosity for polychloroprene and polybutadiene samples in good and θ solvent systems.	138
3.2	The values of Martin constant, K_M and expansion factor α_3 for polychloroprene-solvent systems.	161
3.3	The values of Martin constant, K_M for polybutadiene samples in good and poor solvents.	171



LIST OF FIGURES

LIST OF FIGURES

<u>Figure No.</u>		<u>Page</u>
1.1	Entanglement coupling of polymer chains	7
1.2	Models of topological restrains	9
2.1	Schematic diagram of the Brookfield synchro-lectric viscometer	42
2.2	Plots of viscosity as a function of shear rate for sample PCF2A in benzene for different concentrations at 45.5°C.	48
2.3	Plots of viscosity as a function of shear rate for sample PCF2A in cyclohexane for different concentrations at 45.5°C.	49
2.4	Capillary viscometer with continuously varying pressure head	51
2.5	Plots of log h vs t	58
2.6	Plots of log h vs t for PCF3B sample (5.07 g/dl) in benzene solution at 25°C and graphical differentiation for determination of m and $\frac{dm}{dt}$ values.	62
2.7	Plots of apparent viscosity vs rate of shear for PCF3B sample in benzene solution (5.07 g/dl) at 25°C.	63
2.8	Debye's plot for polychloroprene fractions in benzene.	76
2.9	Debye's plot for polybutadiene fractions in cyclohexane	77
2.10	Plots of η_{sp}/c vs c for polychloroprene fractions in benzene at 25°C.	79

2.11	Plots of η_{sp}/c vs c for polychloroprene fractions in benzene at 45.5°C .	80
2.12	Plots of η_{sp}/c vs c for polychloroprene fractions in butanone at 25°C .	81
2.13	Plots of η_{sp}/c vs c for polybutadiene fractions in benzene at 20.5°C .	82
2.14	Plots of η_{sp}/c vs c for polybutadiene fractions in benzene at 25°C .	83
2.15	Plots of η_{sp}/c vs c for polybutadiene fractions in benzene at 32°C .	84
2.16	Plots of η_{sp}/c vs c for polybutadiene fractions in cyclohexane at 25°C .	85
2.17	Plots of η_{sp}/c vs c for polybutadiene fractions in dioxane at 20.2°C .	86
2.18	Plots of η_{sp}/c vs c for polybutadiene fractions in isobutyl acetate at 20.5°C .	87
2.19	Log-log plots of intrinsic viscosity vs molecular weight for polychloroprene samples.	91
2.10	Log-log plots of intrinsic viscosity vs molecular weight for polybutadiene samples.	92
3.1	Plots of $\log \eta^{\circ}$ vs $\log c$ for polychloroprene samples in good solvents.	120
3.2	Plots of $\log \eta^{\circ}$ vs $\log c$ for polychloroprene samples in poor solvents.	121
3.3	Plots of $\log \eta^{\circ}$ vs $\log c$ for polybutadiene samples in good and poor solvents.	122
3.4	Composite curves for polychloroprene samples in good and poor solvents at 45.5°C .	124

3.5	Composite curves for polychloroprene samples in good and poor solvents at 25°C.	125
3.6	Composite curve for polybutadiene samples in benzene.	126
3.7	Composite curve for polybutadiene samples in poor solvents.	127
3.8	Plots of $\log \eta_r^0$ vs $5 \log c + 3.4 \log \bar{M}_w$ for polychloroprene samples in good and poor solvents.	129
3.9	Plots of $\log \eta_r^0$ vs $5 \log c + 3.4 \log \bar{M}_w$ for polybutadiene samples in good and poor solvents.	130
3.10	Plots of $\log \eta_{sp}^0$ vs $\log c$ for polychloroprene samples in good and poor solvents at 45.5°C.	133
3.11	Plots of $\log \eta_{sp}^0$ vs $\log c$ for polychloroprene samples in good and poor solvents at 25°C.	134
3.12	Plots of $\log \eta_{sp}^0$ vs $\log c$ for polybutadiene samples in good and poor solvents (benzene-IBA).	135
3.13	Plots of $\log \eta_{sp}^0$ vs $\log c$ for polybutadiene samples in good and poor solvents (benzene-dioxane).	136
3.14	Plots of $\log \bar{M}_v$ vs $\log c_{cross}$ for polychloroprene samples in good and poor solvents.	144
3.15	Plots of $\log \bar{M}_v$ vs $\log c_{cross}$ for polybutadiene samples in good and poor solvents.	145
3.16	Plots of $\log \eta_r^0$ vs $c [\eta]$ or $0.77 (c [\eta] / 0.77)^{1/2a}$ for polychloroprene samples in good and poor solvents at 45.5°C.	150

3.17	Plots of $\log \eta_r^0$ vs $c[\eta]$ or $0.77 (c[\eta]/0.77)^{1/2a}$ for polychloroprene samples in good and poor solvents at 25°C.	151
3.18	Plots of $\log \eta_r^0$ vs $c[\eta]$ or $0.77 (c[\eta] / 0.77)^{1/2a}$ for polybutadiene samples in good and poor solvents.	153
3.19	Plots of $\log \bar{\eta}$ vs $c[\eta]$ for polychloroprene samples in different good solvents.	159
3.10	Plots of $\log \bar{\eta}$ vs $c[\eta]$ for poly- chloroprene samples in cyclohexane and butanone solution	160
3.21	Plots of $\log \bar{\eta}$ vs $K_M c[\eta]$ for polychloroprene samples in good and poor solvents.	163
3.22	Plots of K_M vs α^3 (expansion factor) for polychloroprene samples.	164
3.23	Plots of $\log \bar{\eta}$ vs $c[\eta]$ for poly- butadiene samples in good solvents (benzene).	167
3.24	Plots of $\log \bar{\eta}$ vs $c[\eta]$ for poly- butadiene samples in poor solvents	168
3.25	Plots of $\log \bar{\eta}$ vs $K_M c[\eta]$ for polybutadiene samples in good and poor solvents.	170



CHAPTER - I
INTRODUCTION

I N T R O D U C T I O N

Rheology is the science of the deformation and flow of matter. Rheology has made important contributions to advances in food technology, medicine, paint and printing ink technology, building and structural engineering, adhesives, cosmetics, oil well drilling operations and elsewhere. Among all these branches of rheology, polymer rheology has received the most intensive attention of rheologists, particularly during the last 15-20 years. The intensity of the study of polymer rheology may be attributable to the steadily increasing world demand for polymeric materials as a suitable substitute for many natural materials such as fibre, wood, metal, rubber and others.

The zero shear viscosity, η^0 is an important rheological parameter used to characterize the flow properties of polymer solution or melt in the linear region of deformation. It is a measure of energy dissipation in the system. Several factors such as the concentration of the solution, its temperature, the molecular weight and the molecular structure of

the polymer and the nature of the solvent are responsible for the viscosity of the polymer solutions. Many endeavours have been made for many years to correlate the data for zero shear viscosity of the polymer solutions obtained at different concentrations (high and low), molecular weights and solvents¹⁻¹⁰. Most recently molecular dynamic models based on reptation in a "tube" formed from entanglement constrains have been successfully compared^{3,5-10} with experimental data in a few cases. Reptation has emerged as a successful model to describe relaxation of polymer fluids and the pattern of observed stress over time, after or during an applied strain. The model thus predicts flow of polymer melts or concentrated solutions (generally solutions that have more than 10% by volume of polymer). The word "reptation" comes from the imagined snakelike or reptilian motion of a polymer chain tangled up in all the others. The reptation model seems vindicated by the correct scaling laws it predicts. Scaling laws are equations¹¹ that relate observed properties like osmotic pressure or viscosity to fundamental characteristics such as molecular weight or concentration raised to some power. The model predicts that the diffusion coefficient of a polymer chain is inversely proportional to the molecular

weight (the length of the snake), which leads to diffusion speeds inversely proportional to the square of the molecular weight and viscosities directly proportional to the cube. Diffusion and viscosity measurements lead to equations with exponents slightly different from -2 and +3 for the molecular weight. However, these discrepancies may be eliminated if we assume that the rapid motion of the snake's head and tail get these portions out of the two ends of the tube, thus shortening the effective length of the tube it must escape from, and if we further assume that the polymer chains that form the tube walls are also moving into and away from the region, thus continuously relaxing and reforming the tube. It may be pointed out that in order to explain the above discrepancies that the terminal relaxation time, T_1 and static shear viscosity, η^0 are found to depend on the third power of the molecular weight, while experiments yields $T_1 \sim \eta^0 \sim M^{3,4}$, Doi¹⁰ has recently proposed a correction applicable for samples of molecular weight of practical importance, which improves the above disagreements. Since entanglement of molecules are responsible for the peculiar properties the polymer melts or concentrated solutions manifest, we will briefly describe the entanglement concept in polymer rheology in the next section.

1.1 The Entanglement Concept in Polymer Rheology

The concept of chain entanglement first arose more than 60 years ago from attempts to explain the mechanical properties of amorphous polymer above the glass transition temperature, T_g . In 1932 Busse¹² noted that if unvulcanized rubber is subjected to a large deformation, held for a short time and released, it recovers its original shape almost completely, while if held for a long time it flows and recovers only partially when released. He pointed out that a physical interlocking of the molecules different from the permanent chemical linkages provided by vulcanization exists and this probably slips to new equilibrium position when given time, causing the above phenomena.

In 1940 Treloar¹³ pointed out that some kind of intermolecular coupling at widely separated points in uncrosslinked rubbery polymers might indeed be expected. Regions where molecules were looped through one another might offer high resistance to deformation for a time, but the loops would eventually slip and would be removed and reformed by random thermal motion. Further Treloar pointed out that most of the observations on unvulcanized rubber (large, recoverable deformations

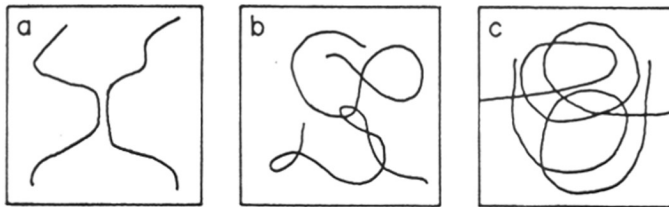
for short times, stress relaxation and viscous flow for long time) could be satisfactorily explained if one regarded entanglements as isolated regions of high viscosity, interconnected by freely extensible molecular segments.

The extensive stress relaxation experiments of Tobolsky on uncross-linked polymers of high molecular weight^{14,15} showed two stages of relaxation with a period in the time scale where the stress relaxed very slowly and this leads to the concept of an entangled network structure.

Bueche^{16,17} has advanced the concept of entanglement network from a quite different type of observation. The concept of entanglement network was advanced from the dependence of viscosity on molecular weight in undiluted polymers or at constant concentration in concentrated solutions. At low molecular weights, η^0 increases only slightly more rapidly than directly proportional to M , but at high molecular weight, η^0 increases with the 3.4 power of the molecular weight. This highly exaggerated molecular weight dependence was attributed by Bueche to entanglement coupling, and on the basis of the dragging of one molecule by another, Bueche calculated^{16,17} that the viscosity

should be proportional to $M^{3.5}$. The magnitude of M at which the slope changes is a characteristic value, M_c , which according to the Bueche theory¹⁷ is related to the average molecular weight spacing between entanglement points, M_e , in a rather complicated manner. M_c is approximately equal to $2M_e$. The change in slope between the regions $M < M_c$ and $M > M_c$ is not really a sharp one. However, in the relaxation and retardation spectra, there is a clear difference, the two maxima appear only for $M > M_c$.

The nature of the coupling is still speculative even though the phenomena is evident. The concept of adherence of polymer molecules at specific loci (Fig. 1.1a) has become necessary in order to explain the two widely separated sets of relaxation times. Such a locus is a temporary cross-link. The effects of entanglement coupling appear universally, both in non-polar (here intermolecular attractive forces are small) and polar polymers. The term "entanglement" is justified because it seems that the coupling must be topological rather than due to intermolecular forces. A concept which retains the idea of the specific locus is an entanglement where the two chains are tightly kinked around each other by bending back

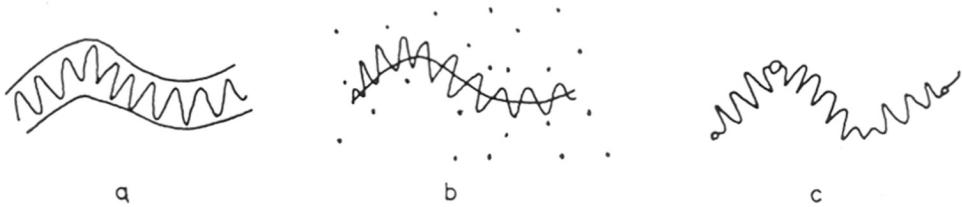


- a LOCUS OF ADHERENCE OF TEMPORARY CROSS LINK
- b LOCAL KINK.
- c LONG RANGE CONTOUR LOOP.

FIG.1-1 ENTANGLEMENT COUPLING OF POLYMER CHAINS

on themselves in short range contour (Fig. 1.1b). However, molecules which are relatively stiff and extended such as cellulose derivatives¹⁹ and even deoxyribonucleic acid^{20,21} and helical poly(amino acid)²² (all in concentrated solution) exhibit the effects of entanglement coupling even more prominently than do highly flexible polymers. Moreover, the presence of enormous bulky side groups does not markedly inhibit the entanglement coupling²³. It seems probable, therefore, that the coupling involves looping of chains around each other in their long-range contour (Fig. 1.1c).

It is somewhat misleading to speak of entanglement "points" or "loci" when an entanglement, whether trapped or not, is pictured as being able to slide along the contours of the two molecules participating in it and continually changes its position with thermal motions. A somewhat different model which introduces topological restraint without placing it at a specific point is that of a tube or tunnel that surrounds a given polymer molecule and conforms to its contorted contour as introduced by Edwards²⁴ and treated by de Gennes³, Doi and Edwards⁵ and Klein⁶. The constraint of the tube (Fig. 1.2a) corresponds to a set of obstacles³ (Fig. 1.2b) or a sequence of slip links⁵ (Fig. 1.2c) which replace the entanglement points of the entanglement



- a VIRTUAL TUBE
- b POINT OBSTACLES
- c SLIP LINKS

FIG. 1.2 MODELS OF TOPOLOGICAL RESTRAINS

conceptual scheme. As pointed out by de Gennes³ the easiest escape for sufficiently long chain will be achieved by sliding along the contorted contour (reptation). Long-range configurational changes could also be achieved if the obstacles rearrange themselves (tube reorganization)^{25,26} but this process should not make a very significant contribution except where M/M_c is only slightly greater than 1 and entanglement behaviour is only incipient.⁶

Although the tube model avoids the specification of an average molecular weight M_e between entanglement points, the diameter, d of the tube is an equivalent parameter and the average number of entanglements per molecule M/M_e can be identified approximately with L/d , where L is the contour length of a random walk with M/M_e steps²⁷. In theory of Klein⁶, M/M_e can be identified approximately with $N/13$, where N is the number of entanglement points per molecule.

1.2 Viscosity of Concentrated Solution

The study of rheological properties of concentrated solutions of polymers has aroused increasing interest as the processing of polymers is associated with the flow behaviour. The study of flow

properties and viscoelastic properties are important not only from the application point of view but also such study may yield valuable information concerning the structure of polymer solutions which is represented as a spatial fluctuational network formed by more or less densely packed aggregates of macromolecules and the solvent molecules are distributed in it. Solutions are usually called concentrated if the solute molecules in them interact with one another. Ferry²⁸ has suggested that the term "concentrated" would be applied to polymer solutions with the product $c[\eta]$ of at least 10. Such a solution has a relative viscosity of the order of at least 100 though it depends on polymer, the solvent and the temperature. The lower limit of polymer concentration in solution may vary from a fraction of a percent for an unusually long stiff molecule to 10 per cent for a flexible polymer of low molecular weight. The upper limit is the undiluted polymer. However, concentrated solutions are conveniently subdivided into moderately concentrated and highly concentrated solutions. The latter include solution containing a volume fraction of a polymer of about 0.30 or more. The intrinsic viscosity at zero shear is concerned with the undeformed polymer molecule

at rest and isolated from its fellows. As the solution increases in concentration there is increasing interference between polymer molecules, and a concentration at which the domains of the molecules overlap is soon reached. At still higher concentrations, the viscosity increases rapidly with increased concentration, and shear effects become large. At these high concentrations, a solution of a high polymer behaves as if its molecules were linked by transient intermolecular attachments which produce clusters at moderate concentrations²⁹ or in undiluted polymers^{30,31}. The nature of intermolecular interactions which are responsible for the rapid rise in viscosity has been described variously as due to association^{30,31}, entanglement^{16,29,30,32,33} or intermolecular attachments³⁴. The idea of entanglement network is very useful for chemists which has been discussed in detail in the previous section. Let us now consider the viscosities of concentrated solutions at zero or low rates of shear, the so-called steady flow viscosities, η° .

1.3 Dependence of Zero Shear Viscosity, η° on Molecular Parameters

When the concentration of polymer is so high that polymer molecules may be regarded as uniformly

draining but still low enough so that entanglements do not complicate the flow, Debye's equation for melt viscosity^{32,35} should apply and may be represented as

$$\eta = (\bar{R}^2 N_a n \zeta \xi) / 36 M \quad (1.1)$$

Here N_a is the Avogadro's number, n is the number of links in the molecular chain (i.e., the number of chain atoms), ζ is the friction coefficient per link ($N\zeta$ is the molecular friction coefficient), ξ is the density of the polymer and \bar{R}^2 is the mean square end-to-end distance of the polymer molecule.

At higher concentrations where entanglements play a major role in determining viscosity, the above equation must include a factor³⁶, such as the factor $(1 + n/3q)$, to take account of entanglements, i.e.,

$$\eta = [\bar{R}^2 N_a n \zeta \xi (1+n/3q)] / 36 M \quad (1.2)$$

where q is the number of links between points of entanglements and n/q is the number of entanglements per molecule. When $n\zeta$ is replaced by $n^*\zeta^0$, here n^* is the effective number of links and ζ^0 is a sliding friction coefficient and ζ^0 is set equal to $2kT/a^2p$

where $3a^2$ is the average distance moved by a segment in one jump and p is the number of jumps per second, the Eq. (1.1) becomes

$$\eta = (\bar{R}^2 N_a \zeta kT n^*) / 16 a^2 pM \quad (1.3).$$

In concentrated solutions and in diluted polymers in which all segments have the same environment, R is usually identified with R_0 , the unperturbed end-to-end distance³⁷ i.e., the expansion factor, α is set equal to unity. This assumption is reasonable³⁸ and has experimental support for concentrated solutions³⁹, but it is not necessarily valid⁴⁰ for solutions that are neither concentrated nor dilute i.e., in the range perhaps 1 to 10 percent.

1.3.1 Effects of Concentration on Zero Shear Viscosity

The viscosity behaviour of the system poly(methyl acrylate) and diethyl phthalate was measured over the entire range of concentration i.e., from 0 to 100% polymer by Fujita and Malkawa⁴¹ which showed a typical behaviour of polymers whose molecules are soft and flexible and have high molecular weights. The plots of $\log \eta^0$ against weight fraction of polymer, w_p showed an S-shaped curve with its inflection

point appearing in the region near $w_p = 0.6$. Similar plots of polymers whose molecules are stiffer have been found to be concave to the axis of concentration¹⁹. When molecular weights and concentrations are high, a double logarithmic plot of zero shear viscosity against concentration can be represented rather well by two intersecting straight lines. Above the concentration c_0 , at which these lines intersect, the viscosity is proportional to a high power, usually a fifth power, of concentration.

$$\eta^0 = k c^5 \quad c > c_0 \quad (1.4)$$

The above relationship holds for a wide variety of polymers over substantial ranges of concentration, but for other polymers (e.g., poly(vinyl acetate)) the relationship holds only over short ranges. When concentrations are less than the concentration c_0 , steady-flow viscosities are proportional to a lower power of concentration i.e., to c^b , at not too far below c_0 . The value of b is less than 5 and varies widely from polymer to polymer.

Cornet⁴² has assumed the concentration c_0 , at which the onset of straight line behaviour appears, to be the concentration at which a uniform segment

density is attained in the solution. He calculated theta dimension for several polymers from c_o , finding reasonably good agreement with literature values. His relation between c_o and $(\bar{R}^2)_\theta$ can be written in the form

$$c_o = 6.14 / [\eta]_\theta \quad (1.5)$$

According to Cornet's criterion, the product $c_o M^{\frac{1}{2}}$ should be constant for a given polymer solvent system.

The viscosity of concentrated solutions must approach the viscosity of the solid polymer as the concentration of solvent decreases. Therefore viscosity must rise rapidly at high concentrations when the polymer is rigid at the temperature of measurement i.e., when the temperature of measurement is near or below the glass transition temperature of the polymer. However, when the polymer is soft at the temperature of measurement i.e., when the temperature of measurement is well above the glass-transition temperature, the viscosity rises less rapidly with increased concentration. The sharp rise in viscosity which accompanies increased polymer content occurs at a higher concentration in poor solvents than in good solvents^{43,44}.

1.3.2 Effects of Molecular Weight on Zero Shear Viscosity

It has been generally accepted that the primary effect of shear is a breaking down of molecular interactions arising from chain entanglement. Since the chain entanglement is a function of both the size and the number of molecules, the molecular weight and molecular weight distribution are controlling factors in determining the viscosity of polymeric materials. However, in most polymer solutions and melts, the viscosity is independent of shear rate at sufficiently low shear rates. As the shear rate is increased, the viscosity begins to decrease from its zero shear values.

The experimental study of the dependence of zero shear viscosity on molecular weight of the polymers by several workers^{19,30,35,45-47} has revealed that there are two regions of molecular weights, which are separated by the critical molecular weight, M_c characteristic of each polymer-homologous series. In both the regions the relationship between η^0 and M can be described by a power law as given below:

$$\begin{aligned} \eta^0(M) &= a M^a & \text{at } M < M_c \\ & b M^b & \text{at } M > M_c \end{aligned} \quad (1.6)$$

678.01:532.135(043)
DEU

Here a and b are constants, the value of a is unity (though greater than unity is found) and β has a value 3.4 to 3.5. The value of M_c depends on concentration and on the particular polymer, and is higher for non-polar polymers^{4,5}. For any given polymer, the product of M_c and ϕ_p the volume fraction of polymer at critical concentration, is roughly constant. The critical molecular weight, M_c can be thought of as the molecular weight which is just large enough to permit an entanglement network to form at the existing concentration. As discussed earlier it may be pointed out here that the recently developed molecular theory of viscoelasticity for entangled polymer liquids^{5,6} based on the reptating chain model of de Gennes³ yielded the results that the terminal relaxation time T_1 and static shear viscosity, η^0 are found to depend on the third power of the molecular weight, M which is slightly less than the experimental results. However, some improvement of the theoretical results can be achieved by a correction¹⁰ applicable for samples of molecular weight of practical importance.

Though it is evident that η^0 is proportional to $M^{3.4}$ over a considerable range of molecular weights for many polymers, some investigators^{4,8-50} have obtained exponents ranging from 3.3 to 3.7. It is

doubtful whether these differences are significant departures, in view of the uncertainties of measuring very high molecular weights and the difficulty of making sure that steady state flow is attained in creep experiments of such materials. The measurement of zero shear viscosity in polymer solution will be discussed briefly later.

When the molecular weights is not too large, the branched molecules have lower viscosities in melts and in concentrated solution than linear molecules of the same molecular weight⁵¹⁻⁵³. Kraus and Gruver^{54,55} observed that at higher molecular weights, η_B^0 increases more rapidly and becomes very much larger than η_L^0 for polybutadiene stars with three or four arms. Graessley⁵⁶ obtained similar results for polyisoprene stars with four and six arms especially in concentrated solutions. The molecular weight dependence of η^0 then corresponds to exponents considerably higher than 3.4 (4.2) although a logarithmic plot of η^0 against M is generally curved.

1.3.3 Effects of Temperature on Zero Shear Viscosity

The viscosity of polymer solutions and of melt polymers decreases rapidly with increased temperature.

At temperature well above the glass transition, the temperature dependence of the viscosity is described by an equation of the Arrhenius type⁵⁷

$$\eta = A \exp (E/RT) \quad (1.7)$$

where E is an apparent activation energy for viscous flow and A is a constant. A temperature 100°C or more above the glass transition, E is substantially constant and has a value in the range 5 to 30 K cal/mole. However, as the temperature is lowered, the value of E becomes dependent on temperature and near the glass transition temperature, the observed value of E for poly(methyl methacrylate) at 10°C above glass transition appears to reach approximately 250 K cal/mole. Below the glass transition, the value of E falls to approximately its value at high temperature^{30,44}. Hence there are two distinct temperature ranges, one is 100°C or more above the glass-transition temperature, where the temperature dependence of viscosity of concentrated polymer solutions and the melts is governed by the above Arrhenius type equation (1.7) based on Eyring hole theory of liquids⁵⁸ and the other range extends from glass transition temperature to roughly 100°C above glass transition, when the Arrhenius type equation is not valid.

The value of E for dilute polymer solutions is very nearly the same as the value of E for the solvent alone, but in more concentrated solutions in which the viscosity of the solution increases rapidly with increasing concentration the energy of activation also increases with concentration. In the temperature range in which the energy of activation for viscous flow is independent of temperature, the value of the energy of activation depends on the type of polymer and increases with increased stiffness of the molecule, with increased bulkness of the monomer units, and with increased polarity. The apparent energy of activation of viscous flow for undiluted polymers like ethylene, propylene, isobutylene, styrene, α -methyl styrene, measured at temperatures 100°C or more, above their glass transition temperatures where an Arrhenius type of equation is obeyed, is found⁵⁹ to be 6.5 - 7.0, 9.0 - 9.6, 12.0 - 16.2, 22.6 and 32 K cal/mole respectively, where it is clearly evident that the value of E increases as the size of the repeating unit increases.

At temperatures near the glass transition temperature, where Arrhenius type equation is not obeyed, the mobility of segments is limited by the limited availability of holes. In this temperature

range, the free volume is low and becomes lower as the temperature decreases. Here the probability of a jump is determined not so much by the rate at which a molecular segment surmounts an energy barrier as by the probability that there is sufficient free volume near the segment to permit a jump. The lower the free volume, the more a molecule or a molecular segment must depend on cooperative motion of its neighbour⁶⁰ to produce the free volume needed for a jump.

In the temperature range in which an Arrhenius type of equation is not applicable, the temperature dependence of viscosity of the molten polymers and of concentrated polymer solutions can be described over a long range of concentrations and temperatures by an equation of the form:

$$\log \eta_R = [-B(T-T_1)] / [C + (T-T_1)] \quad (1.8)$$

in which viscosities are expressed as reduced viscosities η_R , defined as

$$\eta_R = \eta_{T_1} \rho_{T_1} / \rho_T \eta_T \quad (1.9)$$

Here T_1 is an arbitrarily chosen reference temperature, η_{T_1} and ρ_{T_1} are the viscosity and density, respectively,

of the polymer at this reference temperature, and η and ρ are the viscosity and density at another temperature T . This equation is frequently referred to as the Williams-Landel-Ferry equation or simply the WLF equation⁶¹. The values of the constants, B and C , depend on the polymer under consideration and on the temperature chosen as reference temperature.

1.3.4 Effects of Solvents on Zero Shear Viscosity

The viscosity of a polymer solution is determined not only by the volume fraction of a polymer, but also by the nature of a solvent. The quality of the solvents have their effect on the viscosity of the polymer solution. If two solvents whose quality to a given polymer is similar, but differ from one another by their viscosity, the viscosity of a solution in a more viscous solvent is always greater than that in a less viscous one. However, the difference in the quality of a solvent can cause an astounding difference in the viscosity of a solution.

Williams and Gandhi^{62,63} have recently examined the effects of solvent power and polymer polarity on viscosity. They found that η^0 tends to increase with concentration more rapidly in the θ solvents than in

good solvents and attributed this result to increased polymer-polymer association in the thermodynamically poor solvents. Dreval and coworkers⁶⁴, and Ferry and coworkers⁶⁵ had earlier noted similar differences between good and poor solvents and drew similar inferences. On the other hand, Simha and Zakin⁶⁶ have pointed out that the least part of the solvent power effect may be accounted for by the expected decrease of coil dimensions in good solvents with increasing concentration. Thus in good solvents the coils are larger at low concentrations due to excluded volume, and the relative viscosity of their solution η_r^0 will be larger. At higher concentrations in good solvents the coil dimensions shrink toward this θ solvent values. The relative viscosity might therefore be expected to become the same at the same polymer concentration in different solvents. Quadrat and Podnecka⁶⁷ have reported by examining the literature data that in case of polyisobutylene in a variety of solvents η_r^0 is found to be the same at the same polymer concentration. The results of Ferry and coworkers⁶⁸ on polyisobutylene also confirm that the relative viscosity in various solvents when compared appears to be the same at the same polymer concentration.

However, in polyvinyl acetate⁶⁵, polystyrene^{62,66,67,43} and poly(methyl methacrylate)^{62,69} the relative viscosities for a θ solvent cross over and become somewhat higher than good solvent values with cross over points at higher than 35% of concentration, in the range of 15-30% of concentration and in the range of 5-7% of concentration of polymer respectively. The results suggest that there is a relationship between viscosity cross over in θ solvents and polymer polarity which supports the idea of enhanced intermolecular association in poor solvents. However after examining these results, Graessley⁷⁰ has stated that a correlation between viscosity cross over in θ solvents and glass transition temperature, T_g of undiluted polymer and hence with T_g for the polymer-solvent mixture can be established. Dreval and coworkers⁷¹ have recently emphasized that such a dependence might develop as free draining behaviour is approached at the higher concentration, since the viscosity must lose its direct proportionality to solvent viscosity and become proportional instead to a local frictional coefficient, ζ_0 . The value of ζ_0 depends on the nature of both solvent and polymer since both influence the free volume and glass temperature of the mixture. The glass

temperature of most solvents is well below the room temperature. In polyisobutylene solutions T_g probably remains relatively constant and always well below room temperature because T_g for pure isobutylene is so low ($T_g = -70^\circ\text{C}$). For pure polyvinyl acetate T_g is 30°C , so T_g for its solutions must rise somewhat with increasing concentrations. Similarly, the effect for polystyrene ($T_g = 95^\circ\text{C}$) should be large, while that for poly(methyl methacrylate) ($T_g = 100^\circ\text{C}$) should not only be large but might be unusual if the unusual dependence of T_g with concentration in diethyl phthalate solutions^{2,72} holds true in other solvents as well.

1.4 Experimental Methods for the Measurement of Rheological Properties

Measurement of rheological properties is very important because of the fact that the knowledge of their values helps one to formulate the polymer systems that would best provide a particular set of physical properties desired of the final product. At present there are several different types of apparatus which may be used for determining the rheological properties, i.e., material functions $\eta(\dot{\gamma})$, $\Psi_1(\dot{\gamma})$ and $\Psi_2(\dot{\gamma})$, of polymeric materials. Here $\eta(\dot{\gamma})$ defines the

shear dependent (i.e., non-Newtonian) viscosity, $\Psi_{11}(\dot{\gamma})$ defines the first normal stress function and $\Psi_2(\dot{\gamma})$ defines the second normal stress function and they depend only on the fluid, not on the particular flow. The above apparatus include (1) the cone-and-plate instrument, (2) the two concentric cylinder instrument, (3) the parallel plate instrument and (4) the capillary instrument. Except the capillary-type instrument, the measurements of rheological properties of polymeric solutions and melts cannot be carried out with the first three types of instrument at reasonably high shear rates, say above 10 sec^{-1} . The polymeric melts give rise to shear stresses of about 10^5 - 10^7 dyne/cm² over a range of shear rates which is of practical interest in industrial polymer processing, whereas the first three types of instruments can be used to shear stresses below 10^5 dynes/cm². Only capillary viscometer or capillary rheometer is used to determine the viscosity of a fluid from measurements of flow rates and pressure drops across the tube. Besides the determination of just the viscosity alone the capillary viscometer can also be used for determining flow properties (i.e. elastic properties) of a test fluid. The word "rheometry"

has been used widely since 1950s to describe studies for determining all components of stress tensors, that is the normal stresses τ_{11} , τ_{22} , τ_{33} or combinations of them, in addition of the shear stresses τ_{12} , τ_{13} and others. As stated earlier that the zero shear viscosity, η^0 is an important rheological parameter used to characterize the flow properties of polymer solution or melt in the linear region of deformation. The study of the effect of solvent, concentration and molecular weight on the zero shear viscosity of polymer solutions has been reported in the thesis. Since we have used the zero shear viscosity measurements in the present investigations, a brief account of the methods for the determination of zero shear viscosity is given in the next section.

1.4.1 Determination of Zero Shear Viscosity

The value of the zero shear viscosity, η^0 is of great importance for the characterization of polymers. Although the zero shear viscosity concept is often used without explicit definition, current theories seem to agree implicitly on η^0 as an actual or estimated lower Newtonian viscosity.

The zero shear viscosity in molecular theories is often that of an unperturbed melt. Strictly speaking,

this would be the viscosity coefficient of a material with zero shear history which is subjected to vanishingly small shear stresses. These conditions are experimentally inaccessible and the utility of the concept is therefore enhanced if it is further assumed that η^0 is finite and that it is a Newtonian viscosity. Newtonian viscosity in this sense means that the apparent viscosity (ratio of corresponding point values of shear stress and shear rate) is constant over a finite range of either of these parameters.

Viscosity-molecular weight (η^0 -M) relations of polymer melts have been studied extensively. It has been found that a double logarithmic plot of zero shear viscosity, η^0 against molecular weight, M consists of two linear portions². At molecular weights less than a critical value, M_c , the viscosity is directly proportional to M and at $M > M_c$, η^0 is proportional to M^3 ,⁴. Experimental studies of the η^0 -M relation of polymers would be confined to rather narrow molecular weight regions if account were taken only of those η^0 values which could be demonstrated to be Newtonian viscosities. Plateau regions in plots of apparent viscosity against shear rate, $\dot{\gamma}$ or shear stress, τ have actually been measured only with fairly low molecular weight parameters.

The viscosities of many of the samples in homologous molecular weight series are non-Newtonian at all conveniently accessible shear rates. In such cases η° is estimated by extrapolating the measured non-Newtonian viscosities to zero shear rate values. However, an equivalent extrapolation is required to zero frequency in the case of dynamic measurements or to steady flow conditions in stress relaxation experiments. Thus most of the η° values available are estimated from non-Newtonian data.

Most studies of polystyrene melt rheology have involved capillary extrusion experiments in which the data were extrapolated to zero shear stress, τ or shear rate, $\dot{\gamma}$ to provide estimates to η° . Studies with cone-and-plate rheometers usually extends to lower shear rates than those with capillary viscometers. Cone-and-plate data may appear to be Newtonian in the log viscosity - log shear rate plots usually used to summarize such observations. The log-log representation compresses the data to such an extent, however of, that an apparently minor extension to what may seem to be an asymptotic value of $\log \eta^{\circ}$ may correspond to a considerable extrapolation to η° from non-Newtonian viscosities at the experimental shear rates.

Similar cautions apply to dynamic measurements in which $\log \eta^0$ may be estimated by extrapolation to zero frequency with the usual assumption of a second order fluid constitutive equation. Assumptions are also implicit in relaxation methods in which generalized Maxwell constitutive equations have been involved.

The good interlaboratory coincidence of η^0 -M results is confined to data for narrow molecular weight distribution polymers. Data on commercial, thermally initiated polystyrenes are much more scattered. The η^0 estimate in these cases is found to be very independent on the method used to extrapolate the non-Newtonian flow data. Large discrepancies are noted between such estimated zero shear viscosities and measured lower Newtonian viscosities.

Since flow curves of polymer melts are often curvilinear at low τ or $\dot{\gamma}$, direct extension of such plots to zero values of the experimental variable can be quite subjective. It would be better if the data is converted to a linear form for subsequent straight line extrapolation to η^0 . A number of linearization methods have been used for this purpose^{73,74}. Two well-known extrapolation methods^{75,76} used for linearising the experimental non-Newtonian data may

be mentioned here. One method involves plots of $1/\eta$ vs. τ and is based on the equation⁷⁵

$$1/\eta = 1/\eta^0 + \tau/(\eta^0 G) \quad (1.10)$$

where G has the dimension of a modulus. This procedure has been used extensively with polyethylene melt data. The second method uses the equation⁷⁶ as given below:

$$1/\eta = 1/\eta^0 + (\alpha \dot{\gamma}^n)/\eta^0 \quad (1.11)$$

This involves the extrapolation of $1/\eta - \dot{\gamma}^n$ plots to zero values of $\dot{\gamma}$. In this equation α is constant and n is a fractional index which is often, but not necessarily, equal to $2/3$. Good results have been obtained by Rudin and Chee⁷⁷ using the second method. Another equation⁷³ which is widely used in this connection is given as under:

$$\ln(1/\eta) = \ln(A/\eta^0) + B\tau \quad (1.12)$$

Here A and B are material constants. Plots of $\ln(1/\eta)$ vs. τ were always linear with the data but intercepts at zero τ contained an unknown factor A .

Recently a new theoretically grounded method has been proposed⁷⁸ for the determination of zero

shear viscosity, η^0 , in which a plot of η as a function of $(\eta\dot{\gamma})^3$ will yield a straight line, the intercept of which give η^0 . The η^0 s obtained by this procedure are found to be in good agreement with directly measured values.

1.5 Viscosity of Concentrated Solutions or Melts at High Rate of Shear

In most polymeric solutions and melts, the viscosity is independent of shear rate at sufficiently low shear rates. As the shear rate is increased, the viscosity begins to decrease from its zero shear value, η^0 . The drop in viscosity has important practical consequences in operations such as spinning, which forces polymer solutions through tiny orifices at high rates and painting, which is done at rates of shear say to range⁷⁹ from 12,000 to 35,000 sec^{-1} . It has generally been accepted that the primary effect of shear in concentrated solutions and in molten polymers is a breaking down of molecular interactions arising from chain entanglement. On the other hand the principal cause of shear effects in dilute polymer solutions is deformation and alignment of molecules. In dilute solution, shear effects are observed only when the molecular weights are very high (i.e. over 400,000 and often not below one million) but in

concentrated solutions and in molten polymers shear effects may become apparent at molecular weights as low as 10,000 or even 3000. The melt viscosities of oligomers with very low molecular weights are independent of shear upto the highest rates of shear attainable experimentally, but as the molecular weight increases, a critical molecular weight, M_c at which viscosity becomes shear dependent at observable rates of shear is soon reached. It has been observed that in case of undiluted poly(dimethyl siloxane)^{80,81}, poly(ethylene glycol) and polyisobutylene, the double logarithmic plots of viscosity versus molecular weights at different shear rates give contiguous curves below the critical molecular weight, whereas above the critical molecular weights the same plots at different shear rates give deviations from the single straight line. Above the critical molecular weight, the slope at low shear is approximately 3.4, but as the shear rate increases, this slope becomes lower. Since the molecular weight at which the zero shear plot changes slope is supposed to be the molecular weight at which an entanglement network forms, it may be concluded that the viscosity of these polymers does not become shear dependent until entanglements form. However, in case of the melt

viscosities of polystyrene and of linear polyethylene⁸¹ it has been observed, contrary to the observation found in case of poly(dimethyl siloxane), that the critical molecular weights vary with shear rates. When the viscosities of these same polymers are measured at various constant shear stresses (instead of at various constant shear rates) and are plotted against molecular weight, the new plot displays only a single critical molecular weight⁸² which is independent of shear stress.

A third type of viscosity-shear dependence is observed in certain copolymers of acrylonitrile. Solutions of these polymers, containing 3 to 8% of polymer dissolved in aqueous sodium thiocyanate have two critical molecular weights⁸³, the higher critical molecular weight marks the formation of an entanglement network and the lower critical molecular weight marks the beginning of shear dependence in viscosity. The lower critical molecular weight (approximately 1500) is much too low to be caused by deformation of individual molecules. These observations suggest that polar solutions may sometimes be characterized by two "entanglement" networks: one corresponding to the entanglement network in solutions of non-polar

polymers, and the other resembling the hydrogen-bonded networks which occur in solutions of poly(carboxylic acids)⁸⁴.

The principal features of the flow curves (i.e. the plots of apparent rate of shear against shearing stress) of polymers at moderate and high concentration (when molecular weight remains constant) are first, at low rates of shear, a linear region in which the solution behaves in a Newtonian manner. This region is followed by a region of non-Newtonian behaviour in which the viscosity decreases with increasing shear rate, causing the flow curve to exhibit a slope that depends on rate of shear. When the polymer is used undiluted or at high concentration and have narrow molecular weight distribution, the change from Newtonian to non-Newtonian behaviour is manifest by an abrupt change in slope of the flow curve⁸⁵, but when concentrations are low, and polymers heterodisperse, the flow curve shows merely an inflection point (instead of distinct break) which may be difficult to locate with certainty⁸⁶. Although shear effects are more pronounced in good solvents in which molecules are extended than in poor solvents, shear effects are present even in θ solvents⁸⁷ in which the molecules are tightly coiled.

1.6 The Present Investigation

Our main work consists of the study of the rheological properties of the samples of two polymers namely polychloroprene and polybutadiene having different molecular weights over a wide range of concentration in both good and θ solvents. Polychloroprene samples with different molecular weights were studied first. Since zero shear viscosity, η^0 of polymer solutions is an important rheological parameter used to characterize the flow properties of polymer solutions and polymer melts in the linear region of deformation, measurements of zero shear viscosity of polymer solutions were carried out in this work. The probability of constructing a zero shear viscosity master curve valid for the entire concentration range independent of molecular weight and nature of solvents has been considered. To correlate the viscosity data obtained in good and poor solvents, two methods, one given by Graessley and the other given by Dreval and coworkers involving the correlating variable, $c[\eta]$ were examined. Dreval and coworkers have used the Martin relation for the correlation of the viscosity data. The solvent-solute interaction constant, K_M which is related to the flexibility of macromolecular

chain and the polymer-solvent interaction, obtained from the Martin equation, has been used to normalize the correlating variable, $c[\eta]$ so as to reduce all experimental data of the polymer samples to a common curve. Further, the method as given by Graessley which has taken into account the contraction of dimensions of chains with concentrations in good solvent, has been employed to correlate the data obtained at good and θ solvents. In case of polychloroprene this approximate correction on correlating variable, $c[\eta]$ though improves the correlation much, but it cannot eliminate completely the difference between the data obtained in good and θ solvents. However, the results indicate that a few more solvent-solute systems need to be studied in detail before coming to a definite conclusion.

The study has further been extended to another polymer, polybutadiene in both good and θ solvents so as to produce additional data involving the effects of solvent, concentration and molecular weight on the zero shear viscosity of polymers and to substantiate our findings and considerations. We have chosen this polymer because of the fact that polybutadiene is a cis compound (100% cis) and the chain of the

polymer is more flexible than that of polychloroprene (probably a trans compound) which was studied earlier. Besides this polychloroprene is a polar compound while polybutadiene is a non-polar one. In this connection it may be mentioned that the relative zero shear viscosity, η_r^0 in a θ solvent crosses over and becomes somewhat higher than the value of the good solvent in the higher concentration range and there seems to have a relationship between the viscosity cross over in θ solvent and polymer polarity supporting the idea of enhanced intermolecular association in poor solvents. Our study of both polar and non-polar polymers may give further insight into this direction also. There are indications from our data on polychloroprene samples that the onset of entanglement has been started at the cross over point concentration, c_{cross} i.e., from this concentration the polymer molecules diffuse by reptation from the virtual tube enclosing each chain and the static shear viscosity depends on 3.4 power on molecular weight. However, in case of polybutadiene samples the data for c_{cross} are found deep inside the zero shear viscosity composite curve made by superposition of viscosity data in the higher concentration region and not at the starting points from where the data deviate

from curve as is found in case of polychloroprene. This implies that entanglement started at higher concentration in polybutadiene samples than in polychloroprene samples.

The zero shear viscosity, η^0 of concentrated polymer solutions was measured by means of a Brookfield LVT viscometer and the solvents and dilute solutions (5% polymer or below) with a Maron-type capillary viscometer with continuously varying pressure head. The molecular weights of the samples were measured by light scattering method and the $[\eta] - \bar{M}_w$ relation was determined by comparing the molecular weights with $[\eta]$ obtained at various solvents.

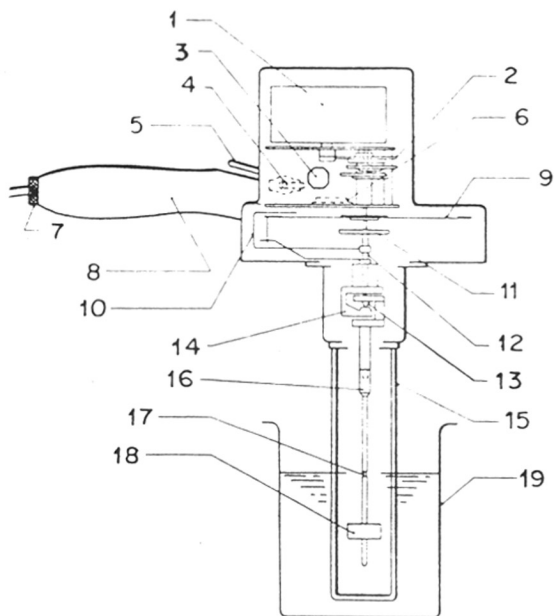


CHAPTER - II
EXPERIMENTAL

EXPERIMENTAL

2.1 Brookfield L V T Viscometer

The zero shear viscosity, η^0 of the polymer solutions was measured by means of a Brookfield LVT viscometer (manufactured by Brookfield Engineering Laboratories, Inc., Massachusetts, U.S.A). The schematic drawing of the Brookfield synchro-lectric viscometer is given in Fig. 2.1. The instrument is powered by a General Electric synchronous induction-type motor, Model 5 SMY 20 J, to ensure the speeds of rotation will be constant. Power is transmitted through a gear train which has eight possible speeds (0.3, 0.6, 1.5, 3, 6, 12, 30 and 60 r.p.m.) (final symbol T indicates the speed). Within the main case is a calibrated spring, one end of which is attached to the gear train and large circular dial. The other end is attached to the pivot shaft to which is affixed a pointer which registers on the dial. The dial is driven directly by the transmission. The pointer and pivot shaft are also driven by the transmission but the power is first transferred through the calibrated spring. The spindles (four in numbers) are attached through an external coupling to the pivot mechanism. The instrument is constructed in such a way that



- | | |
|-------------------------|-----------------------------|
| 1 SYNCHRONOUS MOTOR | 10 POINTER |
| 2 GEAR TRAIN | 11 CALIBRATED SPIRAL SPRING |
| 3 SPEED SELECTOR KNOB | 12 UPPER SHAFT |
| 4 ON-OFF TOGGLE SWITCH | 13 PIVOT POINT |
| 5 CLUTCH LEVER | 14 JEWEL BEARING SUPPORT |
| 6 CIRCULAR BUBBLE LEVEL | 15 REMOVABLE SPINDLE GUARD |
| 7 KNURLED NUT | 16 SPINDLE COUPLING NUT |
| 8 HANDLE | 17 IMMERSION MARK |
| 9 DIAL | 18 SPINDLE BODY |
| | 19 SAMPLE CONTAINER |

FIG. 2-1. SCHEMATIC DRAWING OF THE
BROOKFIELD SYNCHRO-LACTRIC VISCOMETER

there are no lower bearings to add friction. All the assembly turns when the motor turns.

When the spindle is immersed in the simple fluid, a viscous drag opposes the forces of the motor. This drag is detected as a strain on the spring which registers as a deflection on the dial. The spring is precalibrated at the factory. It is made with beryllium copper. It is claimed by the manufacturer that the spring made with this material would not show any change in characteristics due to fatigue even after hundreds of thousands of flexings. For this reason, a check of the spring is not considered necessary. There is no zero adjustment on the viscometer since experience has shown that the zero will never change due to changes in the spring⁹⁰.

The torsion springs are available in several degrees of stiffness and in LVT Model the torque for full-scale deflection is 673 dyne-cm. In this instrument the rate of shear is not known. The viscometer is designed to operate in any size container and rate of shear is, of course, dependent on the gap size. It may be calculated for infinite cup radius in fluids without a yield value by equation⁹²

$$\dot{\gamma} = -2 \frac{d\tau}{d \ln \tau}$$

Here ω is the angular velocity and τ is the stress at the inner wall. $\dot{\gamma}$ can be found directly from a plot of ω versus $\ln \tau$. τ and ω are both obtained from experimental data; hence the rate of shear at the inner cylinder $\dot{\gamma}$ is determined. The solution is valid for any fluid that does not have a yield value.

The removable guard leg which come attached to the instrument is meant to afford protection for the spindle when exposed to fairly rough service. With the legs installed and the assembly immersed in a container, the effective gap becomes reduced and the readings obtained are higher than without the guards. However, the LV model is calibrated in an "infinite body" with guard in place⁹². This "infinite body" concept simply means that the radius of the cup is sufficiently large so that when $1/R_{\text{cup}}^2$ is neglected, the error is less than the 1% accuracy specified. Use of the guards on the Model LV is optional and depends on the service to which the instrument is to be put. In this work we have not used the guard leg and instead of using a cup of large radius, a smaller radius cup has been used (described later).

The reading is taken through the window in the main case. For low values of the speed (r.p.m.) the

reading is taken by observing the pointer and dial when they come in view during rotation. For the higher speeds, the dial and pointer are stopped or "frozen" by proper manipulation of the clutch and motor switch.

The Model LV comes with four spindles, one cylindrical (No.1), two disc types (Nos.2 and 3) and one straight shaft (No.4) (also cylindrical). The spindles have all been calibrated for Newtonian liquids by the manufacturer, and the direct readings in centipoises are found from a specially provided table called "Fact Finder". For apparent viscosity determination all that is needed is the spindle number, speed (r.p.m.) at which the spindle rotates and the dial reading. The minimum range of viscosity that can be measured with LVT model is 0 - 1.0 poise and the maximum range is 0 - 2×10^4 poises. The lowest limit of effective measurement is 15 cps - below this viscosity, the use of UL adapter is recommended for truly accurate results. The adapter consists of a cylindrical cup and spindle of small clearance. The cup is closed at the lower end and holds 24 to 25 ml sample. An accuracy of 2×10^{-4} Poise is claimed for this attachment.

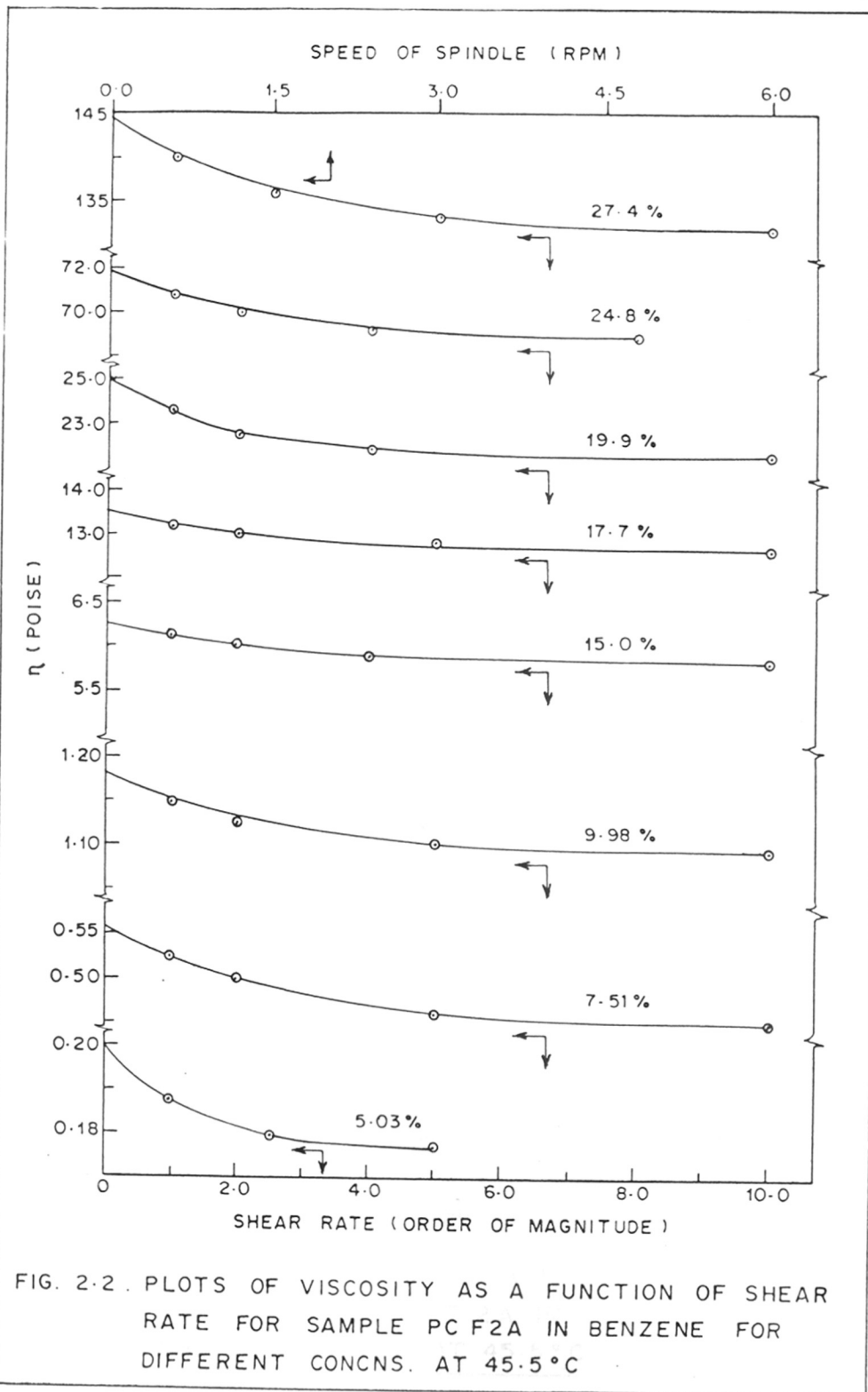
The manufacturer supplies special stand for supporting and levelling the Brookfield viscometers.

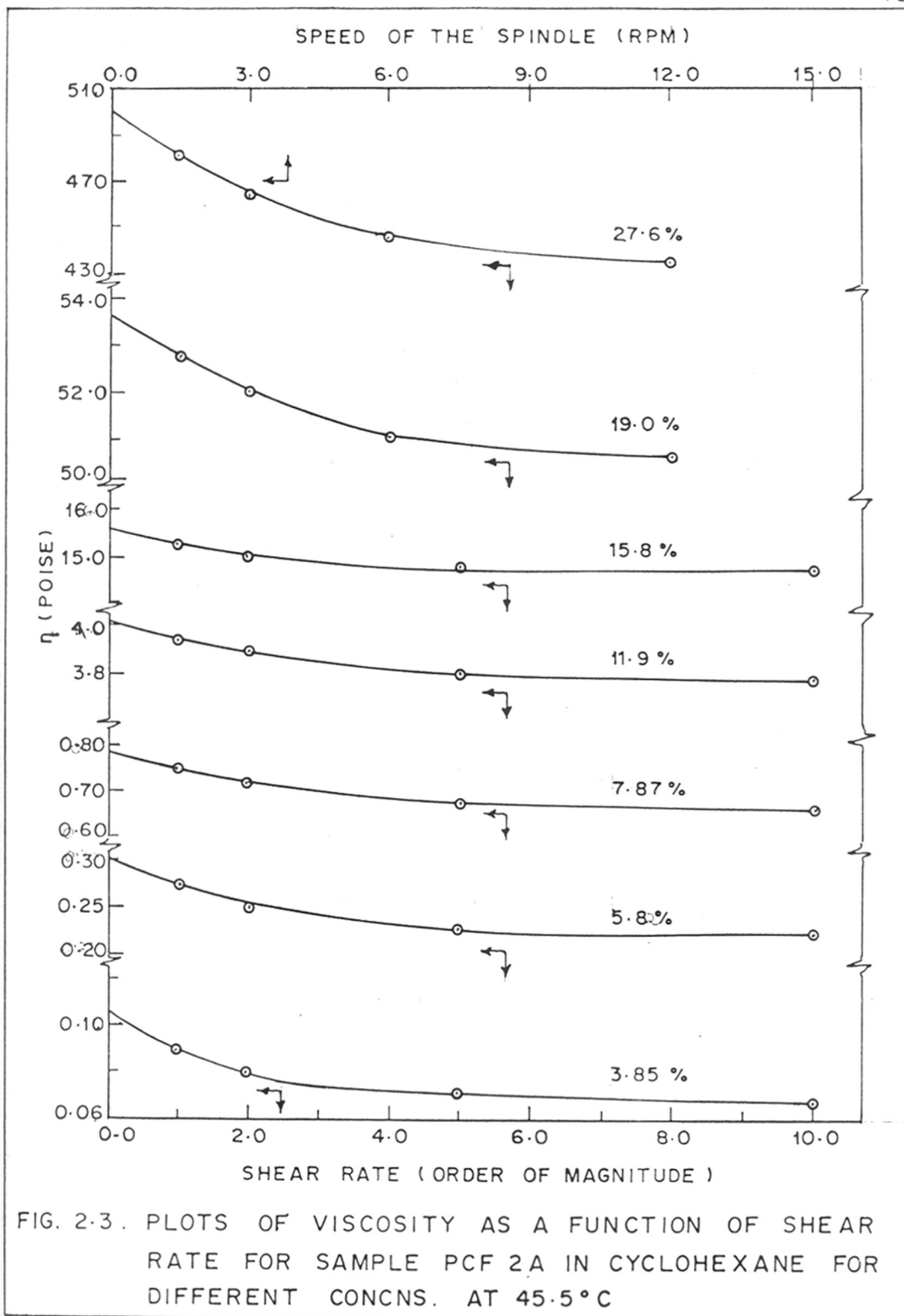
These stands are superior to the usual laboratory ring stand in that there are levelling adjustments in the support. The viscometer with eight speeds (T series) are reasonably well suited for measuring effects dependent on rate of shear. Lower shearing rates are obtained with the instrument as purchased. Some time dependent effects may be measured with the Brookfield, although recording viscometers are much more superior in this respect.

2.1.1. Zero Shear Viscosity Measurement of Polymer Solutions with Brookfield LVT Viscometer

In Brookfield LVT viscometer the rate of shear and shear stress cannot be readily calculated, but the simple approximation that the shear rate is approximately 0.2 times the revolutions per minute of the cylinder is useful^{93,94}. The viscosity of non-Newtonian fluids is dependent on the rate of shear at which they are measured and the shearing rate depends on the speed at which the spindle rotates. Since the rate of shear is directly proportional to r.p.m. of the spindle at which the measurements are made, the η values taken at different speeds (r.p.m.) were extrapolated to zero for the determination of the zero shear viscosity, η^0 in this work.

The Brookfield viscometer was recalibrated with a smaller container (cell) (35 mm diameter) made with stainless steel and with this container the measurement was carried out with 63 cc of solution. The cell was kept immersed into thermostatic water bath maintained at different temperatures (20.2° , 20.5° , 25.0° and 45.5°C) with an accuracy of $\pm 0.02^{\circ}\text{C}$. Only three spindles, Nos. 2, 3 and 4 were used. The viscosity of each polymer solution was measured at least with 4 different speeds and the plot of apparent viscosity, η versus speed (r.p.m.) was extrapolated to zero for the determination of zero shear viscosity, η^0 . The typical plots of viscosity as a function of speed at which the spindle rotates (i.e., shear rate) corresponding to the highest viscosity's and then an order of magnitude of the shear rate for all other concentrations for one polychloroprene sample(PCF2A) in benzene and cyclohexane are given in Figs. 2.2 and 2.3 respectively. Since the flow curves are curvilinear at low shear rate, direct extension of such plots to zero values of the experimental variable is somewhat subjective. However, the plots on semi-log paper converted the data to a somewhat linear form and subsequent extrapolation to η^0 produced the same results.





2.2. Maron-type Capillary Viscometer with Continuously Varying Pressure Head

The zero shear viscosity, η^0 of the solvents were measured at different temperatures by a capillary viscometer with a continuously varying pressure head as designed by Maron and coworkers⁹⁵. A sketch of the capillary viscometer is shown in Fig. 2.4. The apparatus constructed entirely of glass, consisting of a capillary unit I and a manometer unit II connected by a standard joint (No. 10). The capillary unit is composed of a water jacket F inside of which are sealed the bulb C and tube D of the same diameter, joined by the capillary A and side arm tube B. The function of the side arm is to facilitate filling of the unit with sample and to speed attainment of hydrostatic balance by by-passing the capillary. During a run the side arm stop-cock is kept closed.

The manometer unit II consists of a precision bore tube (3.4 mm diameter and 100 cm long) and a 20 ml hypodermic syringe G, joined to the manifold as indicated in Fig. 2.4. The manometer tube with mercury is placed against a scale of mm graph paper, to permit reading of the mercury column heights. The syringe is

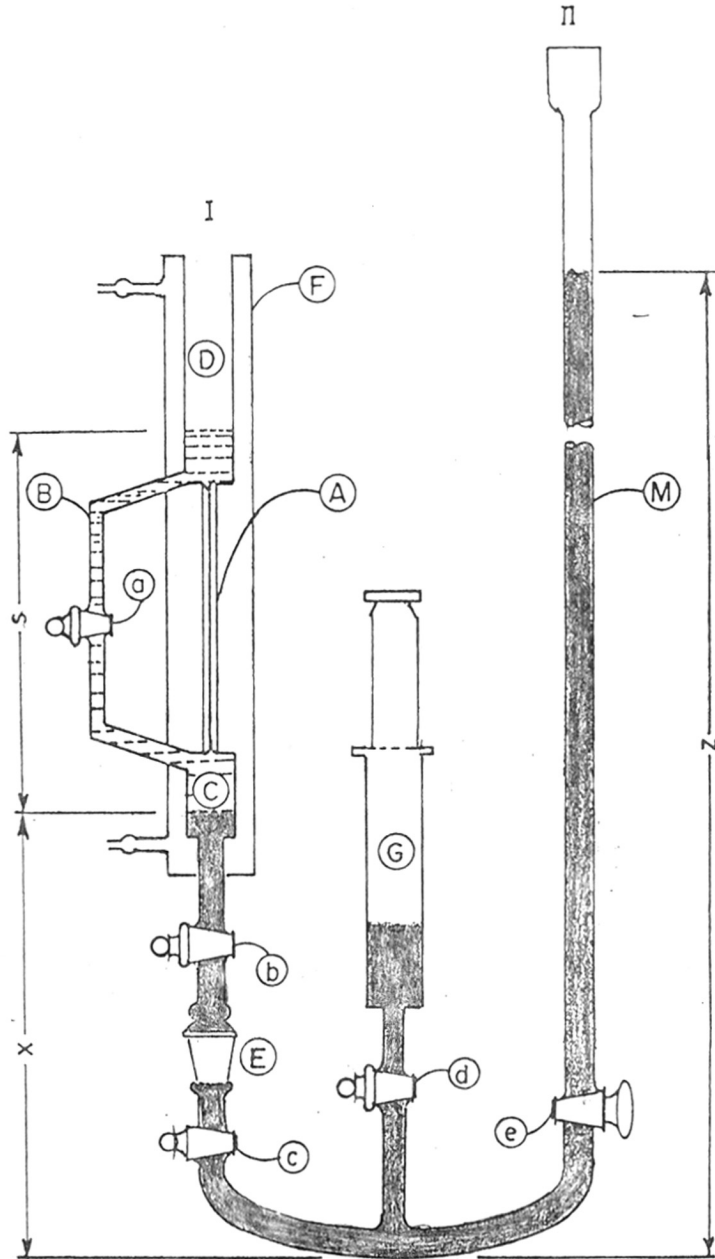


FIG. 2.4. CAPILLARY VISCOMETER WITH CONTINUOUSLY VARYING PRESSURE HEAD

used to adjust the amount of mercury in the system and the mercury levels. All the stopcocks shown are of 2 mm bore and fitted with pressure adapters.

To permit variation of capillary size, three units such as I were constructed. These units only differed in the bore of the capillary sealed in (radii of three capillaries A, B and C used are 0.1462, 0.1985 and 0.3058 mm respectively) and they can be interchanged through the standard joint connection. Approximately 15 ml of the sample is required for the measurement. The water from the thermostatic water bath maintained at different temperatures (20.2° , 20.5° , 25.0° and 45.5°C) with an accuracy of $\pm 0.02^{\circ}\text{C}$ was circulated through the water jacket F for performing the measurements at constant temperature.

Principle of Operation: When the sample is flowing through the capillary tube with a volume of flow Q , the pressure drop P across the capillary is

$$P = Z \rho_m g - (x \rho_m g + s \rho_s g) \quad (2.1)$$

where ρ_m and ρ_s are respectively the densities of mercury and sample, while g is the acceleration due to gravity. When the system is in hydrostatic balance, the heights of the mercury columns x and z in the U tube

system above a horizontal base line, becomes $x = x_0$ and $z = z_0$, s is the height of the sample column and thus

$$0 = z_0 \rho_m g - (x_0 \rho_m g + s \rho_s g) \quad (2.2)$$

Subtracting Eq. (2.2) from Eq. (2.1), we have

$$P = [(z - z_0) - (x - x_0)] \rho_m g \quad (2.3)$$

Since the volume of mercury in the system remains constant,

$$(x - x_0) = (r_m^2 / R_c^2) (z - z_0) \quad (2.4)$$

Where r_m and R_c are respectively the radius of the manometer tube and the bulbs C and D which are of the same diameter.

Hence Eq. (2.3) becomes

$$P = (z - z_0) \rho_m g [1 + (r_m^2 / R_c^2)] \quad (2.5)$$

$$= h \rho_m g [1 + (r_m^2 / R_c^2)] \quad (2.6)$$

$$= \alpha_m h \quad (2.7)$$

The volume rate of flow is given by

$$Q = - \pi r_m^2 (dh/dt) \quad (2.8)$$

From the Eqs. (2.6) and (2.8), it is evident that determination of h as a function of t , as the sample

flows through the capillary under the driving pressure of the manometer, allows calculation of both P and Q. However the density of the sample ρ_s does not enter the equation and hence need not be known.

Flow of Newtonian Fluids in Viscometer: According to Poiseuille's equation the viscosity of a Newtonian fluid is given by

$$\eta = (\pi R^4 P / 8LQ) \quad (2.9)$$

Substituting the relations for P and Q determined above, we have

$$\eta = [(R^4 \alpha_m) / (8Lr_m^2) (1/d \ln h / dt)] \quad (2.10)$$

$$\text{or } (d \log_{10} h / dt) = m = \left\{ [(R^4 \alpha_m) / (8 \times 2.303 L r_m^2)] \right.$$

$$\left. (1/\eta) \right\} = - (B/\eta) \quad (2.11)$$

For Newtonian fluid a plot of $\log_{10} h$ vs. t should be linear and the viscosity would be obtained from the slope of this line and the instrumental parameters.

Flow of Non-Newtonian Fluids in Viscometer: In case of non-Newtonian fluid the plot of $\log_{10} h$ vs. t produces a nonlinear graph. The problem involved then is the computation of the rate of shear - shear stress relation

of the non-Newtonian fluid.

The mean rate of flow \bar{Q} may be defined as

$$\bar{Q} = \left\{ \pi r_m^2 (h_2 - h_1) \right\} / (t_2 - t_1) \quad (2.12)$$

and a logarithmic mean pressure head may be defined as

$$\bar{h} = (h_2 - h_1) / \ln (h_2 / h_1) \quad (2.13)$$

as the effective head for the Newtonian liquids.

This mean value of h is usable for non-Newtonian fluids if $(h_2 - h_1)h_1 \ll 1$. In terms of these, the apparent fluidity, $1/\eta$ becomes,

$$1/\eta = (8L\bar{Q}) / (\pi R^4 \alpha_m \bar{h}) \quad (2.14)$$

and the maximum shearing stress, τ

$$\tau = RP/2L = (R\alpha_m \bar{h})/2L \quad (2.15)$$

From Eq. (2.11)

$$= -[8(2.303)L r_m^2] / (R^4 \alpha_m) = m/B \quad (2.16)$$

Krieger and Maron⁹⁶ have shown the relation between shearing stress, τ and the rate of shear, $\dot{\gamma}$ at capillary wall as

$$\dot{\gamma}/\tau = (1/\eta) \left[1 + (1/4) \left\{ \frac{d \ln (1/\eta)}{d \ln \tau} \right\} \right] \quad (2.17)$$

Substituting Eq. (2.16) into Eq. (2.17) we have

$$\begin{aligned} &= -(m/B) \left[1 + \left\{ 1/(4 \times 2.303) \right\} \left\{ (dm/dt)/m^2 \right\} \right] \\ &= -(m/B) \left[1 + \left\{ 1/(9.212 \text{ m}^2) \right\} (dm/dt) \right] \end{aligned} \quad (2.18)$$

When $\log_{10} h$ is plotted as a function of time, t and differentiated graphically, it will give m . The m values are then to be plotted as a function of t and the plot again is to be differentiated graphically to get dm/dt . When these derivatives are substituted into Eqs. (2.16) and (2.18), $(1/\eta)$ and $\dot{\gamma}/\tau$ would be obtained.

2.2.1 Zero Shear Viscosity Measurements of Solvents and Dilute Polymer Solutions with Capillary Viscometer with Varying Pressure Head

The zero shear viscosity of solvents were measured at different temperatures by a capillary viscometer with a continuously varying pressure head as described above. For taking measurements at constant temperature, the water from thermostatic water bath maintained at the required temperatures (20.2°, 20.5°, 25.0 and 45.5°)

with an accuracy of $\pm 0.02^{\circ}\text{C}$ was circulated through the instrument. For Newtonian fluids, the viscosity was calculated by the Eq. (2.11)

$$(1/\eta) = -(1/B) (d \log_{10} h) dt = - (m/B)$$

where h is the height of the mercury manometer from its equilibrium position and B is the apparatus constant. As stated earlier three interchangeable capillaries of radius 0.1462, 0.1985 and 0.3058 mm were used in this work and the apparatus constant B values with these capillaries have been obtained as 0.58890×10^{-4} , 1.96706×10^{-4} and 11.4046×10^{-4} respectively. The typical plots of $\log_{10} h$ as a function of time for different solvents using a capillary of radius 0.1462 mm (Capillary A) is shown in Fig. 2.5. For avoiding crowding of lines, the same plot for cyclohexane has not been shown on the same graph. The solvents used in this work showed Newtonian flow as $d \log_{10} h/dt$ was constant. The viscosity data (η°) for the solvents are given in Table 2.1.

Further, the zero shear viscosity for some dilute solutions (5% and below) having non-Newtonian flow was also measured with this instrument. A typical plot of $\log_{10} h$ as a function of time for PC F3B

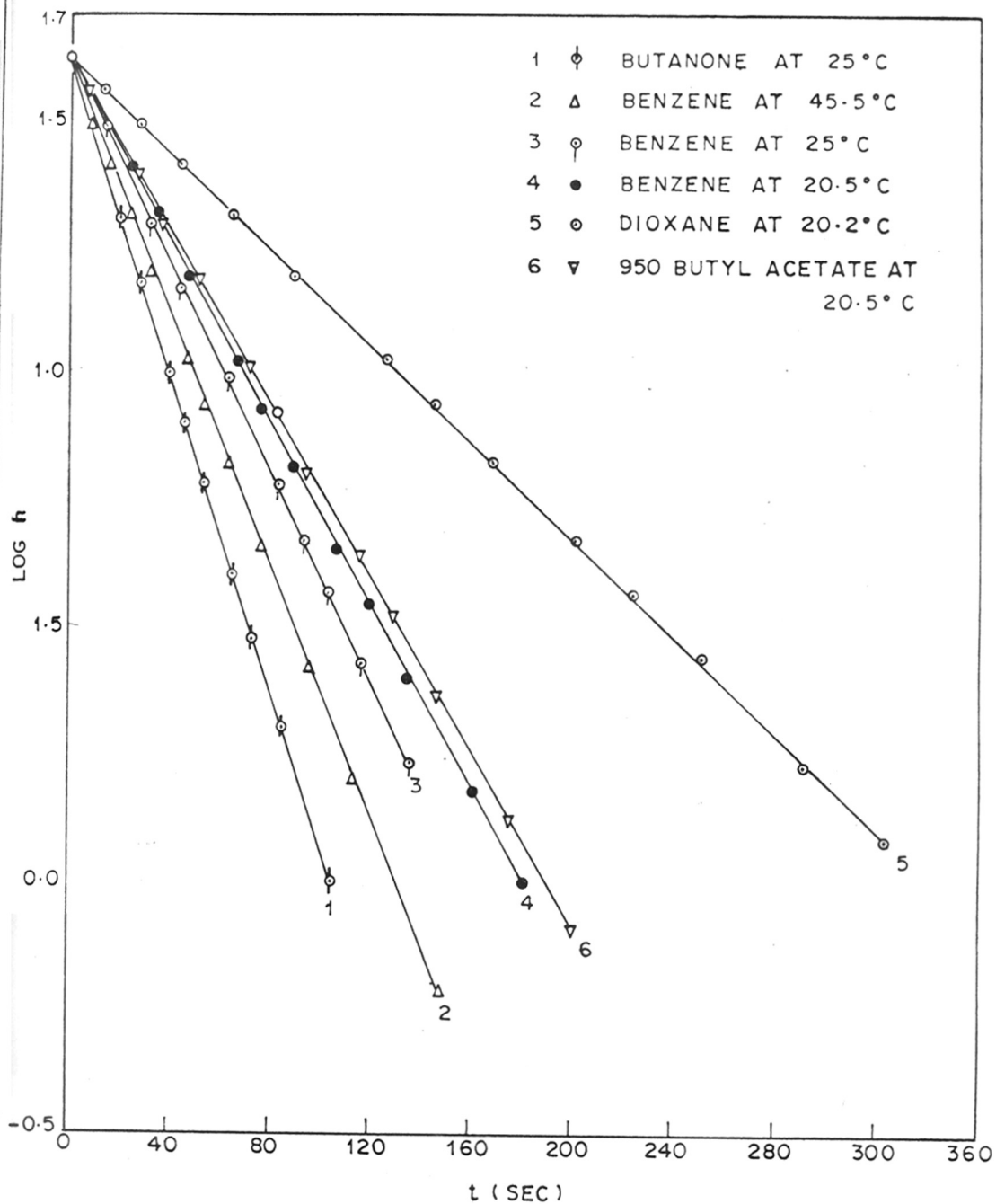
FIG. 2-5. PLOTS OF LOG h vs. t

Table 2.1

The zero shear viscosity, η^0 and θ temperature for the solvents

Solvent	Temperature (°C)	η^0 (CPS)	θ temperature (°C) for polymers
Benzene	20.5	0.655	good solvent for PB
Benzene	25	0.598	good solvent for PC and PB
Benzene	45.5	0.473	good solvent for PC
Cyclohexane	45.5	0.648	45.5 for PC ^a
Butanone	25	0.381	25 for PC ^a
Isobutyl acetate	20.5	0.698	20.5 for PB ^a
Dioxane	20.2	1.240	20.2 for PB ^a

a : From ref. 97

Table 2.2

The summary of data obtained by the capillary viscometer for PC F3B sample in benzene solution (5.07 gm/dl) at 25°C

Capillary A : $R = 1.4628 \times 10^{-2}$ cm, $L = 14.344$ cm

Mercury manometer: $r_m = 0.2047$ cm, $R_c = 0.7526$ cm,

$\alpha_m = 1.4246 \times 10^4$

h cm	t sec	$-m \times 10^3$	(dm/dt) $\times 10^6$	$(\dot{\gamma}/\tau)^a$	τ^b (dynes/cm ²)	$\dot{\gamma}$ (Sec ⁻¹)	$\eta_a = -(B/m)$ (Poise)
41.4	0	1.25	1.890	24.013	601.4	14,442	0.0471
30.7	131	1.09	0.973	19.699	446.0	8,786	0.0540
20.7	304	1.02	0.410	18.061	300.7	5,431	0.0577
10.7	605	0.944	0.307	16.629	155.4	2,585	0.0624
6.7	833	0.896	0.256	15.742	97.33	1,532	0.0657
4.7	1015	0.880	0.205	15.372	68.28	1,050	0.0669
3.7	1143	0.864	0.154	14.998	53.75	806	0.0682
2.7	1286	0.832	0.102	14.354	39.22	563	0.0708
1.7	1540	0.800	0.051	13.702	24.70	338	0.0736

$$a : (\dot{\gamma}/\tau) = (m/B) [1 + (1/(9.212 \text{ m}^2) (dm/dt))]$$

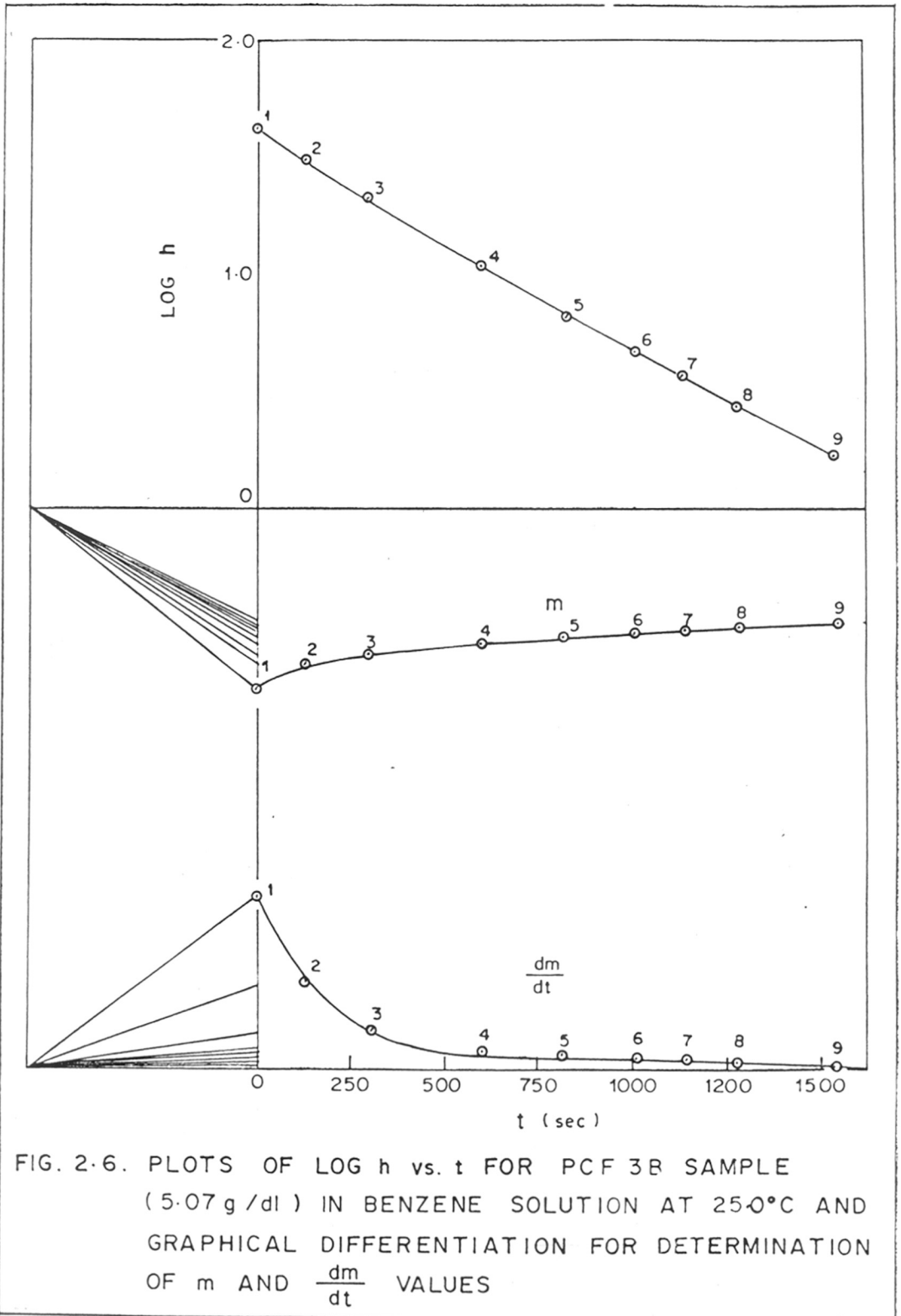
$$b : \tau = (R \alpha_m h)/L, \alpha_m = \rho_m g [1 + (r_m^2/R_c^2)]$$

sample (5.07 gm/dl) in benzene solution at 25°C and the graphical differentiation for determination of m and dm/dt values of it, is given in Fig. 2.6. The shear stress, τ , the apparent viscosity, η_a and rate of shear, $\dot{\gamma}$ were calculated employing the equations given in (2.15), (2.16) and (2.18) respectively.

The typical data for measurements in capillary viscometer or 5.07% PC F3B sample in benzene solution at 25°C are given in Table 2.2. The plots of apparent viscosity, η_a versus rate of shear, $\dot{\gamma}$ for the polychloroprene sample are shown in Fig. 2.7 and the zero shear viscosity, η^0 determined by extrapolation of the plots, was obtained as 7.90×10^{-2} Poise.

2.3 Density Measurement

The density of each solvent was measured as the mean of three measurements using 30 cc Ostwald-type pycnometers, and the agreement between the measurements was ± 0.00002 or better. The density of each polymer was measured employing two specific gravity bottles (25 cc) using ethylene glycol as confining liquid. Both the pycnometers and specific gravity bottles were filled carefully to avoid trapping of air bubbles, equilibrated for 20 minutes in water thermostat maintained



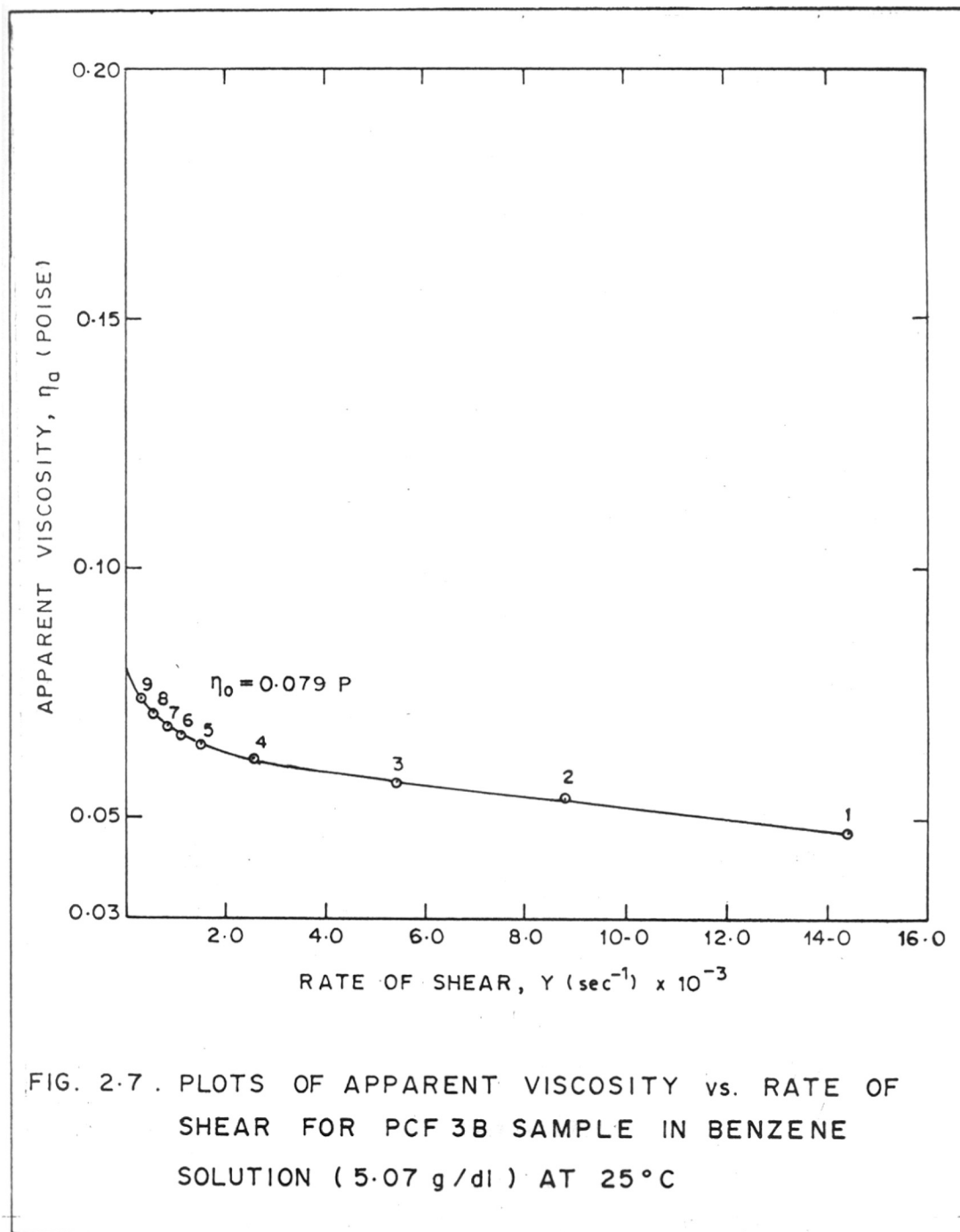


FIG. 2.7 . PLOTS OF APPARENT VISCOSITY vs. RATE OF SHEAR FOR PCF 3B SAMPLE IN BENZENE SOLUTION (5.07 g /dl) AT 25 °C

at different temperatures (as required) with an accuracy of $\pm 0.02^{\circ}\text{C}$, capped, washed, dried and equilibrated at room temperature for 30 minutes to constant weight. The densities were calculated from the mass of solvent (or polymer) and the volumes were obtained from the mass of the pure solvent they held at the corresponding temperature and its density. All weighings were reduced to the vacuum standard.

With the density data, the apparent specific volume, V_s of the solvents namely benzene, cyclohexane, butanone, isobutyl acetate (IBA) and dioxane was determined at five different temperatures starting with 20°C (20° , 30° , 40° , 50° and 60°C), which were represented by the following equations.

The apparent specific volume of two polymers, V_p namely, polychloroprene and polybutadiene, were determined in the similar way with the density data (measured at 20° , 30° , 40° , 50° and 60°C) and they were represented by the equations given below:

Solvents

$$V_s \text{ (benzene)} = 1.1386 + 14.28 \times 10^{-4} (\theta - 20^{\circ})$$

$$V_s \text{ (butanone)} = 1.2421 + 17.40 \times 10^{-4} (\theta - 20^{\circ})$$

$$V_s \text{ (cyclohexane)} = 1.2849 + 16.30 \times 10^{-4} (\theta - 20^{\circ})$$

$$V_s \text{ (dioxane)} = 0.9677 + 10.67 \times 10^{-4} (\theta - 20^\circ)$$

$$V_s \text{ (isobutyl acetate)} = 1.1519 + 14.06 \times 10^{-4} (\theta - 20^\circ)$$

Polymer

$$V_p \text{ (polychloroprene)} = 0.8230 + 6.36 \times 10^{-4} (\theta - 20^\circ)$$

$$V_p \text{ (polybutadiene)} = 1.1055 + 9.00 \times 10^{-4} (\theta - 20^\circ)$$

where θ is the temperature.

2.4 Purification of Solvents and Preparation of Solutions

The solutions of higher concentrations were prepared by mixing the weighed amounts of the polymer and the solvent and the relations for V_p and V_s were used to calculate the concentration of the solutions (gm/dl) assuming that there was no volume change on mixing. However, in higher concentrations (>30%) this assumption is not correct. Dilution was carried out by adding solvents by weight and polymer concentration was converted to gm/dl. In case of polychloroprene samples (PC) benzene at two different temperatures (25° and 45.5°C) was used as two good solvents, and cyclohexane and butanone were used as θ solvents. On the other hand, in case of polybutadiene samples (PB), benzene at 20.5°C was used as good solvent and dioxane and isobutyl acetate (IBA) were used as θ solvents.

The θ temperature of the solvents used in polychloroprene and polybutadiene samples are listed in Table 2.1.

All solvents used were dried primarily with fused CaCl_2 and carefully distilled. Benzene (thiophane free), cyclohexane and dioxane were refluxed with sodium and the distillate was stored under sodium wires. To prevent the degradation, nitrogen gas was passed into the polymer solution and stored in inert nitrogen atmosphere under dark in dry places, mostly in desiccator.

2.5 Purification and Fractionation of Polymers

2.5.1 Polychloroprene (Denkaprene M-40)

Polychloroprene (PC) (Denkachloroprene type M-40) was obtained as a gift from Swastic Rubber Products Ltd., Poona. The polymer was fractionated into three main fractions without any purification from benzene solution at 25°C with the addition of acetone as non-solvent. Further each fraction was refractionated at least into two fractions. The samples were dried in vacuo to constant weight and stored in vacuum desiccator in cold. The molecular weight of the samples used in this work were calculated from the intrinsic viscosities, $[\eta]$ measured in benzene solution at 25°C . The relation between intrinsic viscosity ($[\eta]$ in dl/gm) and molecular weight, \bar{M}_w as $[\eta] = 63.28 \times 10^{-5} \bar{M}_w^{0.62}$ was determined

in this work (described in detail in the next section) using light scattering values of \bar{M}_w in benzene solution for five polychloroprene fractions. The data for intrinsic viscosity and molecular weight of the samples used in this work are given in Table 2.3.

2.5.2 Polybutadiene

The sample poly(cis 1,4 butadiene) (PB) was obtained from Polysciences, Inc. Warrington, Pennsylvania, U.S.A. The polymer was fractionated in a similar way as of polychloroprene from benzene solution at 25°C with addition of acetone as non-solvent. The samples were dried in vacuo to constant weight and stored in cold and dark place under a vacuum desiccator. The molecular weight of the polybutadiene samples used in this work for zero shear viscosity measurements was calculated from the intrinsic viscosities measured in benzene solution at 25°C ($[\eta]$ in dl/gm). The \bar{M}_w - $[\eta]$ relation was determined in this work as $[\eta] = 16.88 \times 10^{-5} \bar{M}_w^{0.748}$ (described in detail in the next section) using the light scattering values of \bar{M}_w in cyclohexane solution for six polybutadiene fractions. The data for intrinsic viscosity, $[\eta]$ and viscosity average molecular weight, \bar{M}_v of the samples used in this work are listed in Table 2.4.

Table 2.3

Values of intrinsic viscosity and molecular weight for the polychloroprene samples

Sample	Solvent	Temperature (°C)	$[\eta]$ dl/gm	$\bar{M}_v \times 10^{-5}$
PCF1B	Benzene	25	2.12	4.85
	Benzene	45.5	2.42	
	Cyclohexane	45.5	0.56	
PCF2A	Benzene	25	1.47	2.69
	Benzene	45.5	1.66	
	Cyclohexane	45.5	0.41	
PCF2B	Benzene	25	1.10	1.68
	Butanone	25	0.38	
PCF2C	Benzene	25	1.00	1.44
	Butanone	25	0.35	
PCF3A	Benzene	25	0.85	1.11
	Benzene	45.5	0.94	
	Cyclohexane	45.5	0.27	
PCF3B	Benzene	25	0.79	0.99
	Butanone	25	0.29	

Table 2.4

Values of intrinsic viscosity and molecular weight for polybutadiene samples

Samples	Solvent	Temperature (°C)	$[\eta]$ (dl/gm)	$\bar{M}_v \times 10^{-5}$
PB2F1	Benzene	32	3.80	6.17
	Benzene	25	3.62	
	Benzene	20.5	3.40	
	Isobutyl acetate	20.5	1.03	
	Dioxane	20.2	1.03	
PB2F2	Benzene	32	2.00	2.61
	Benzene	25	1.90	
	Benzene	20.5	1.82	
	Isobutyl acetate	20.5	0.68	
	Dioxane	20.2	0.68	
PB2F3	Benzene	32	1.32	1.54
	Benzene	25	1.28	
	Benzene	20.5	1.24	
	Isobutyl acetate	20.5	0.52	
	Dioxane	20.2	0.52	

2.6 Determination of Weight Average Molecular Weight of Polychloroprene and Polybutadiene Fractions by Light Scattering Method

The weight average molecular weight of polychloroprene and polybutadiene (100% cis) fractions were determined with a Brice-Phoenix light scattering photometer with monochromatic blue light of wavelength 4360 Å. The equation for calculating molecular weight from light scattering data is

$$(KC/R_{\theta}) = 1/\bar{M}_w P(\theta) + 2 B c \quad (2.19)$$

where R_{θ} = measured Rayleigh ratio at angle θ to the incident beam

\bar{M}_w = weight average molecular weight of the scattering polymer

$P(\theta)$ = particle scattering factor

B = second virial coefficient of the system under study

c = concentration in gm/ml

$$K = \frac{2 \pi^2 n_1^2 (dn/dc)^2}{N_a \lambda^4}$$

where N_a = Avogadro's number

* λ = wavelength of the incident light in vacuo

Experimentally determined quantities were Rayleigh ratios, R_{θ} , evaluated from the galvanometer deflection, refractive index gradient, dn/dc , the refractive index of the solvent, n_1 and wavelength, λ .

Measurement of R_{θ} : An optically homogeneous cylindrical cell having flat entrance and exit windows and no cement joints was used. Black paint was applied at the frosted semicircular part of the cell to avoid back reflection. The primary intensity data for each solution at each angle θ was the galvanometer deflections. The value of R_{θ} of the above equation (2.19) was calculated by means of the formula

$$R_{\theta} = \frac{TDakn_1}{1.045 \pi h} \cdot \frac{R_w}{R_c} \left\{ \frac{\sin \theta}{1 + \cos \theta} 2_{\theta} \left[(F G_{\theta}/G_o)_{\text{soln}} - (F G_{\theta}/G_o)_{\text{solv}} \right] - \frac{I}{20} \right\} \quad (2.20)$$

where $TD = 0.340$, the product of the diffuse transmittance of the opal glass reference standard and a diffuser correction factor

h = slit width (0.40 cm)

$R_w/R_c = 1.067$, a factor relating to the geometry and optics of the instrument

- $a = 0.0211$, a constant relating on every day working standard to the opal reference standard
 $k = 1$, the ratio of the 90° scattering of a solution of fluorescence in the square cell to the 90° scattering of the same solution in the cylindrical cell
 G_0 = observed galvanometer deflection at 0° angle
 G_θ = observed galvanometer deflection when the phototube is an angle θ to the incident beam
 F = the product of the transmittance of the neutral filters which were used
 $0.05 I'$ = correction for the back reflection (= 0 for our case)

Neutral filters were calibrated for transmission values for light of wavelength 4360 \AA .

The calibration of the photometer was checked by taking measurements with pure benzene and toluene and the values for R_{90} were compared with the values of Edsall and Doty for benzene (49.9×10^{-6}) and of Maron and Low for toluene (60.3×10^{-6})⁹⁸. Due corrections were made for the difference between the experimental and literature values.

Refractive Index Gradient Measurement: The refractive index gradient, dn/dc for polychloroprene and polybutadiene fractions in benzene and cyclohexane solutions respectively was determined with a Rayleigh Interference Diffractational Refractometer (Hilger Watts, England) with a single piece two compartment cell. The instrument was calibrated with aqueous sodium chloride solution at room temperature ($\sim 25^{\circ}\text{C}$). The dn/dc values for polychloroprene in benzene solution and polybutadiene in cyclohexane solution were obtained as 0.042 and 0.114 $(\text{gm/ml})^{-1}$ respectively.

The weight average molecular weight, \bar{M}_w for the polychloroprene and polybutadiene fractions was estimated using benzene and cyclohexane as solvents respectively. The solution was clarified by filtration through $3\text{-}\mu$, $1.5\text{-}\mu$, $0.45\text{-}\mu$ and $0.30\text{-}\mu$ Millipore filters in succession. The results for light scattering measurements for polychloroprene and polybutadiene samples are shown in Tables 2.5 and 2.6 respectively and the corresponding Debye's plots, Kc/R_{90} versus c , employed to estimate the value of the \bar{M}_w are shown respectively in Figs. 2.8 and 2.9. The dissymmetry ratios I_{45}/I_{135} were evaluated to obtain the particle scattering factor, $P(\theta)$ for correction of the light

Table 2.5

Summary of results for light scattering measurements of polychloroprene fractions in benzene solution at room temperature ($\sim 25^{\circ}\text{C}$)

$$K = 3.6076 \times 10^{-8} \quad dn/dc = 0.042 \text{ (gm/ml)}^{-1}$$

Fractions	$\frac{1 \times 10^5}{\bar{M}_w P(\theta)}$	Z_0	$1/P(\theta)$	$\bar{M}_w \times 10^{-5}$
PC2F1A	0.17	1.88	1.70	10.0
PC2F1B	0.29	1.70	1.52	5.24
PC2F2	0.54	1.62	1.44	2.67
PC2F1C	0.61	1.60	1.43	2.34
PC2F3	1.51	1.45	1.33	0.88

Table 2.6

Summary of results for light scattering measurements of polybutadiene fractions in cyclohexane solution at room temperature ($\sim 25^{\circ}\text{C}$)

$$K = 2.39028 \times 10^{-7} \quad dn/dc = 0.114 \text{ (gm/ml)}^{-1}$$

Fractions	$\frac{1 \times 10^5}{\bar{M}_w P(\theta)}$	Z_0	$1/P(\theta)$	$\bar{M}_w \times 10^{-5}$
PB1F1A	0.22	1.50	1.37	6.23
PB1F1B	0.37	1.42	1.32	3.57
PB1F2	0.39	1.40	1.30	3.33
PB1F3	0.56	1.37	1.27	2.27
PB1F4	0.77	1.25	1.19	1.54
PB1F1C	0.95	1.22	1.16	1.22

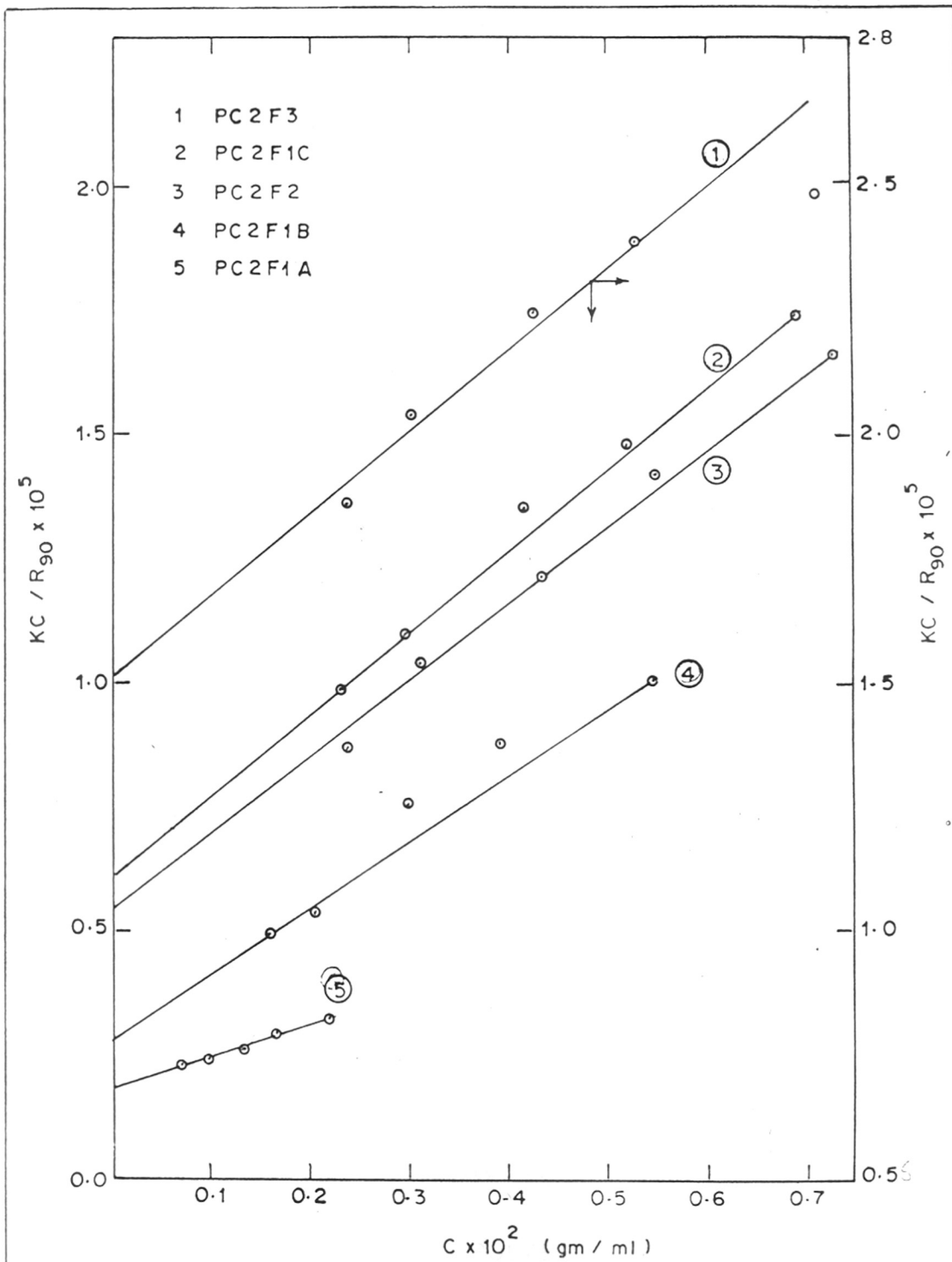


FIG. 2-8. DEBYE'S PLOT FOR POLYCHLOROPRENE FRACTIONS IN BENZENE

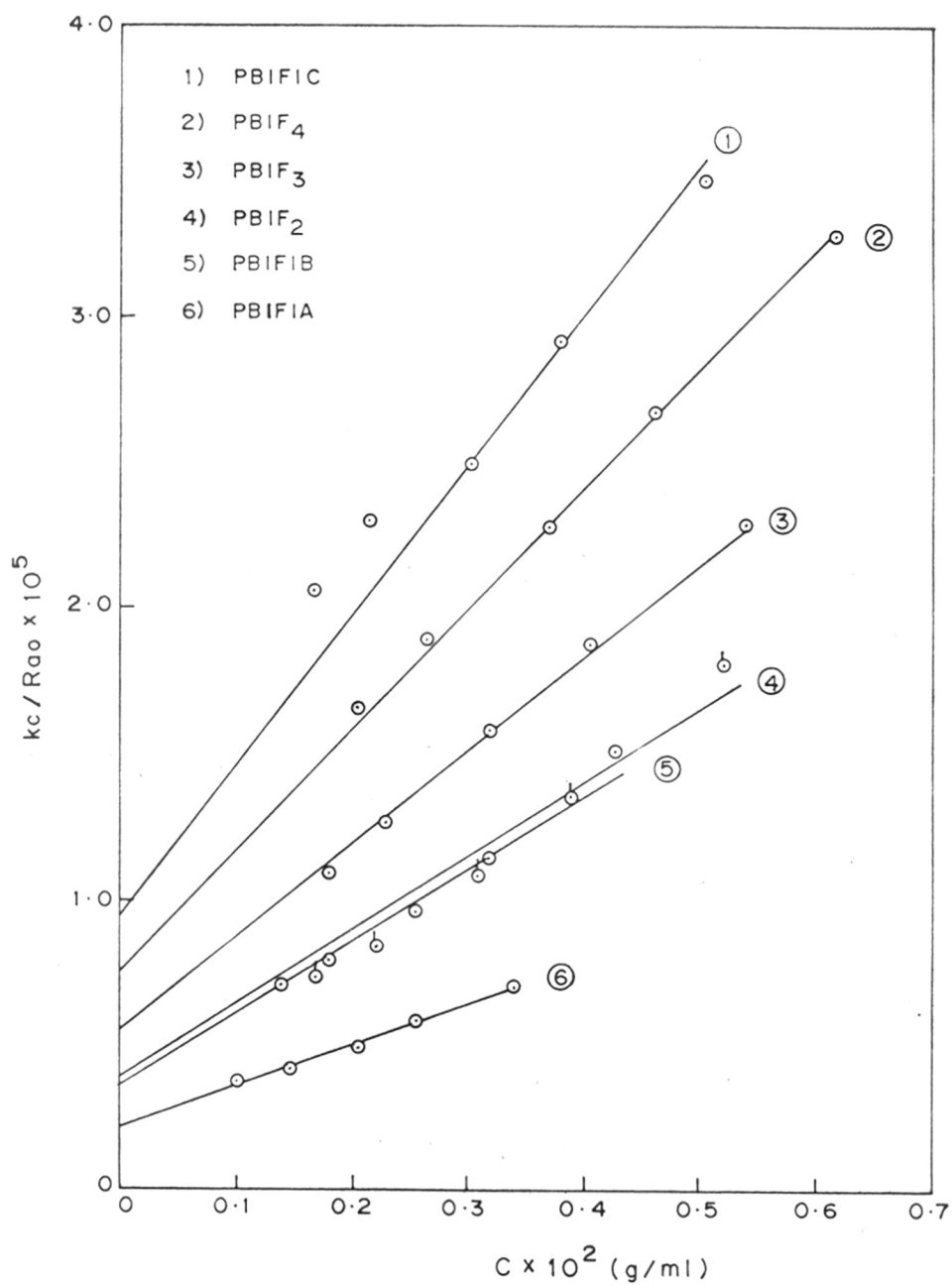


FIG. 2.9 DEBYE'S PLOT FOR POLYBUTADIENE FRACTIONS IN CYCLOHEXANE.

scattering data, Z_0 , the extrapolated value obtained for dissymmetry at infinite dilution, given in the same table along with $1/P(\theta)$.

2.7 Measurement of Intrinsic Viscosity

The viscosity of polymer samples in different solvents and at different temperatures was measured with Ubbelohde dilution viscometer. The flow time of solvents at all the experimental temperatures was more than 200 seconds and hence no kinetic energy correction was made. The viscometer was kept immersed in a thermostatic water bath maintained at the requisite temperature (20.2° , 20.5° , 25° and 45.5°C) with an accuracy of $\pm 0.02^\circ\text{C}$. Intrinsic viscosity, $[\eta]$ was obtained by extrapolation to infinite dilution, according to the relation $\eta_{sp}/c = [\eta] + k'[\eta]^2 c$, where k' is the Huggins constant. The typical plots of η_{sp}/c as a function of concentration for different fractions of polychloroprene and polybutadiene in different solvents and temperatures are shown in Figs. 2.10 to 2.18, and the corresponding data for intrinsic viscosity, $[\eta]$ for polychloroprene and polybutadiene samples are given in Tables 2.7 and 2.8 respectively.

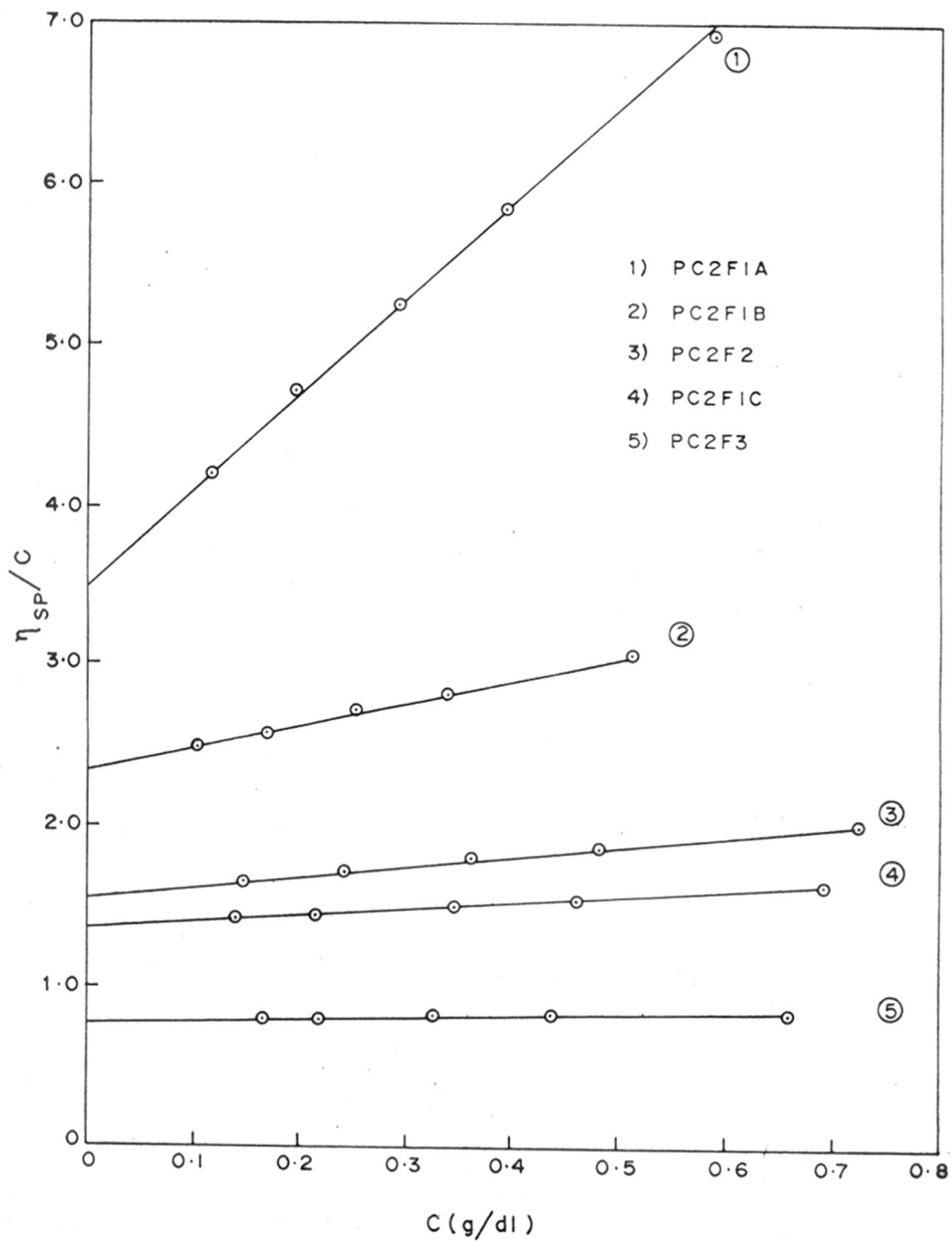


FIG. 2-10 PLOTS OF η_{SP}/C vs C FOR POLYCHLOROPRENE FRACTIONS IN BENZENE AT 25°C

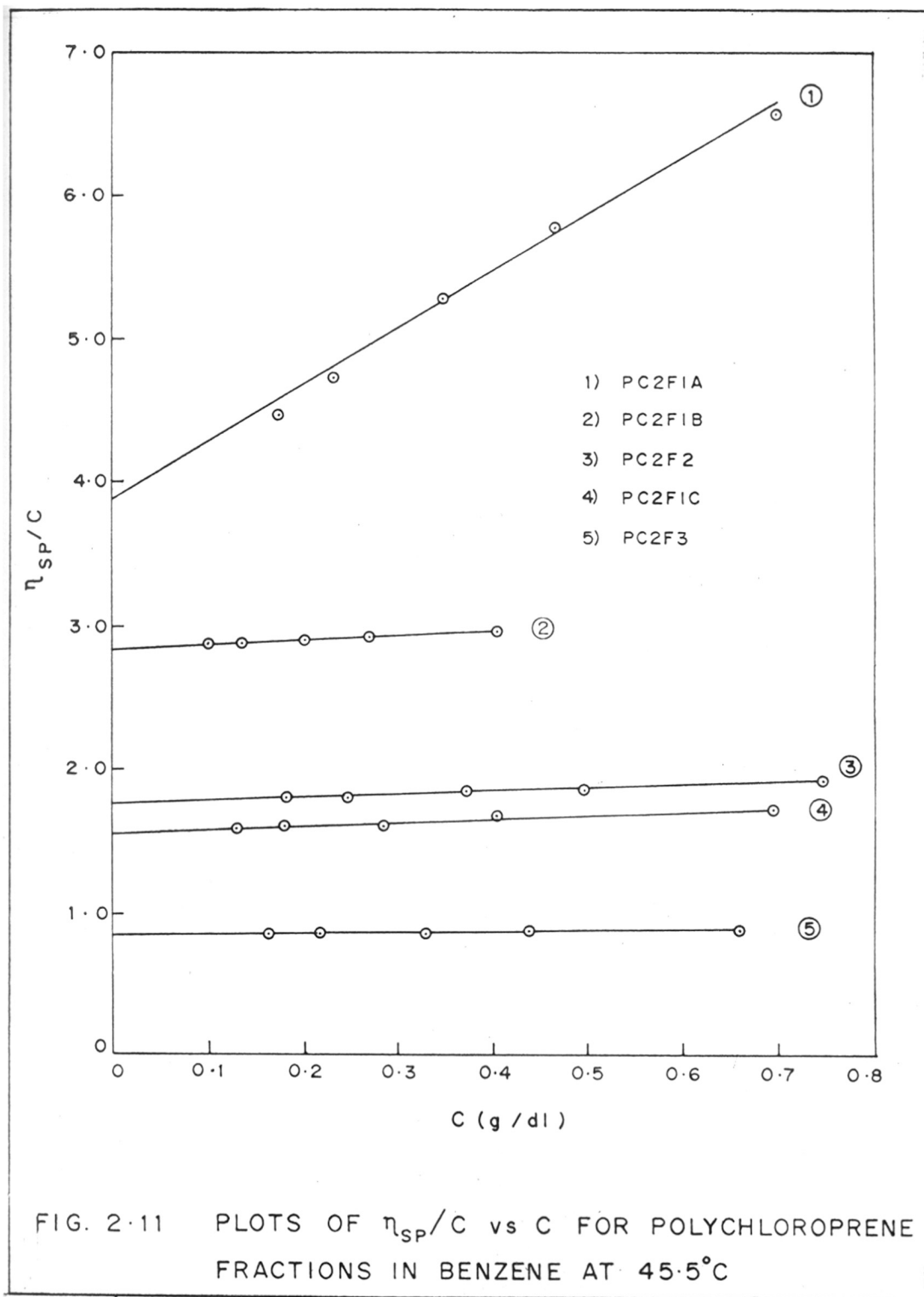


FIG. 2.11 PLOTS OF η_{sp}/C vs C FOR POLYCHLOROPRENE FRACTIONS IN BENZENE AT 45.5°C

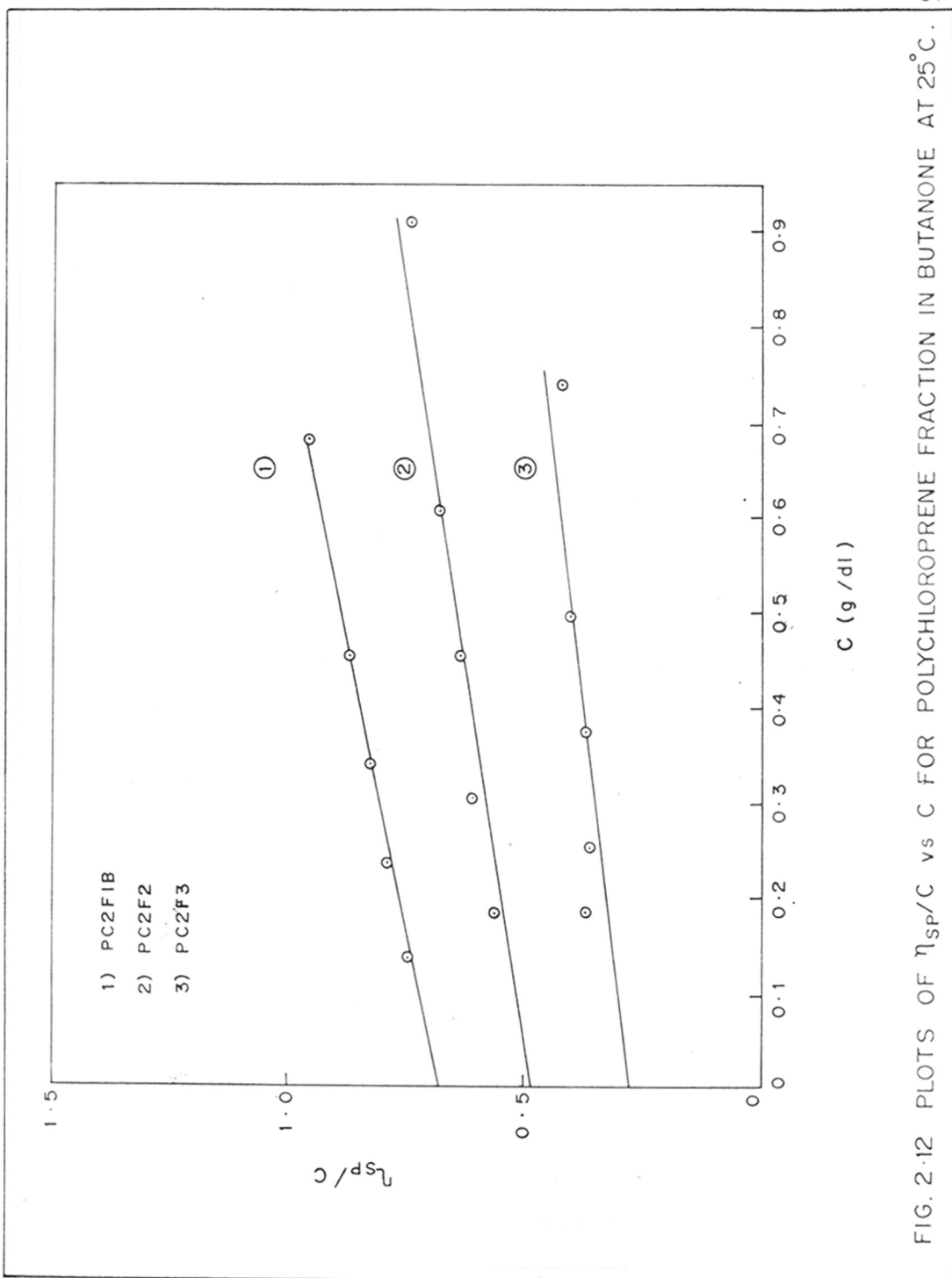


FIG. 2.12 PLOTS OF η_{sp}/C vs C FOR POLYCHLOROPRENE FRACTION IN BUTANONE AT 25°C.

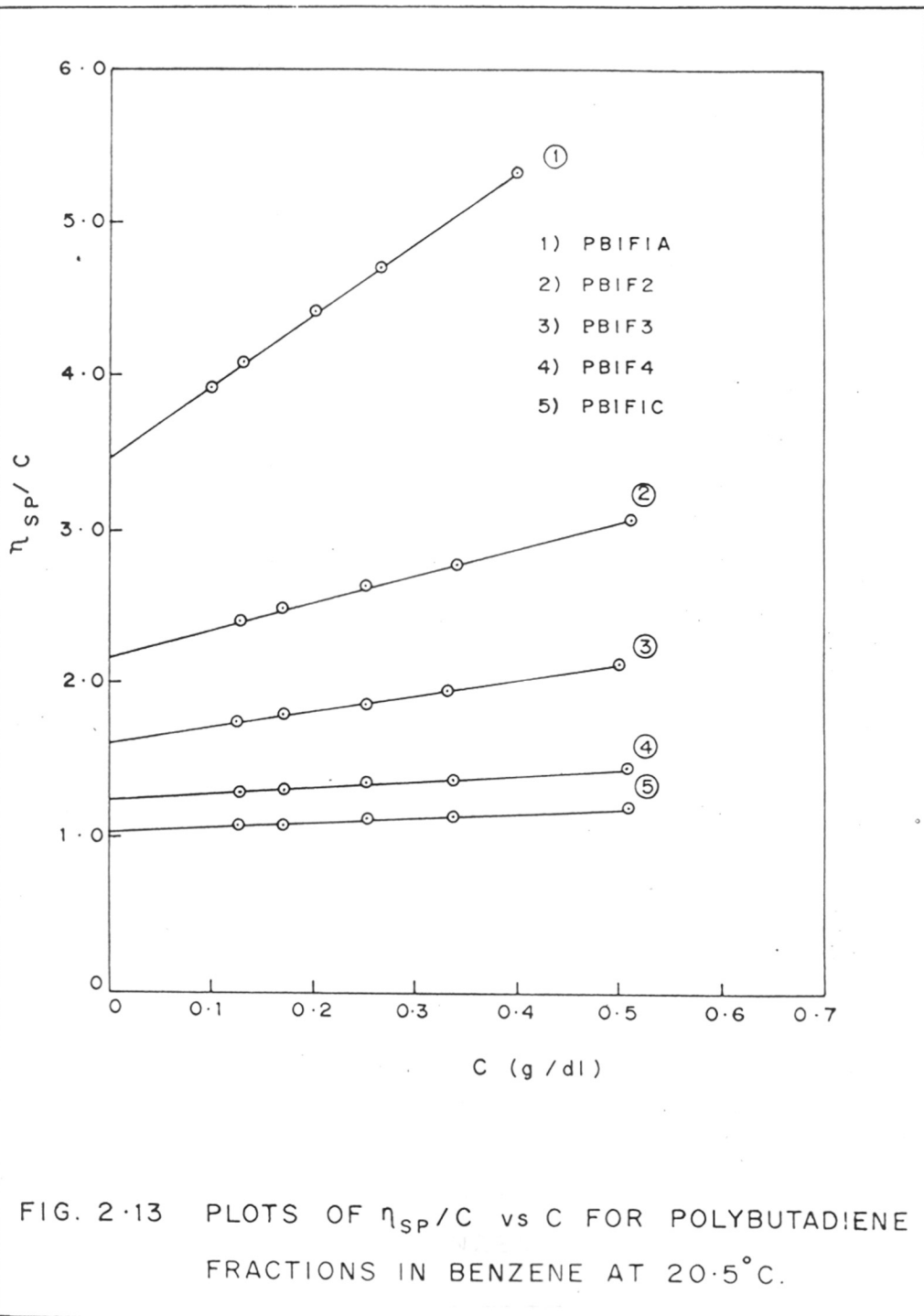


FIG. 2.13 PLOTS OF η_{SP}/C vs C FOR POLYBUTADIENE FRACTIONS IN BENZENE AT 20.5°C.

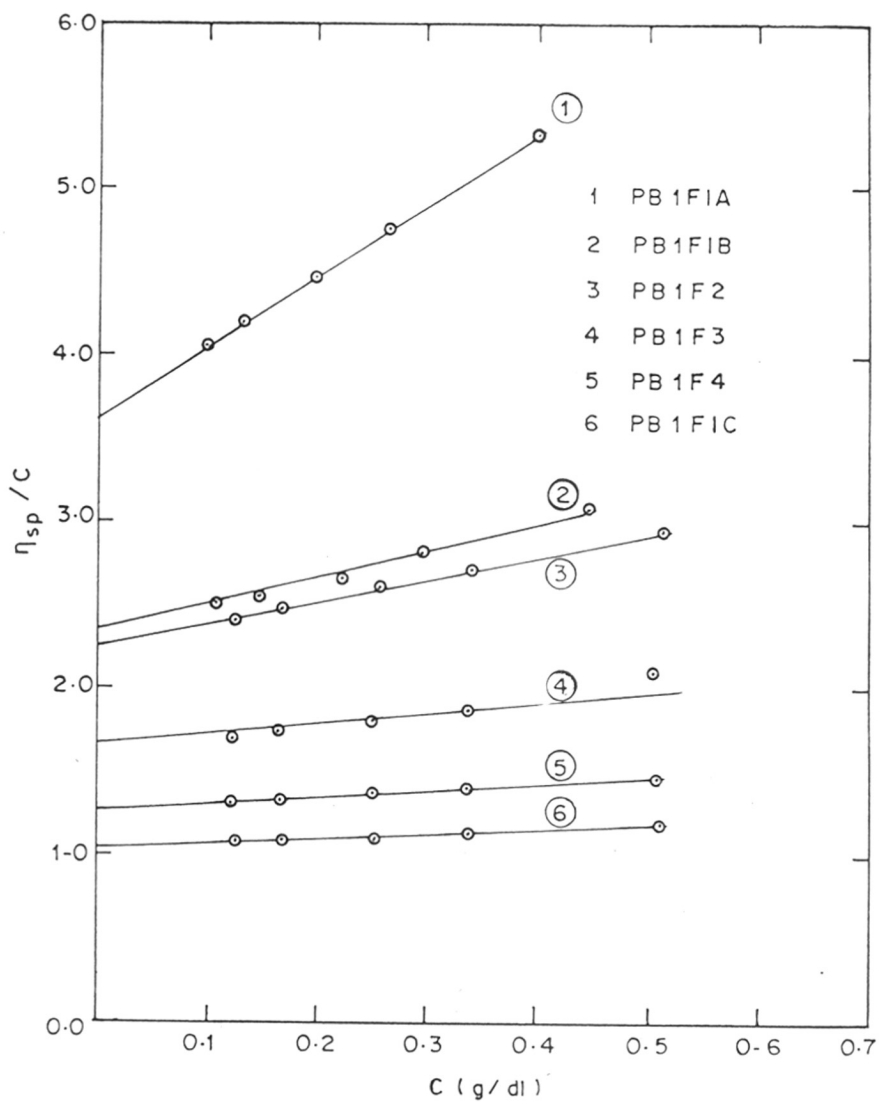


FIG. 2.14. PLOTS OF η_{sp}/C vs C FOR POLYBUTADIENE FRACTIONS IN BENZENE AT 25°C

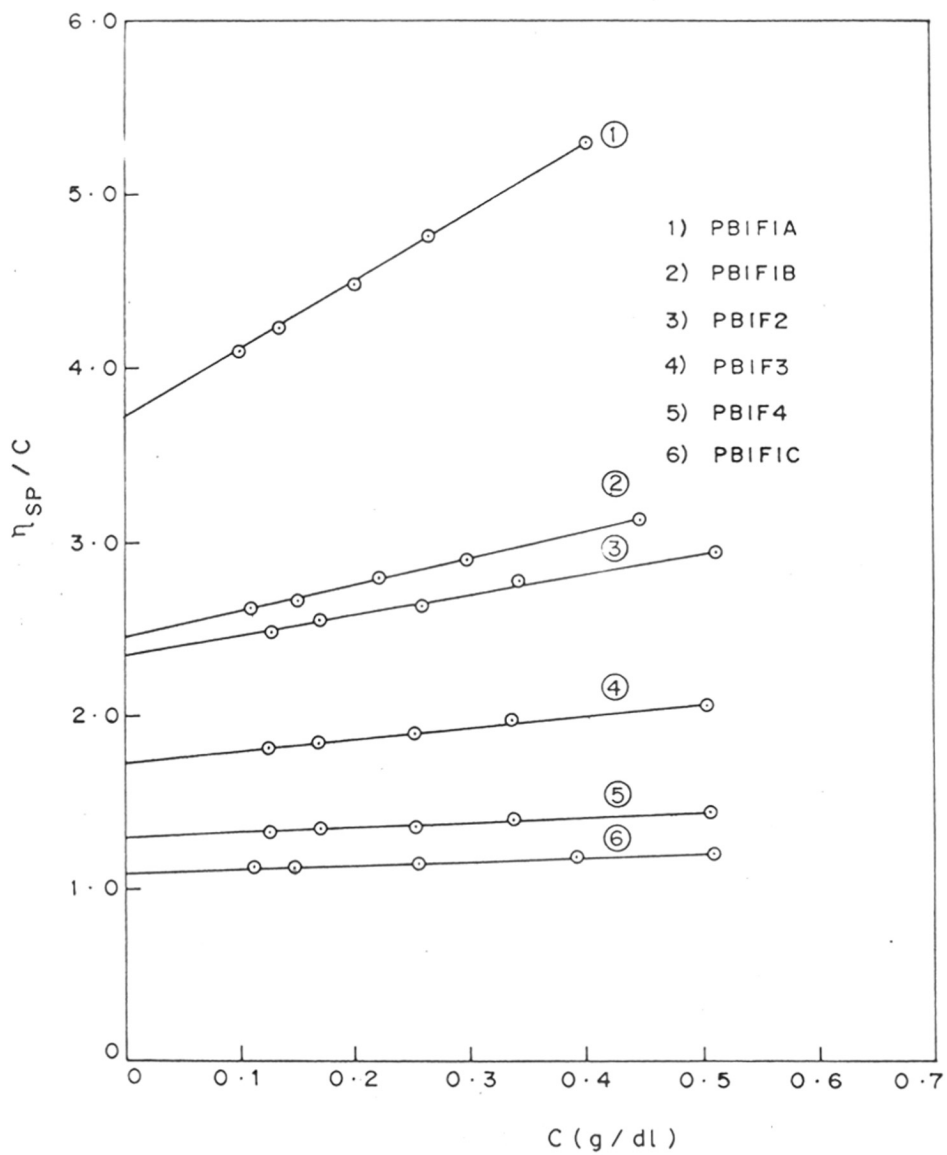


FIG. 2.15 PLOTS OF η_{sp}/C vs C FOR POLYBUTADIENE IN BENZENE AT 32°C.

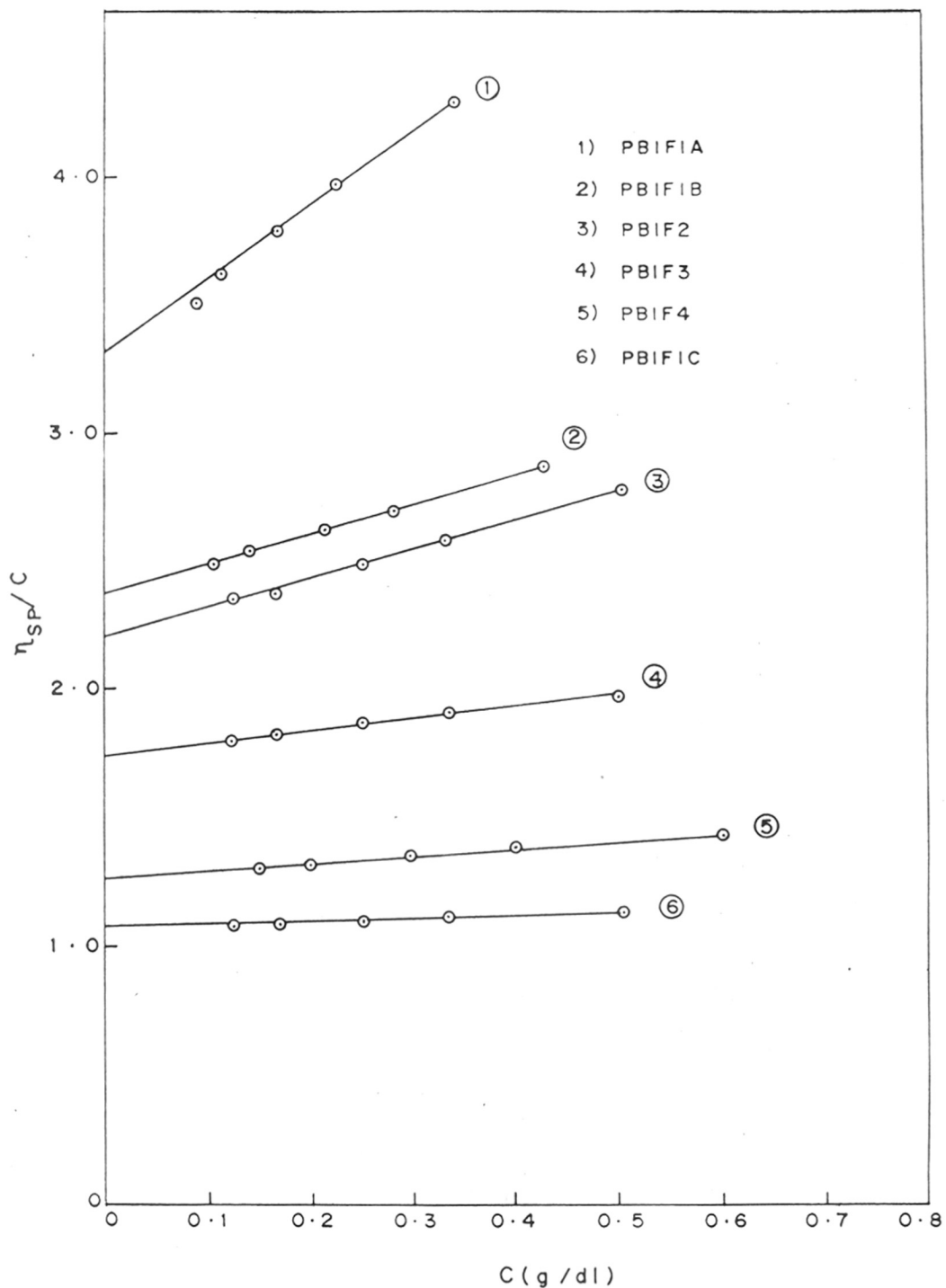
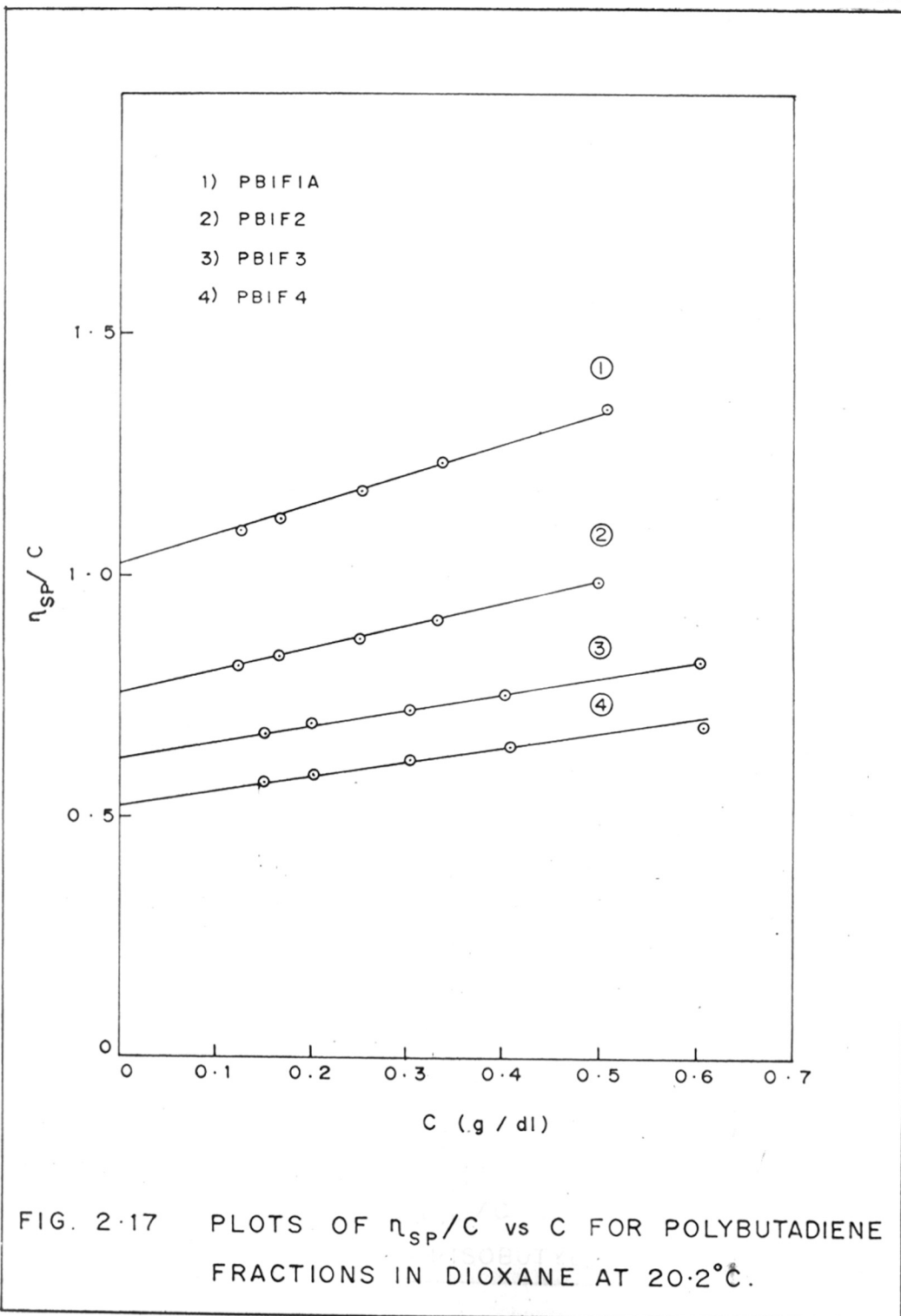


FIG. 2-16 PLOTS OF η_{sp}/C vs C FOR POLYBUTADIENE FRACTIONS IN CYCLOHEXANE AT 25°C.



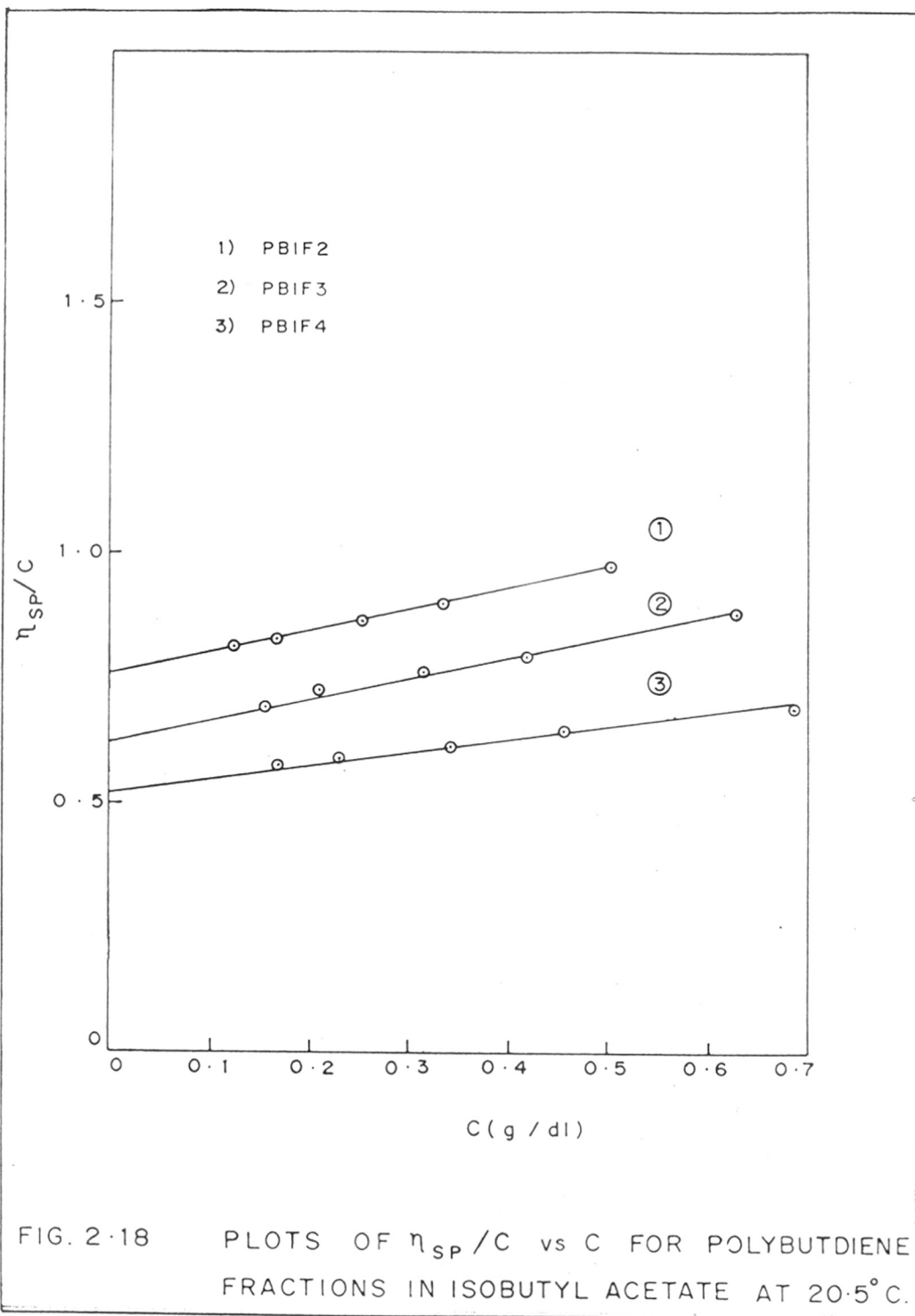


Table 2.7

Summary of results for intrinsic viscosity measurements in different solvents and temperatures for polychloroprene fractions.

Fractions	$\bar{M}_w \times 10^{-5}$	$[\eta]^{25}$ Benzene (dl/gm)	$[\eta]^{45.5}$ Benzene (dl/gm)	$[\eta]^{25}$ Butanone (dl/gm)
PC2F1A	10.0	3.50	3.90	-
PC2F1B	5.24	2.34	2.84	0.68
PC2F2	2.67	1.54	1.76	0.48
PC2F1C	2.34	1.36	1.55	-
PC2F3	0.88	0.77	0.84	0.28

Table 2.8

Summary of results for intrinsic viscosity measurements in different solvents and temperatures for polybutadiene fractions.

Fractions	\bar{M}_w $\times 10^{-5}$	$[\eta]^{20.5}$ Benzene (dl/gm)	$[\eta]^{25}$ Benzene (dl/gm)	$[\eta]^{32}$ Benzene (dl/gm)	$[\eta]^{25}$ Cyclo- hexane (dl/gm)	$[\eta]^{20.5}$ I B A (dl/gm)	$[\eta]^{20.2}$ Dioxane (dl/gm)
PB1F1A	6.23	3.48	3.62	3.72	3.40	-	1.03
PB1F1B	3.57	-	2.40	2.44	2.37	-	-
PB1F2	3.33	2.18	2.29	2.34	2.20	0.76	0.76
PB1F3	2.27	1.62	1.69	1.72	1.74	0.62	0.62
PB1F4	1.54	1.27	1.29	1.30	1.26	0.52	0.52
PB1F1C	1.22	1.06	1.07	1.08	1.08	-	-

2.8 Relationship between Intrinsic Viscosity and Molecular Weight

The relationship between intrinsic viscosity, $[\eta]$ and molecular weight, \bar{M}_w for two polymers, polychloroprene and polybutadiene, in both good and θ solvents was determined according to the Mark-Hauwink equation

$$[\eta] = K \bar{M}_w^a$$

A set of constants K and a for the polymers in each solvent at a particular temperature was evaluated by comparing $[\eta]$ of five or six fractions with their molecular weight determined by the light scattering method. The data of $[\eta]$ and \bar{M}_w for polychloroprene and polybutadiene fractions (as given in Tables 2.7 and 2.8) are shown as log-log plots in Figs. 2.19 and 2.20 respectively. In case of polychloroprene, the data of $[\eta]$ and \bar{M}_w in cyclohexane and butanone were taken from Table 2.3 (shown by the symbol \odot in Fig. 2.19). The straight lines drawn through these points were computed by the least square method and the constants K and a were evaluated from intercepts and slopes of the lines. The results are summarized in Table 2.9. It should be mentioned that Cooper and coworkers⁹⁹ had

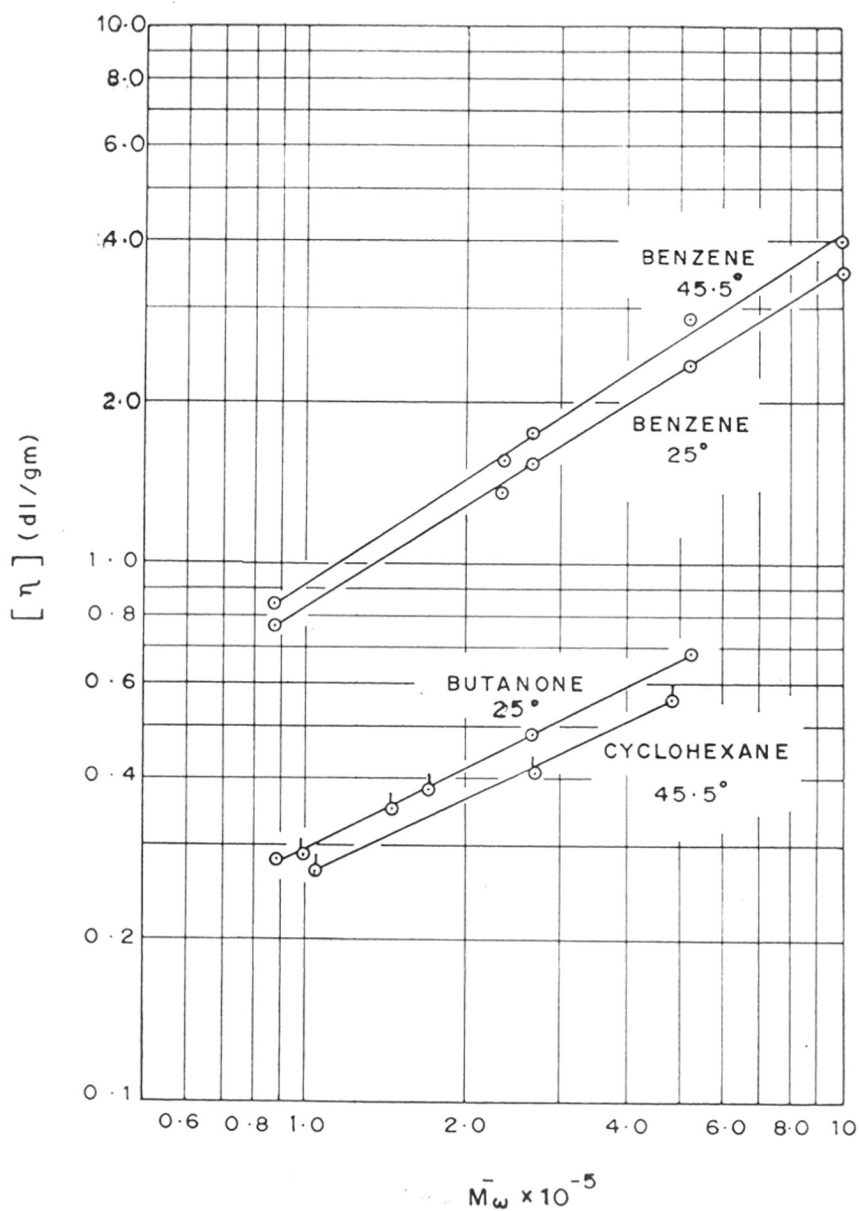


FIG. 2-19 LOG-LOG PLOTS OF INTRINSIC VISCOSITY vs MOLECULAR WEIGHT FOR POLYCHLOROPRENE SAMPLES.

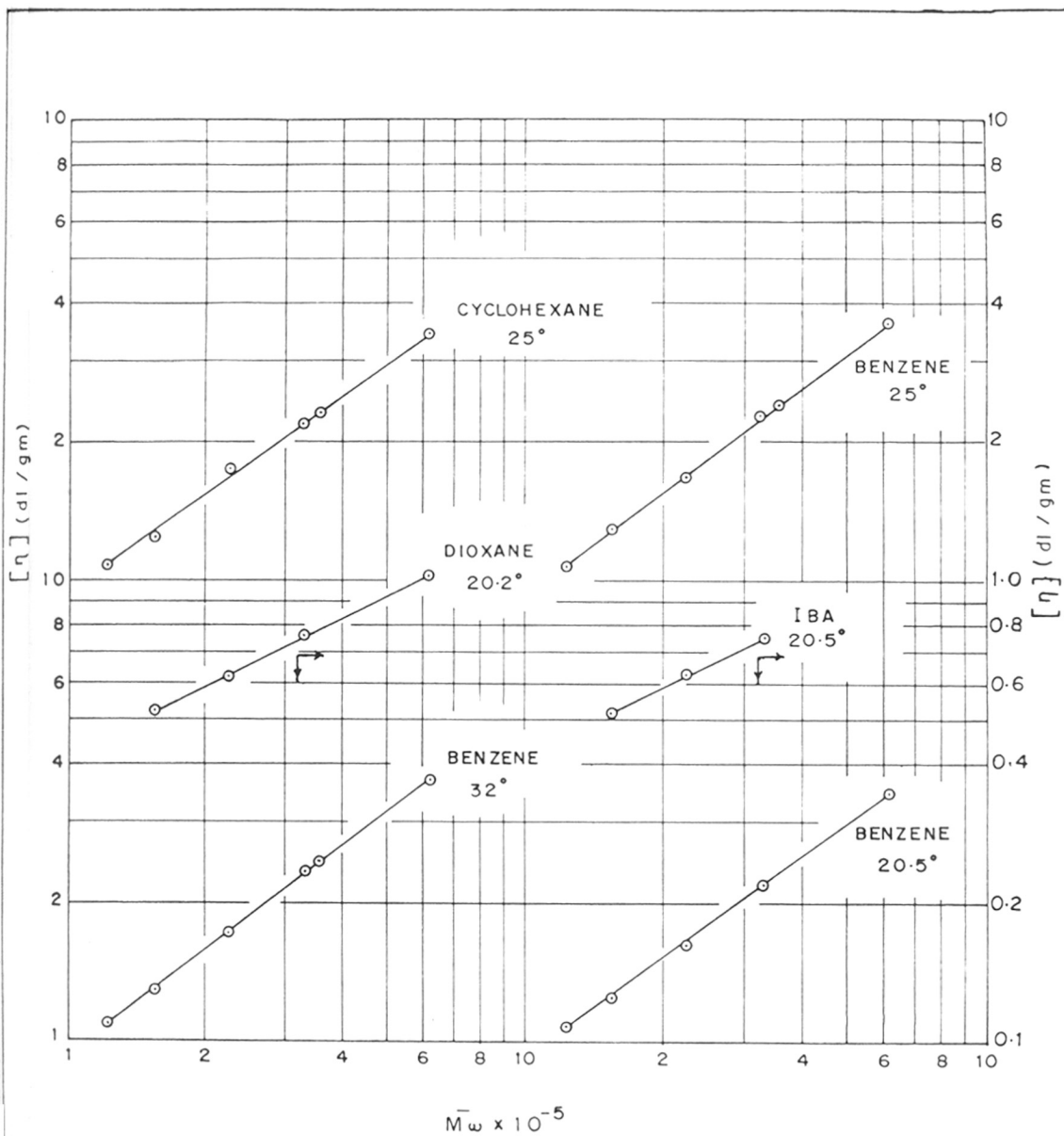


FIG. 2.20 LOG-LOG PLOTS OF INTRINSIC VISCOSITY vs MOLECULAR WEIGHT FOR POLYBUTADIENE SAMPLES.

Table 2.9

The values of K and a for polychloroprene and polybutadiene in good and θ solvents.

Polymer	Solvent	Temperature (°C)	K x 10 ⁵ (dl/gm)	a
Polychloroprene	Benzene	25	63.28	0.62
		45.5	57.32	0.64
	Butanone	25	89.50	0.50
	Cyclohexane	45.5	13.92	0.50
Polybutadiene	Benzene	20.5	21.30	0.73
		25	16.88	0.74 _a
		32	14.88	0.76
	Cyclohexane	25	30.52	0.70
	Dioxane	20.2	14.15	0.50
	IBA	20.5	14.15	0.50

obtained $[\eta] - \bar{M}_w$ relation for polybutadiene (100% cis) with $[\eta]$ measured at 32°C in benzene as $[\eta] = 14.5 \times 10^5 \bar{M}_w^{0.76}$ which is in excellent agreement with that obtained in this work.

2.9 Zero Shear Viscosity of Polychloroprene Samples in Benzene and Cyclohexane Solutions at 45.5°C

The zero shear viscosity, η^0 of three polychloroprene samples, namely PCF1B, PCF2A and PCF3A has been measured in benzene and cyclohexane solutions at 45.5°C. Benzene was used as a good solvent and cyclohexane (45.5°C) was used as a θ solvent. As mentioned earlier Brookfield LVT viscometer was used to measure the viscosity of the concentrated polymer solutions, whereas a Maron-type capillary viscometer with a continuously varying pressure head was used for the measurement of viscosity of solvents and comparatively less concentrated (5% and below) solutions. In Brookfield viscometer about 63 cc solution was used in the stainless steel cell (35 mm diameter) and the cell was kept immersed in a water thermostat maintained at $45.5 \pm 0.02^\circ\text{C}$. The viscosity for each solution was measured at least with 4 different speeds and the plot of η versus speed (r.p.m.) was extrapolated to zero for the determination of the zero shear viscosity.

In the capillary viscometer about 15 cc solution was used and through the capillary part of the instrument water was circulated from a thermostat maintained at $45.5^{\circ}\text{C} \pm 0.02^{\circ}\text{C}$. The apparent viscosity, η_a was calculated by the following equation:

$$1/\eta_a = -(m/B) [1 + \{1/(9.212 \text{ m}^2)\} dm/dt]$$

The zero shear viscosity, η^0 was determined by extrapolating the rate of shear to zero.

The results for zero shear viscosity measurements are summarized in Tables 2.10 to 2.15.

2.10 Zero Shear Viscosity, η^0 for Polychloroprene Samples in Benzene and Butanone Solutions at 25°C

The zero shear viscosity, η^0 of three more polychloroprene samples, PCF2B, PCF2C and PCF3B in both good and θ solvents has been determined in the same way as described earlier. The three polymer samples have comparatively lower molecular weights (1.68×10^5 , 1.44×10^5 and 0.99×10^5 respectively) than the earlier ones. Benzene at 25°C was used here as a good solvent whereas butanone (25°C) was used as a θ solvent. The results for zero shear viscosity measurements are given in Tables 2.16 to 2.21.

Table 2.10

Summary of results for zero shear viscosity, η° measurements for polychloroprene sample PCF1B in benzene solution at 45.5°C.

$$(\bar{M}_v = 4.85 \times 10^5), [\eta] = 2.42 \text{ dl/gm}, K_M = 0.071$$

Conc. at 45.5°C (gm/dl)	η° (poise)	η°_{sp}	$c[\eta]$	$\bar{\eta}$	$K_M c[\eta]$
0.00	$0.473 \times 10^{-2}{}^a$	-	-	-	-
1.26	$2.56 \times 10^{-2}{}^a$	4.41	3.05	1.45	0.22
2.53	$8.40 \times 10^{-2}{}^a$	16.76	6.12	2.74	0.43
5.08	4.25×10^{-1}	88.85	12.29	7.23	0.87
7.57	1.46×10^0	307.7	18.32	16.79	1.30
10.0	3.79×10^0	800.3	24.20	33.07	1.72

a : Capillary viscometer with varying pressure head was used

Table 2.11

Summary of results for zero shear viscosity, η^0
 measurements for polychloroprene sample PCF1B in
 cyclohexane solution at 45.5°C

$$(\bar{M}_v = 4.85 \times 10^5), [\eta] = 0.56 \text{ dl/gm}, K_M = 0.497$$

Conc. at 45.5°C (dl/gm)	η^0 (Poise)	η_{sp}^0	$c[\eta]$	$\bar{\eta}$	$K_M c[\eta]$
0.00	$0.648 \times 10^{-2}^a$	-	-	-	-
2.02	$2.91 \times 10^{-2}^a$	4.50	1.13	3.98	0.56
4.05	2.12×10^{-1}	31.72	2.27	13.98	1.13
5.42	6.35×10^{-1}	96.99	3.03	31.96	1.51
8.12	3.63×10^0	559.2	4.55	123.0	2.26
10.4	1.14×10^1	1758	5.82	301.8	2.89

a : Capillary viscometer with varying pressure
 head was used

Table 2.12

Summary of results for zero shear viscosity, η^0 measurements for polychloroprene sample PCF2A in benzene solution at 45.5°C.

$$(\bar{M}_V = 2.69 \times 10^5), [\eta] = 1.66 \text{ dl/gm}, K_M = 0.085$$

Conc. at 45.5°C (dl/gm)	η^0 (Poise)	η_{sp}^0	$c[\eta]$	$\bar{\eta}$	$K_M c[\eta]$
0.00	$0.473 \times 10^{-2} \text{ }^a$	-	-	-	-
2.55	$5.20 \times 10^{-2} \text{ }^a$	9.99	4.23	2.36	0.36
5.03	1.99×10^{-1}	41.07	8.35	4.92	0.71
7.51	5.55×10^{-1}	116.3	12.47	9.33	1.06
9.98	1.18×10^0	248.5	16.57	15.00	1.41
15.0	6.22×10^0	1314	24.90	52.77	2.12
17.7	1.35×10^1	2853	29.38	97.10	2.50
19.9	2.47×10^1	5221	33.03	158.05	2.81
24.8	7.17×10^1	15,157	41.17	368.17	3.50
27.4	1.44×10^2	30,443	45.48	669.31	3.87

a : Capillary viscometer with varying pressure head was used

Table 2.13

Summary of results for zero shear viscosity, η^0 measurements for polychloroprene sample PCF2A in cyclohexane solution at 45.5°C.

$$(\bar{M}_V = 2.69 \times 10^5), [\eta] = 0.41 \text{ dl/gm}, K_M = 0.497$$

Conc. at 45.5°C (gm/dl)	η^0 (Poise)	η^0_{sp}	$c[\eta]$	$\bar{\eta}$	$K_M c[\eta]$
0.00	$0.648 \times 10^{-2}^a$	-	-	-	-
1.89	$2.60 \times 10^{-2}^a$	3.01	0.77	3.88	0.38
3.85	1.03×10^{-1}	14.89	1.58	9.43	0.78
5.82	3.00×10^{-1}	45.30	2.39	18.99	1.19
7.87	7.80×10^{-1}	119.4	3.23	36.99	1.60
11.9	4.00×10^0	616.3	4.88	126.3	2.42
15.8	1.55×10^1	2391	6.48	369.1	3.22
19.0	5.37×10^1	8286	7.79	1064	3.87
21.9	1.07×10^2	16,511	8.98	1839	4.46
27.6	5.03×10^2	77,622	11.32	6859	5.63

a : Capillary viscometer with varying pressure head was used

Table 2.14

Summary of results for zero shear viscosity, η^0 measurements for polychloroprene samples PCF3A in benzene solution at 45.5°C.

$$(\bar{M}_V = 1.11 \times 10^5), [\eta] = 0.94 \text{ dl/gm}, K_M = 0.099$$

Conc. at 45.5°C (gm/dl)	η^0 (Poise)	η_{sp}^0	c[η]	$\bar{\eta}$	$K_M c[\eta]$
0.00	$0.473 \times 10^{-2}{}^a$	-	-	-	-
2.45	$2.41 \times 10^{-2}{}^a$	4.09	2.30	1.78	0.23
5.19	$7.60 \times 10^{-2}{}^a$	15.07	4.88	3.09	0.48
10.1	4.13×10^{-1}	86.31	9.49	9.09	0.94
15.0	1.54×10^0	324.6	14.10	23.02	1.40
20.1	4.50×10^0	950.4	18.89	50.30	1.87
25.1	1.25×10^1	2642	23.59	111.96	2.34
30.0	2.80×10^1	5919	28.20	209.9	2.79
35.1	6.22×10^1	13,149	32.99	398.5	3.27

a : Capillary viscometer with varying pressure head was used.

Table 2.15

Summary of results for zero shear viscosity, η^0 measurements for polychloroprene sample PCF3A in cyclohexane solution at 45.5°C.

$$(\bar{M}_v = 1.11 \times 10^5), [\eta] = 0.27 \text{ dl/gm}, K_M = 0.497$$

Conc. at 45.5°C (gm/dl)	η^0 (Poise)	η^0_{sp}	$c[\eta]$	$\bar{\eta}$	$K_M c[\eta]$
0.00	$0.648 \times 10^{-2}{}^a$	-	-	-	-
2.50	$2.61 \times 10^{-2}{}^a$	3.03	0.67	4.49	0.33
4.87	$7.55 \times 10^{-2}{}^a$	10.65	1.31	8.10	0.65
10.5	4.55×10^{-1}	69.22	2.83	24.41	1.40
15.0	2.00×10^0	307.6	4.05	75.96	2.01
20.0	5.92×10^0	912.6	5.40	169.0	2.68
25.1	1.82×10^1	2808	6.78	414.3	3.37
30.1	4.80×10^1	7406	8.13	911.3	4.04
32.5	6.65×10^1	10,261	8.77	1169	4.36

a : Capillary viscometer with varying pressure head was used.

Table 2.16

Summary of results for zero shear viscosity, η^0
 measurements for polychloroprene sample PCF2B in
 benzene solution at 25°C.

$$(\bar{M}_V = 1.68 \times 10^5), [\eta] = 1.10 \text{ dl/gm}, K_M = 0.127$$

Conc. at 25°C (gm/dl)	η^0 (Poise)	η_{sp}^0	$c[\eta]$	$\bar{\eta}$	$K_M c[\eta]$
0.00	$0.598 \times 10^{-2}{}^a$	-	-	-	
2.54	$4.94 \times 10^{-2}{}^a$	7.26	2.79	2.60	0.35
5.53	2.46×10^{-1}	40.14	6.08	6.60	0.77
7.54	5.25×10^{-1}	86.79	8.29	10.47	1.05
10.0	1.44×10^0	239.8	11.00	21.80	1.40
15.0	6.70×10^0	1119	16.50	67.82	2.09
20.0	2.95×10^1	4932	22.00	224.18	2.79
22.9	5.86×10^1	9798	25.19	389.0	3.20

a : Capillary viscometer with varying pressure
 head was used

Table 2.17

Summary of results for zero shear viscosity, η^0 measurements for polychloroprene sample PCF2B in butanone solution at 25°C.

($\bar{M}_v = 1.68 \times 10^5$), $[\eta] = 0.38$ dl/gm, $K_M = 0.497$

Conc. at 25°C (gm/dl)	η^0 (Poise)	η^0_{sp}	$c[\eta]$	$\bar{\eta}$	$K_M c[\eta]$
0.00	$0.381 \times 10^{-2}{}^a$	-	-	-	-
2.51	$1.47 \times 10^{-2}{}^a$	2.85	0.95	2.99	0.47
4.47	$6.40 \times 10^{-2}{}^a$	15.80	1.70	9.30	0.84
7.50	3.34×10^{-1}	86.66	2.85	30.41	1.42
10.1	9.90×10^{-1}	258.8	3.84	67.43	1.91
15.0	4.79×10^0	1256	5.70	220.3	2.83
20.0	2.46×10^1	6456	7.60	849.5	3.78
24.2	7.60×10^1	19,947	9.20	2169	4.57

a : Capillary viscometer with varying pressure head was used.

Table 2.18

Summary of results for zero shear viscosity, η^0 measurements for polychloroprene sample PCF2C in benzene solution at 25°C.

$$(\bar{M}_V = 1.44 \times 10^5), [\eta] = 1.00 \text{ dl/gm}, K_M = 0.127$$

Conc. at 25°C (gm/dl)	η^0 (Poise)	η_{sp}^0	c [η]	$\bar{\eta}$	$K_M c [\eta]$
0.00	0.598×10^{-2} ^a	-	-	-	-
2.49	3.96×10^{-2} ^a	5.63	2.49	2.26	0.32
5.01	1.29×10^{-1}	20.58	5.01	4.11	0.64
7.51	3.00×10^{-1}	49.17	7.51	6.52	0.95
10.0	7.41×10^{-1}	122.9	10.00	12.29	1.27
15.2	3.64×10^0	607.7	15.20	39.93	1.93
20.1	1.35×10^1	2256	20.10	112.2	2.55
25.4	5.04×10^1	8427	25.40	331.8	3.23

a : Capillary viscometer with varying pressure head was used

Table 2.19

Summary of results for zero shear viscosity, η^0 measurements for polychloroprene sample PCF2C in butanone solution at 25°C.

$$(\bar{M}_V = 1.44 \times 10^5), [\eta] = 0.35 \text{ dl/gm}, K_M = 0.497$$

Conc. at 25°C (gm/dl)	η^0 (Poise)	η^0_{sp}	$c[\eta]$	$\bar{\eta}$	$K_M c[\eta]$
0.00	$0.381 \times 10^{-2}^a$	-	-	-	-
2.62	$1.39 \times 10^{-2}^a$	2.64	0.92	2.88	0.46
5.23	$5.20 \times 10^{-2}^a$	12.66	1.83	6.92	0.91
7.51	1.95×10^{-1}	50.10	2.63	19.05	1.31
10.0	4.90×10^{-1}	127.6	3.50	36.46	1.74
15.0	3.01×10^0	789.0	5.25	150.2	2.61
20.1	1.45×10^1	3805	7.03	541.2	3.49
25.3	4.72×10^1	12,387	8.85	1400	4.40

a : Capillary viscometer with varying pressure head was used.

Table 2.20

Summary of results for zero shear viscosity, η^0
 measurements for polychloroprene sample PCF3B in
 benzene solution at 25°C.

$$(\bar{M}_V = 0.99 \times 10^5), [\eta] = 0.79 \text{ dl/gm}, K_M = 0.127$$

Conc. at 25°C (gm/dl)	η^0 (Poise)	η_{sp}^0	$c[\eta]$	$\bar{\eta}$	$K_M c[\eta]$
0.00	0.598×10^{-2} ^a	-	-	-	-
2.50	2.38×10^{-2} ^a	2.98	1.97	1.51	0.25
5.07	7.90×10^{-2} ^a	12.21	4.00	3.05	0.51
6.75	1.90×10^{-1}	30.77	5.33	5.77	0.68
11.2	7.20×10^{-1}	119.4	8.85	13.49	1.12
15.0	1.49×10^0	248.2	11.85	20.94	1.50
20.1	4.15×10^0	693.0	15.88	43.64	2.02
23.8	8.90×10^0	1487	18.80	79.10	2.39

a : Capillary viscometer with varying pressure
 head was used

Table 2.21

Summary of results for zero shear viscosity, η^0 measurements for polychloroprene sample PCF3B in butanone solution at 25°C.

$$(\bar{M}_V = 0.99 \times 10^5), [\eta] = 0.29 \text{ dl/gm}, K_M = 0.497$$

Conc. at 25°C (gm/dl)	η^0 (Poise)	η_{sp}^0	$c[\eta]$	$\bar{\eta}$	$K_M c[\eta]$
0.00	$0.381 \times 10^{-2}{}^a$	-	-	-	-
2.52	$1.07 \times 10^{-2}{}^a$	1.81	0.73	2.47	0.36
4.76	$3.10 \times 10^{-2}{}^a$	7.14	1.38	5.17	0.69
7.08	$9.55 \times 10^{-2}{}^a$	24.07	2.05	11.72	1.02
10.0	2.90×10^{-1}	75.11	2.90	25.90	1.44
15.1	1.26×10^0	329.7	4.38	75.29	2.18
20.0	4.18×10^0	1096	5.80	188.96	2.88
25.1	1.26×10^1	3319	7.28	455.97	3.62
29.5	2.92×10^1	7663	8.55	895.73	4.25

a : Capillary viscometer with varying pressure head was used.

2.11 The Zero Shear Viscosity for Polybutadiene Samples in Good and θ Solvents

The study of zero shear viscosity, η^0 has been extended to another polymer, polybutadiene in both good and θ solvents. Dioxane (20.2°C) and isobutyl acetate (20.5°C) have been used as two θ solvents and benzene at 20.5°C as a good solvent. We have chosen this polymer because of the fact that polybutadiene is a cis compound (100% cis) and the chain of this polymer is more flexible than that of polychloroprene (probably trans compound) which was studied earlier. Besides this polychloroprene is a polar compound while polybutadiene is a non-polar one. The zero shear viscosity of the solutions were measured in the similar way. The results are summarized in Tables 2.22 to 2.30.

Table 2.22

Summary of results for zero shear viscosity, η^0 measurements for polybutadiene sample PB2F1 in benzene solution at 20.5°C.

$$(\bar{M}_V = 6.17 \times 10^5), [\eta] = 3.40 \text{ dl/gm}, K_M = 0.120$$

Conc. at 20.5°C (gm/dl)	η^0 (Poise)	η^0_{sp}	$c[\eta]$	$\bar{\eta}$	$K_M c[\eta]$
0.00	$0.655 \times 10^{-2}^a$	-	-	-	-
0.99	$7.20 \times 10^{-2}^a$	9.99	3.40	2.97	0.41
2.52	5.20×10^{-1}	78.4	8.57	9.15	1.03
5.07	5.41×10^0	825	17.2	47.8	2.07
7.50	3.31×10^1	5052	25.5	198.1	3.06
9.78	1.65×10^2	25,190	33.2	757.5	4.00
13.1	1.14×10^3	174,045	44.5	3908	5.34

a : Capillary viscometer with varying pressure head was used.

Table 2.23

Summary of results for zero shear viscosity, η^0
 measurements for polybutadiene sample PB2F1 in
 isobutyl acetate solution at 20.5°C.

$$(\bar{M}_V = 6.17 \times 10^5), [\eta] = 1.03 \text{ dl/gm}, K_M = 0.424$$

Conc. at 20.5°C (gm/dl)	η^0 (Poise)	η^0_{sp}	$c[\eta]$	-	$K_M c[\eta]$
0.00	$0.698 \times 10^{-2} \text{ }^a$	-	-	-	-
1.01	$2.20 \times 10^{-2} \text{ }^a$	2.15	1.04	2.07	0.44
2.51	2.70×10^{-1}	37.7	2.58	14.6	1.10
5.00	3.85×10^0	551	5.15	106.9	2.18
7.50	2.74×10^1	3925	7.72	508.1	3.27
10.0	1.80×10^2	25,787	10.3	2504	4.37
13.0	$1.24_2 \times 10^3$	177,936	13.4	13,289	5.68

a : Capillary viscometer with varying pressure
 head was used

Table 2.24

Summary of results for zero shear viscosity, η^0 measurements for polybutadiene sample PB2F1 in dioxane solution at 20.2°C.

$$(\bar{M}_V = 6.17 \times 10^5), [\eta] = 1.03 \text{ dl/gm}, K_M = 0.424$$

Conc. at 20.2°C (gm/dl)	η^0 (Poise)	η^0_{sp}	$c[\eta]$	$\bar{\eta}$	$K_M c[\eta]$
0.00	$1.24 \times 10^{-2}^a$	-	-	-	-
1.04	$5.20 \times 10^{-2}^a$	3.19	1.07	2.98	0.45
2.42	3.82×10^{-1}	29.8	2.49	12.0	1.06
4.99	5.80×10^0	466.7	5.14	90.8	2.18
7.51	5.05×10^1	4072	7.73	526	3.28
9.53	2.09×10^2	16,854	9.81	1717	4.16
11.6	8.90×10^2	71,773	11.95	6007	5.07

a : Capillary viscometer with varying pressure head was used

Table 2.25

Summary of results of zero shear viscosity, η^0
 measurements for polybutadiene sample PB2F2 in
 benzene solution at 20.5°C.

$$(\bar{M}_V = 2.61 \times 10^5), [\eta] = 1.82 \text{ dl/gm}, K_M = 0.120$$

Conc. at 20.5°C (gm/dl)	η^0 (Poise)	η^0_{sp}	c [η]	$\bar{\eta}$	$K_M c [\eta]$
0.00	$0.655 \times 10^{-2}^a$	-	-	-	-
2.51	$9.40 \times 10^{-2}^a$	13.55	4.57	2.92	0.55
5.00	8.10×10^{-1}	122.7	9.10	13.5	1.09
7.50	3.64×10^0	554.7	13.65	40.6	1.64
10.1	1.14×10^1	1739	18.38	94.6	2.21
15.1	8.56×10^1	13,068	27.48	475	3.30
18.9	3.49×10^2	53,281	34.45	1546	4.13
20.1	4.50×10^2	68,701	36.58	1878	4.39
24.8	$1.56_2 \times 10^3$	238,472	45.14	5283	5.42
25.2	$1.63_8 \times 10^3$	250,075	45.90	5548	5.51

a : Capillary viscometer with varying pressure
 head was used

Table 2.26

Summary of results of zero shear viscosity, η^0 measurements for polybutadiene sample PB2F2 in isobutyl acetate solution at 20.5°C.

$$(\bar{M}_v = 2.61 \times 10^5), \quad [\eta] = 0.68 \text{ dl/gm}, \quad K_M = 0.398$$

Conc. at 20.5°C (gm/dl)	η^0 (Poise)	η_{sp}^0	c [η]	$\bar{\eta}$	$K_M c[\eta]$
0.00	$0.698 \times 10^{-2}{}^a$	-	-	-	-
2.51	$4.60 \times 10^{-2}{}^a$	5.59	1.71	3.27	0.68
5.03	5.10×10^{-1}	72.1	3.42	21.1	1.36
7.57	2.65×10^0	378.7	5.15	73.6	2.05
9.99	8.40×10^0	1202	6.79	177.0	2.70
12.4	2.44×10^1	3495	8.43	414.4	3.36
15.0	6.35×10^1	9096	10.20	891.8	4.06
20.0	3.90×10^2	55,873	13.60	4108	5.41
23.5	$1.20_6 \times 10^3$	172,778	15.98	10,812	6.36

a : Capillary viscometer with varying pressure head was used

Table 2.27

Summary of results of zero shear viscosity, η^0 measurements for polybutadiene sample PB2F2 in dioxane solution at 20.2°C.

$$(\bar{M}_V = 2.61 \times 10^5) \quad [\eta] = 0.68 \text{ dl/gm}, \quad K_M = 0.398$$

Conc. at 20.2°C (gm/dl)	η^0 (Poise)	η_{sp}^0	$c[\eta]$	$\bar{\eta}$	$K_M c[\eta]$
0.00	$1.24 \times 10^{-2}^a$	-	-	-	-
2.51	$9.25 \times 10^{-2}^a$	6.46	1.71	3.78	0.68
5.01	8.20×10^{-1}	65.1	3.41	19.1	1.36
7.50	4.25×10^0	341.7	5.10	67.0	2.03
9.97	1.46×10^1	1176	6.78	173.4	2.70
12.5	4.55×10^1	3668	8.50	431.5	3.38
15.0	1.26×10^2	10,160	10.20	996.1	4.06
19.0	5.54×10^2	44,676	12.92	3458	5.14
20.7	8.71×10^2	70,241	14.08	4990	5.60
22.7	1.57×10^3	126,612	15.44	8202	6.14

a : Capillary viscometer with varying pressure head was used

Table 2.28

Summary of results of zero shear viscosity, η^0 measurements for polybutadiene sample PB2F3 in benzene solution at 20.5°C.

$$(\bar{M}_V = 1.54 \times 10^6), [\eta] = 1.24 \text{ dl/gm}, K_M = 0.120$$

Conc. at 20.5°C (gm/dl)	η^0 (Poise)	η^0_{sp}	$c[\eta]$	$\bar{\eta}$	$K_M c[\eta]$
0.00	$0.655 \times 10^{-2}^a$	-	-	-	-
2.50	$4.60 \times 10^{-2}^a$	6.02	3.10	1.94	0.37
5.01	2.09×10^{-1}	30.9	6.21	4.97	0.74
7.55	8.20×10^{-1}	124.2	9.36	13.3	1.12
10.1	2.58×10^0	393	12.52	31.4	1.50
15.0	1.12×10^1	1709	18.60	91.9	2.23
20.1	4.50×10^1	6869	24.92	275.6	2.99
25.2	1.44×10^2	21,984	31.25	703.5	3.75
30.3	4.30×10^2	65,848	35.57	1747	4.27
32.9	6.68×10^2	101,984	40.80	2500	4.89
35.5	9.25×10^2	141,220	44.02	3208	5.28

a : Capillary viscometer with varying pressure head was used

Table 2.29

Summary of results of zero shear viscosity, η° measurements for polybutadiene sample PB2F3 in isobutyl acetate solution at 20.5°C.

$$(\bar{M}_v = 1.54 \times 10^5), [\eta] = 0.52 \text{ dl/gm}, K_M = 0.352$$

Conc. at 20.5°C (gm/dl)	η° (Poise)	η_{sp}°	$c[\eta]$	$\bar{\eta}$	$K_M c[\eta]$
0.00	$0.698 \times 10^{-2}{}^a$	-	-	-	-
2.50	$3.20 \times 10^{-2}{}^a$	3.58	1.30	2.76	0.46
5.03	$1.07 \times 10^{-1}{}^a$	14.3	2.61	5.48	0.92
7.51	6.00×10^{-1}	85.0	3.90	21.8	1.37
10.0	2.07×10^0	295.6	5.20	58.8	1.83
15.0	1.05×10^1	1503	7.80	192.7	2.74
19.8	4.03×10^1	5773	10.30	560.7	3.62
24.7	1.43×10^2	20,486	12.84	1595	4.52
30.0	4.55×10^2	65,185	15.60	4178	5.49
34.0	9.06×10^2	129,798	17.68	7341	6.22

a : Capillary viscometer with varying pressure head was used

Table 2.30

Summary of results of zero shear viscosity, η^0 measurements for polybutadiene sample PB2F3 in dioxane solution at 20.2°C.

$$(\bar{M}_v = 1.54 \times 10^5), [\eta] = 0.52 \text{ dl/gm}, K_M = 0.352$$

Conc. at 20.2°C (gm/dl)	η^0 (Poise)	η_{sp}^0	$c[\eta]$	$\bar{\eta}$	$K_M c[\eta]$
0.00	$1.24 \times 10^{-2}^a$	-	-	-	-
2.50	$6.40 \times 10^{-2}^a$	4.16	1.30	3.20	0.46
5.00	$3.45 \times 10^{-1}^a$	26.8	2.60	10.3	0.91
7.56	1.10×10^0	87.7	3.93	22.3	1.38
10.2	3.66×10^0	294.2	5.30	55.5	1.87
15.1	1.84×10^1	1483	7.85	195.6	2.76
20.3	7.68×10^1	6192	10.55	568.6	3.72
25.0	2.93×10^2	23,628	13.00	1817	4.76
30.0	7.75×10^2	62,499	15.60	4006	5.49
33.3	1.34×10^3	108,064	17.32	6241	6.10

a : Capillary viscometer with varying pressure head was used

CHAPTER - III

DISCUSSION

DISCUSSION

The zero shear viscosity, η° of polychloroprene and polybutadiene samples of different molecular weights over a wide range of concentration (1.0 to 35.0 gm/dl) in both good and θ solvents were studied. In case of polychloroprene, butanone and cyclohexane were used as θ solvents and benzene at two different temperatures (25° and 45.5°C) was used as two good solvents, whereas in case of polybutadiene, isobutyl acetate (IBA) and dioxane were used as θ solvents and benzene at 20.5°C was used as good solvent. In case of polychloroprene six samples (PCF1B, PCF2A, PCF2B, PCF2C, PCF3A and PCF3B) in the range of molecular weight of $0.99 - 4.85 \times 10^5$ were used, while in case of polybutadiene only three samples (PB2F1, PB2F2 and PB2F3) in the range of molecular weight of $1.54 - 6.17 \times 10^5$ were used. Polybutadiene is a non-polar flexible chain polymer whereas polychloroprene is a polar one.

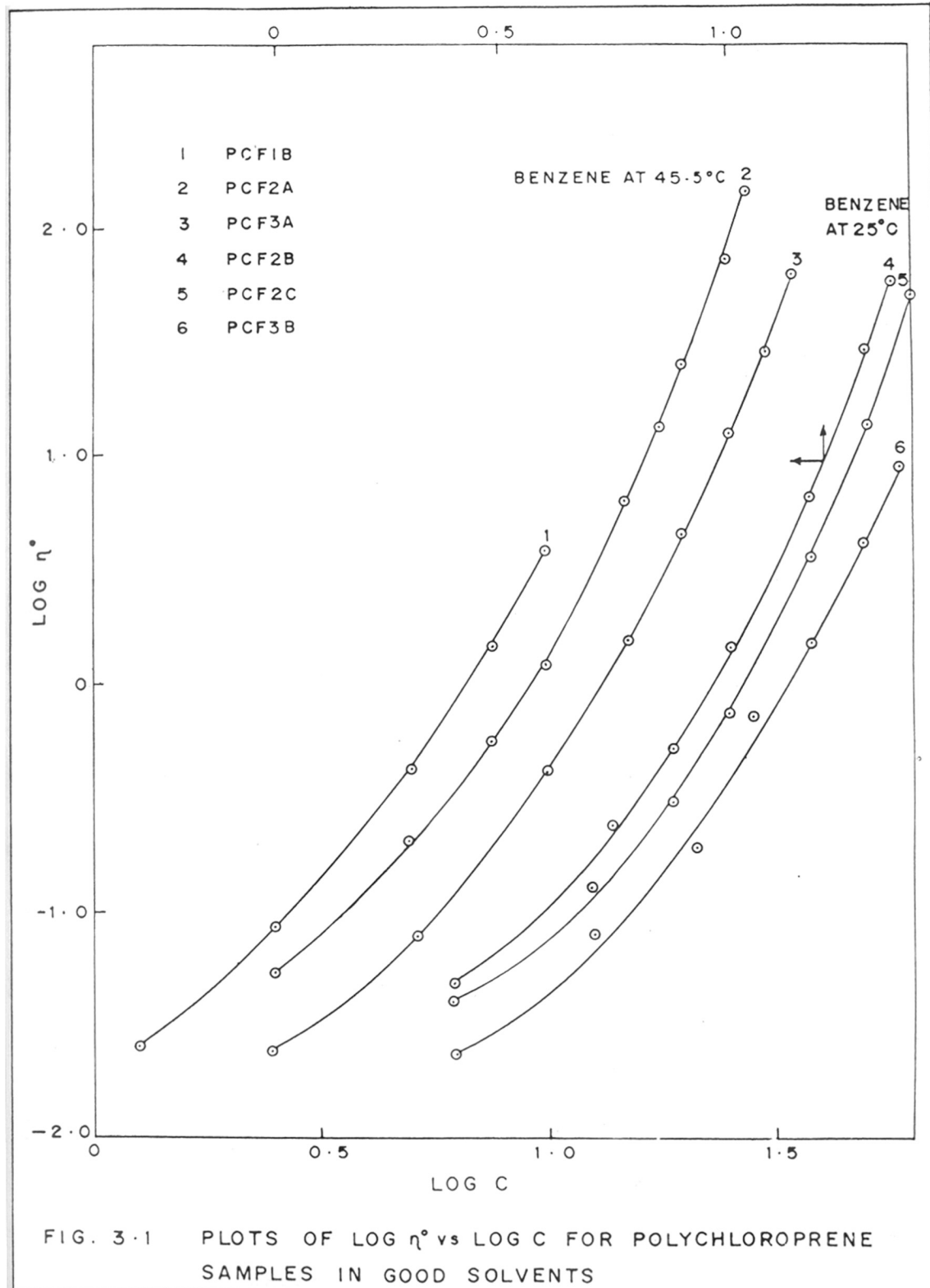
3.1 Dependence of Zero Shear Viscosity on Concentration

The experimental data for zero shear viscosity, η° measurements for polychloroprene samples are given in Tables 2.10 to 2.21 and the same data for polybutadiene

samples are given in Tables 2.22 to 2.30. The viscosity data given in those tables have been plotted as $\log \eta^0$ vs. $\log c$ in Figs. 3.1 to 3.3. Fig. 3.1 shows the double logarithmic plots of zero shear viscosity as a function of concentration for polychloroprene samples in two good solvents (benzene at 45.5° and benzene at 25°C) whereas Fig. 3.2 shows the same plots in two θ solvents (butanone and cyclohexane). The plots for polybutadiene samples in good (benzene) and θ solvents (IBA and dioxane) are shown in Fig. 3.3. The viscosity is strongly dependent on concentration. The $d\log \eta^0/d\log c$ becomes steeper with increasing concentration as entanglement of polymer chains and cross linkings are increased with increasing concentration.

3.2 Dependence of Zero Shear Viscosity on Molecular Weight

The superposition of data for polychloroprene samples in Figs. 3.1 and 3.2 and for polybutadiene samples in Fig. 3.3 have been made to obtain a single composite curve in each solvent by shifting them vertically by a factor $(M^0/M)^{3.4}$. Here M^0 represents the molecular weight of the reference sample (in case of polychloroprene PCF1B or PCF2B was used as reference



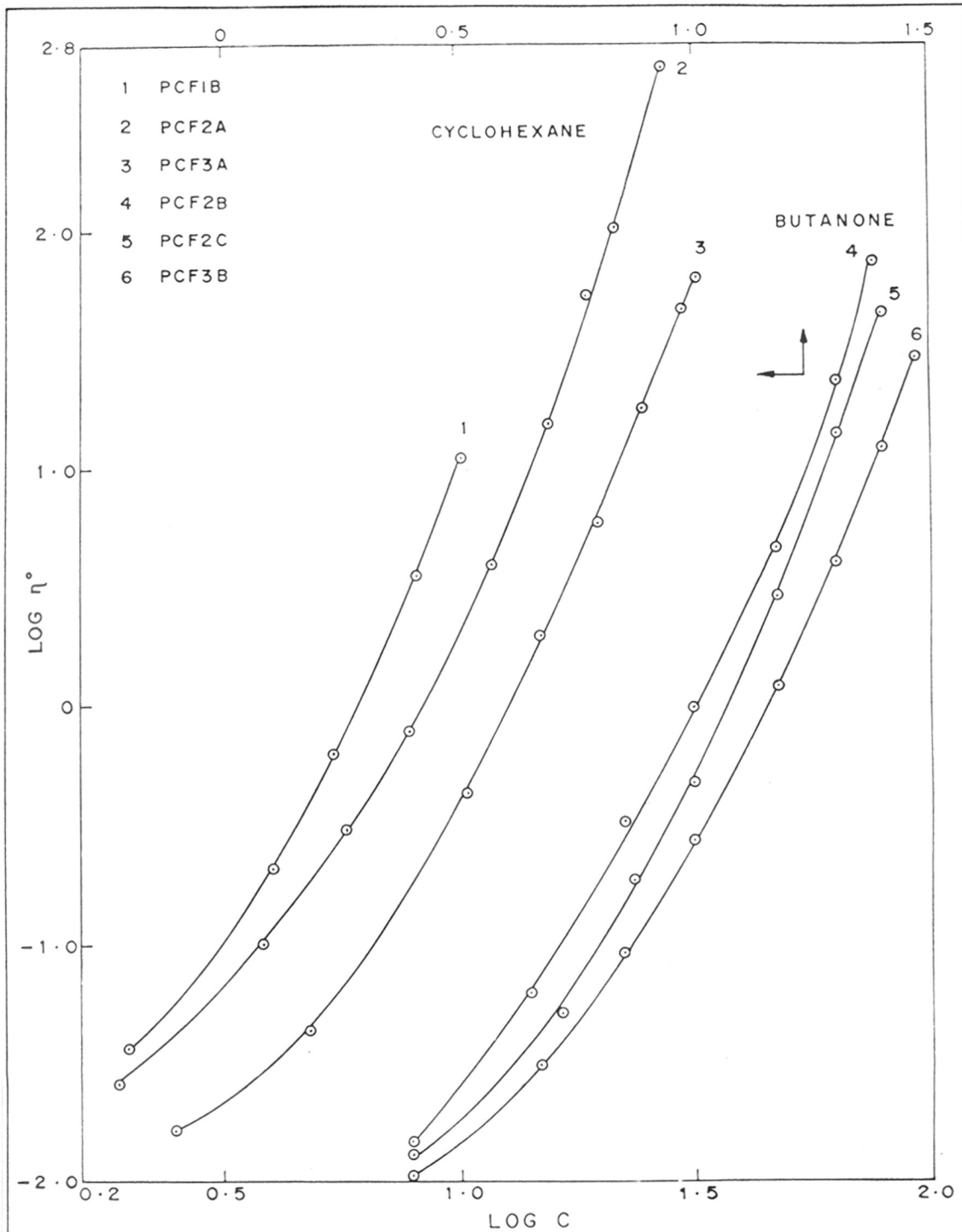


FIG. 3.2 PLOTS OF $\text{LOG } \eta^\circ$ vs $\text{LOG } C$ FOR POLYCHLOROPRENE SAMPLES IN POOR SOLVENTS.

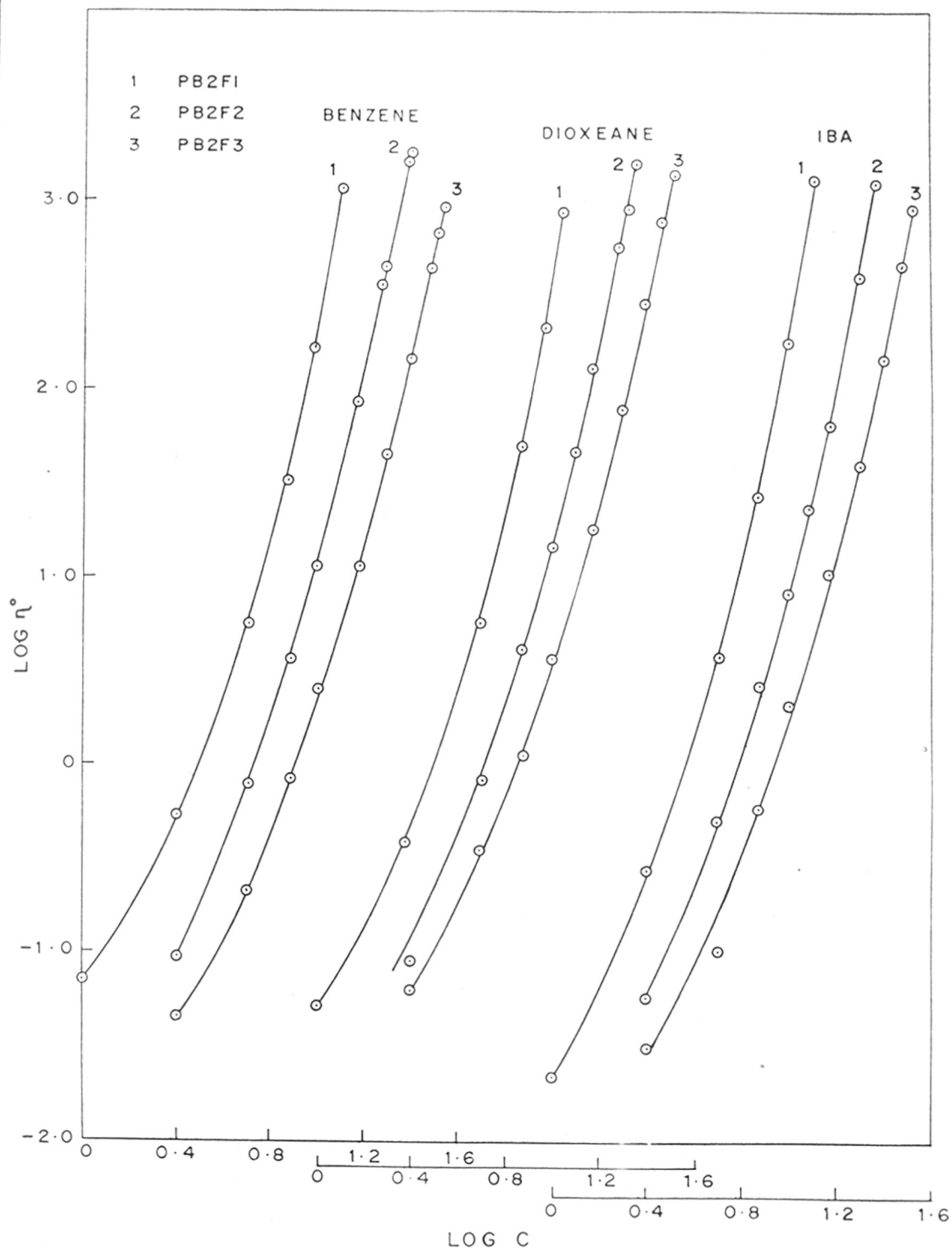


FIG. 3-3 PLOTS OF $\text{LOG } \eta^\circ$ vs $\text{LOG } C$ FOR POLYBUTADIENE SAMPLES IN GOOD AND POOR SOLVENTS.

sample and in case of polybutadiene, PB2F1 was used as reference sample). The composite curves thus obtained for polychloroprene in benzene and cyclohexane solutions at 45.5°C and in benzene and butanone solutions at 25°C are shown in Figs. 3.4 and 3.5 respectively, while the composite curves for polybutadiene in good (benzene) and θ solvents (IBA and dioxane) are shown in Figs. 3.6 and 3.7 respectively, where K is chosen as $3.4 \log (M^0/M)$. The superposition is not successful, however, over the entire range of concentration. The shift factor is found to be proportional to $M^{3.4}$ in the range of higher concentration for both the polymers. The data deviated from the composite curves (at the lower concentration region) are shown by dashed lines. The results indicate that the relation $\eta^0 \propto M^{3.4}$ was obeyed by the data obtained for both polychloroprene samples and polybutadiene samples. In this connection it may be mentioned that similar to our results Kraus and Gruver^{54,55} observed that the zero shear viscosity, η^0 for linear polybutadiene melts increased in a 3.4th power proportion to molecular weight, M above a certain critical molecular weight, M_c . In case of polychloroprene the data for cross over point concentration, c_{cross} (denoted by parentheses in the

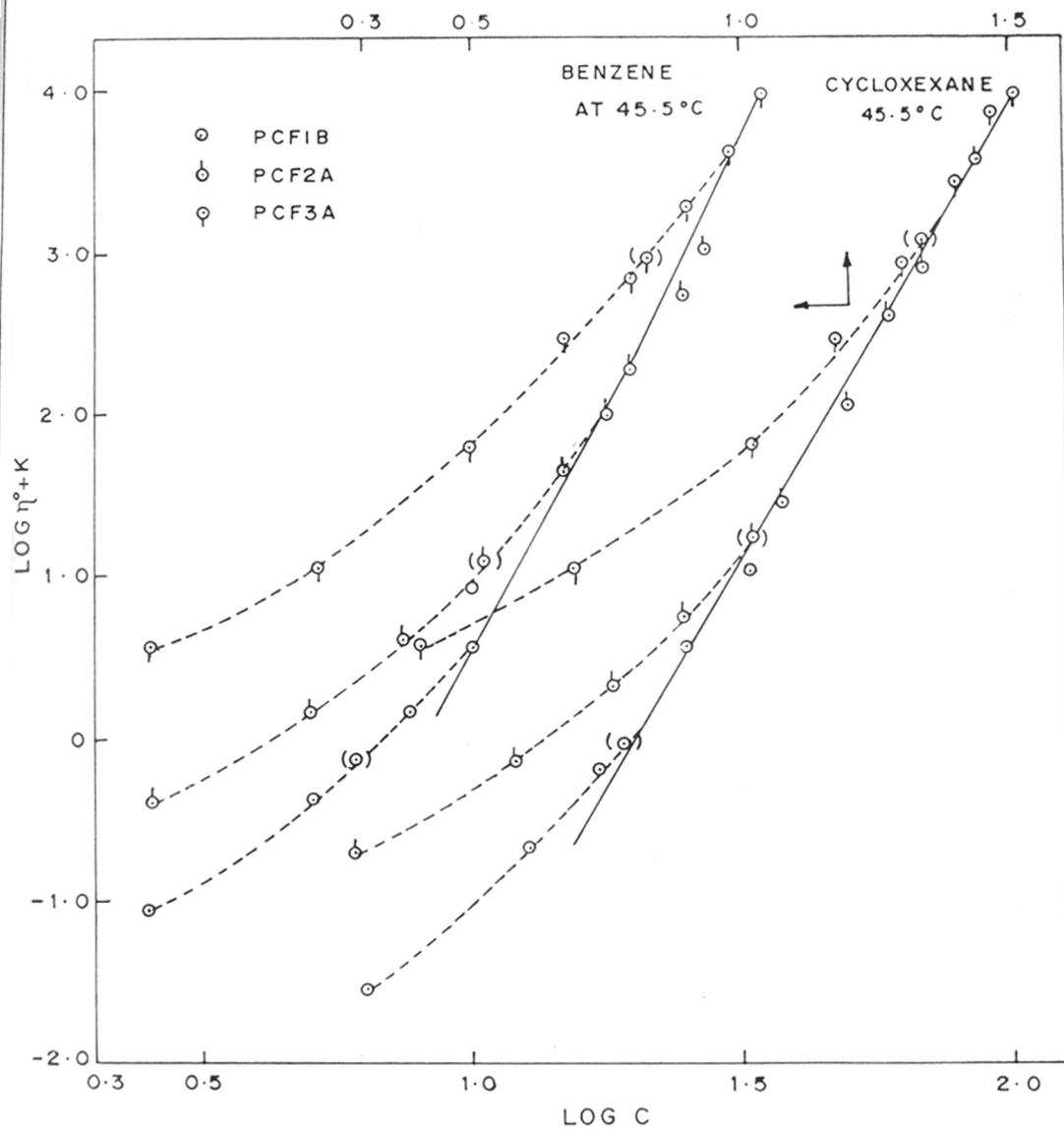


FIG. 3-4 COMPOSITE CURVES FOR POLYCHLOROPRENE SAMPLES IN GOOD AND POOR SOLVENTS AT 45.5°C

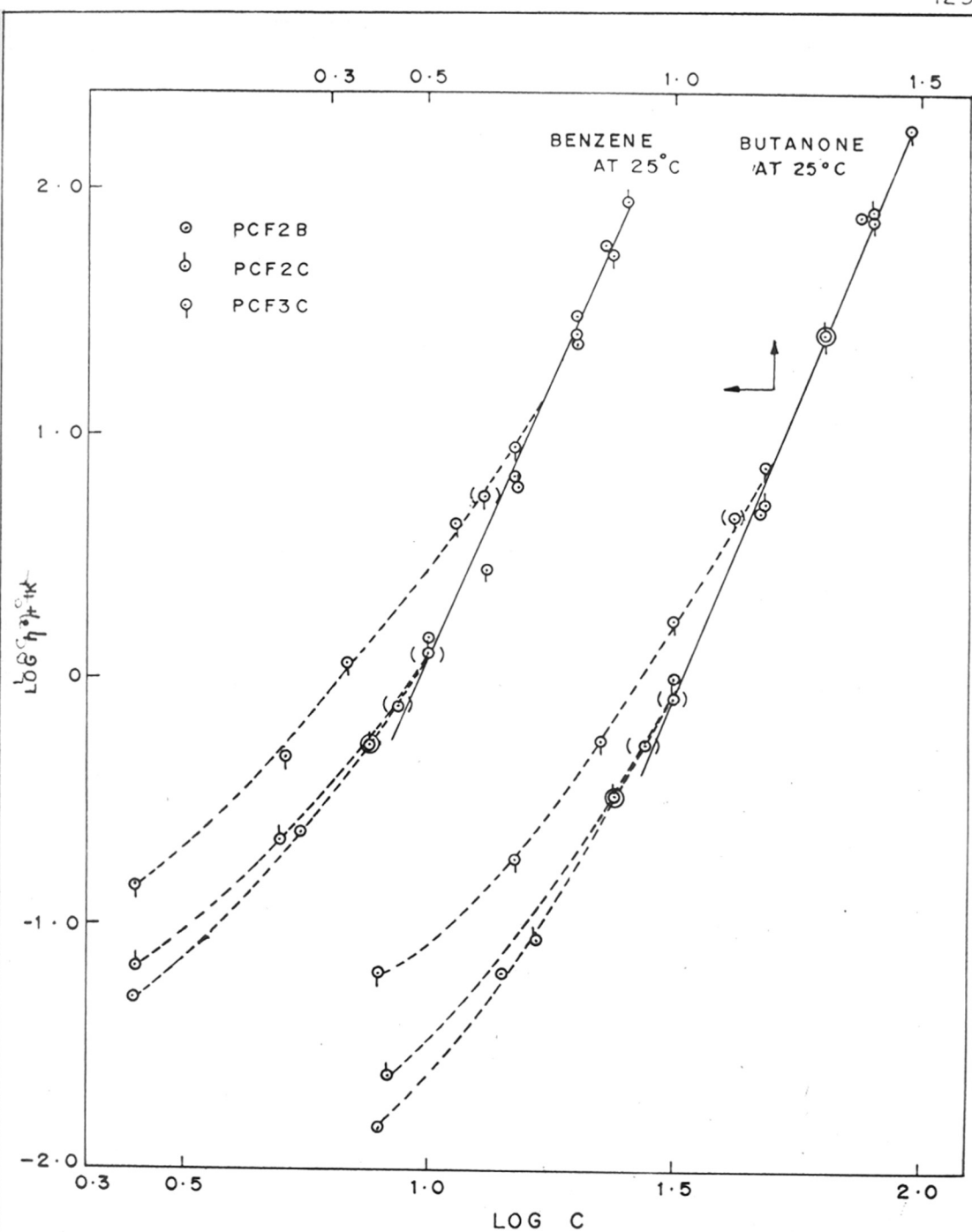


FIG. 3.5 COMPOSITE CURVES FOR POLYCHLOROPRENE SAMPLES IN GOOD AND POOR SOLVENTS AT 25°C

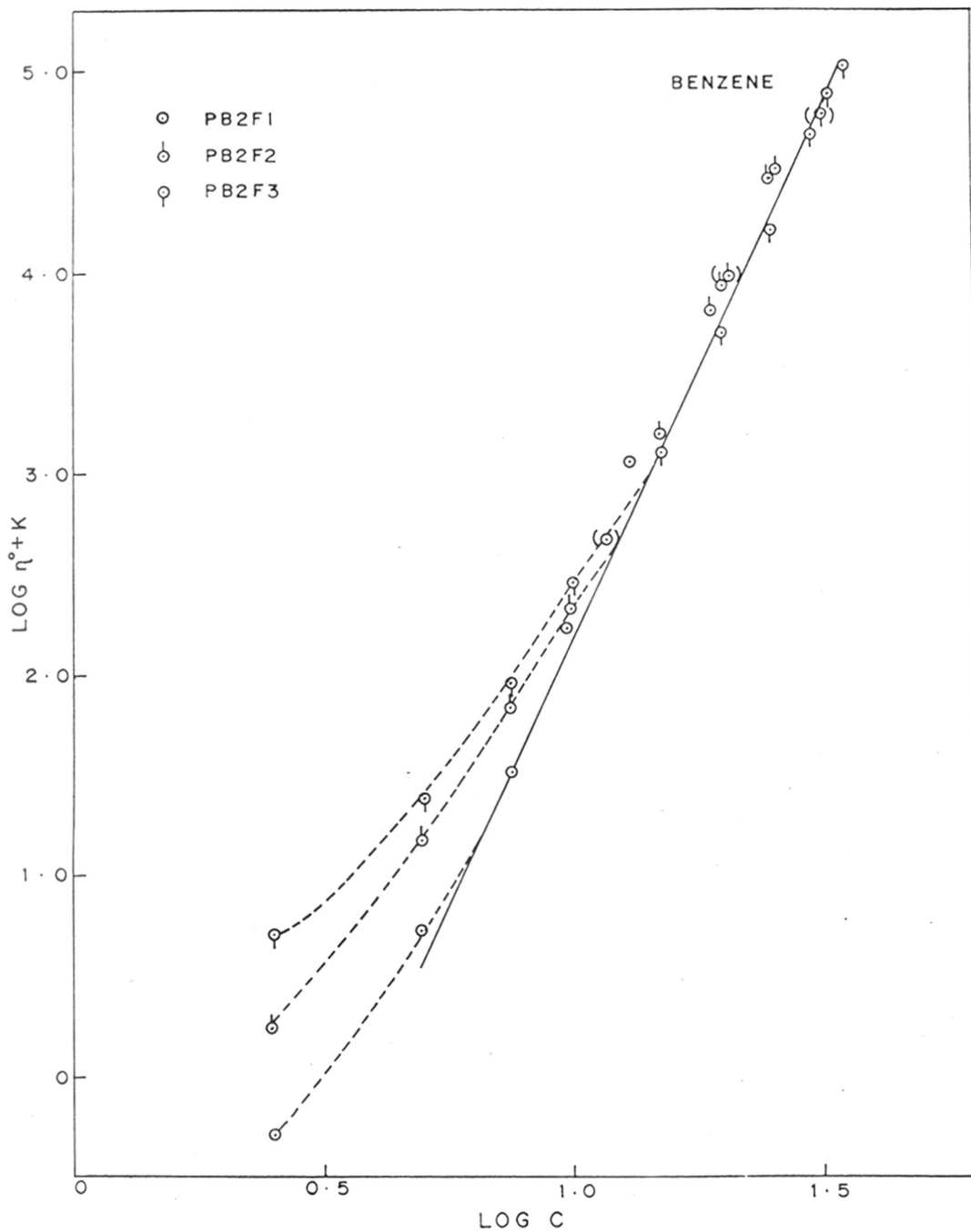


FIG. 3.6 COMPOSITE CURVE FOR POLYBUTADIENE SAMPLES IN BENZENE.

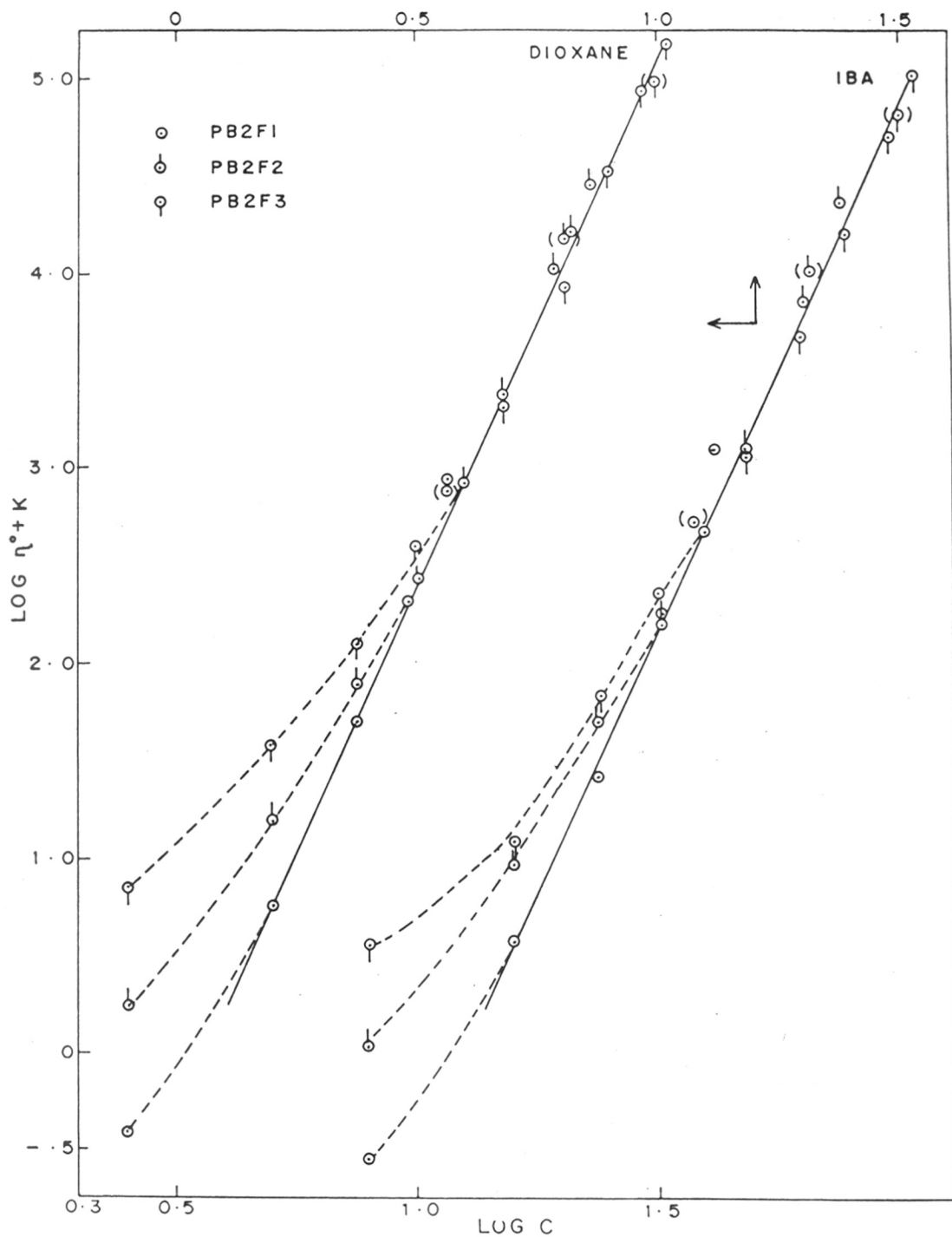


FIG. 3.7 COMPOSITE CURVES FOR POLYBUTADIENE SAMPLES IN POOR SOLVENTS

graph) are found exactly at the starting points from where the composite curves (Figs. 3.4 and 3.5) have started, (however, for benzene solutions the data for c_{cross} are slightly away from the composite curve), whereas in case of polybutadiene the same data are found deep inside the composite curve (Figs. 3.6 and 3.7). (The viscosity cross over in θ solvents will be discussed later). The shift factor in case of polychloroprene is found to be approximately proportional to M in the lower concentration (below the cross over point) range. Superposition curves for lower concentration range are not shown here.

3.3 Dependence of Zero Shear Viscosity on Both Concentration and Molecular Weight

The onset of entanglement can be identified by rather abrupt change of slope in the plots of relative viscosity, $\eta_r(c)$ versus concentration c , $\eta_r(M)$ versus molecular weight, M or $\eta_r(c, M)$ versus $c M^b$. At high $c M^b$ it is frequently reported¹⁹ that the relative viscosity, η_r is a single function of $c^5 M^{3.4}$. The plots of $\log \eta_r$ versus $5 \log c + 3.4 \log M$ for polychloroprene and polybutadiene samples are shown in Figs. 3.8 and 3.9 respectively. In case of

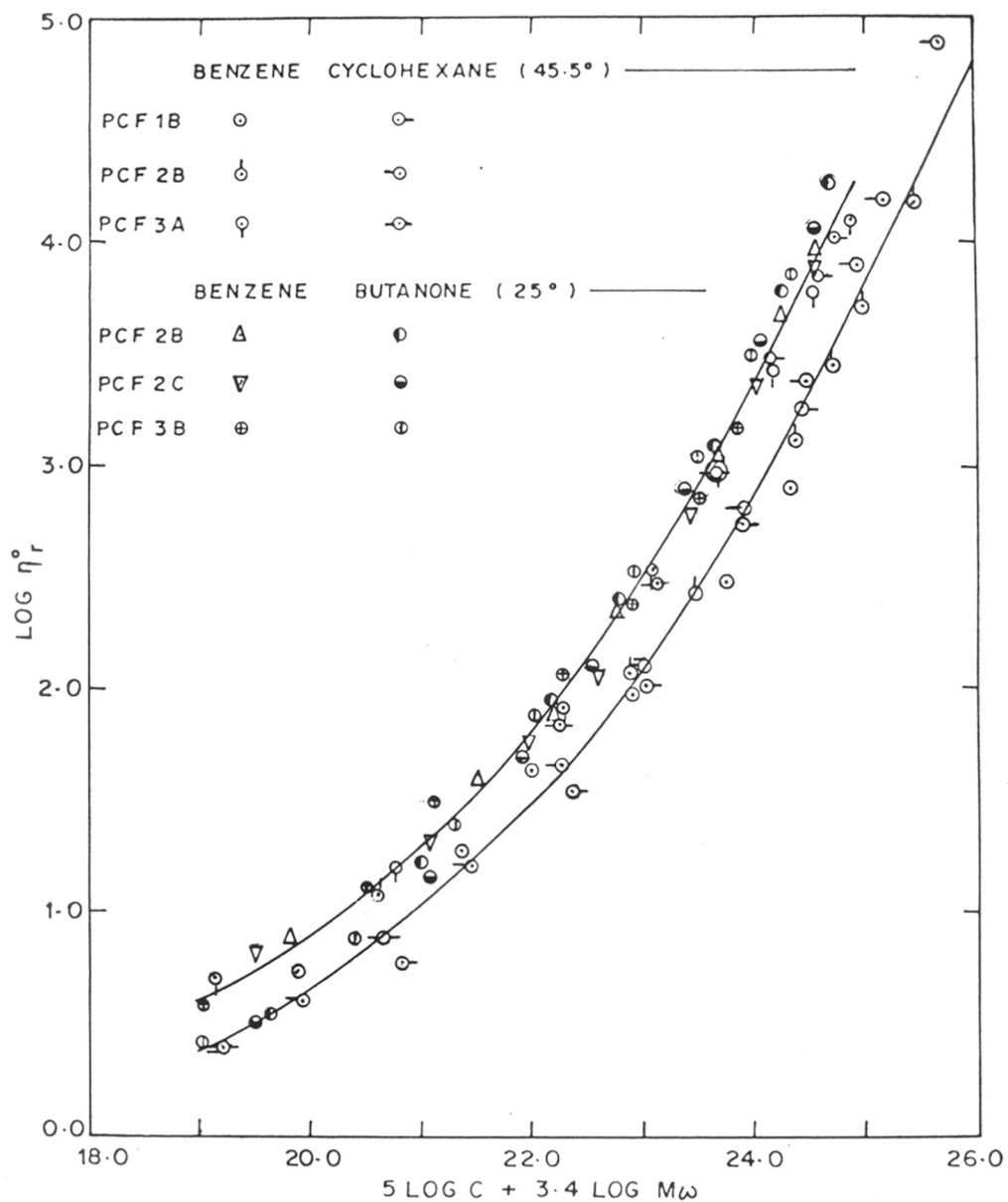


FIG. 3·8. PLOTS OF $\text{LOG } \eta_r^0$ vs $5 \text{ LOG } C + 3.4 \text{ LOG } M_w$
 FOR POLYCHLOROPRENE SAMPLES IN GOOD AND POOR SOLVENTS

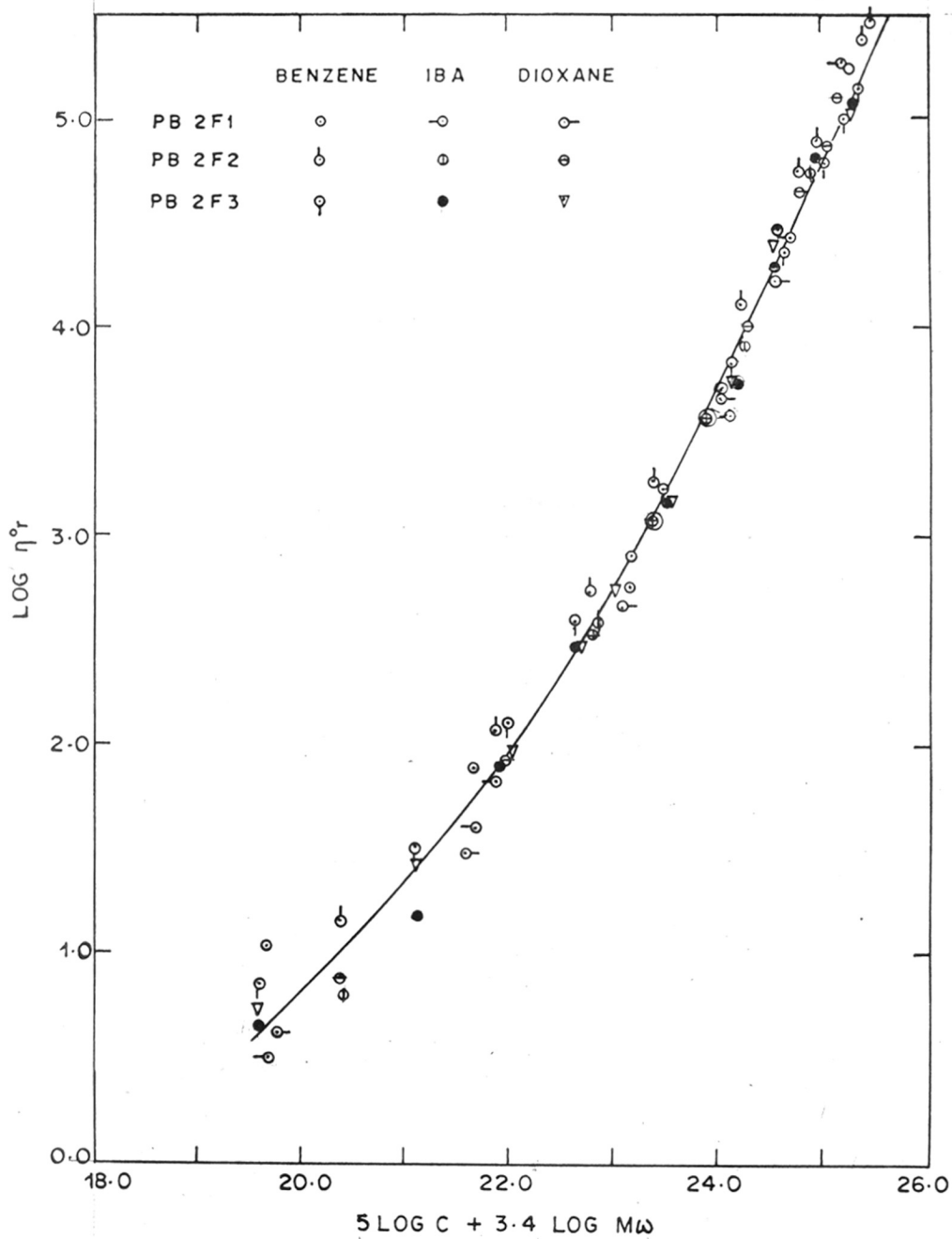


FIG. 3.9. PLOT OF $\text{LOG } \eta^{\circ r}$ vs $5 \text{ LOG } C + 3.4 \text{ LOG } M\omega$ FOR POLYBUTADIENE SAMPLES IN GOOD AND POOR SOLVENTS

polybutadiene (Fig. 3.9) a single composite curve has been obtained with good coincidence for the three samples of different molecular weights both in good and θ solvents. At higher values of the variables (concentration and molecular weight), the logarithmic plots produced a straight line with slope of unity, but at the lower values, the scattering of data are more and the slope of the curve changed gradually. This confirmed that the relation $\eta_r \propto c_M^{3.4}$ was obeyed by the data for polybutadiene samples.

In case of polychloroprene samples (Fig. 3.8) the data were fitted in two different curves (instead of a single one) parallel to each other. The data taken in benzene and butanone solutions at 25°C were fitted in one curve and the data for benzene and cyclohexane solutions at 45.5°C (excluding the data for PCF3A in benzene) were fitted to another one. Since the data taken at two different temperatures (25° and 45.5°C) are fitted in two separate curves instead of a single one, the discrepancy probably is due to two temperatures used for measurements. However, at both the two temperatures, the logarithmic

plots at higher values of the variables (concentration and molecular weight) yield a straight line with slope of unity. The results indicate that over a considerable range of the variables (concentration and molecular weight) at a constant temperature the relative viscosity is a single function of $c^5 M^{3.4}$. In the lower values of the variables, the slope changes gradually and hence the concentration or molecular weight (critical) at entanglement composition cannot be ascertained.

3.4 Dependence of Zero Shear Viscosity on Quality (Good and θ) of Solvents

The zero shear specific viscosity, η_{sp}^0 for the polymers studied here are listed in Tables 2.10 to 2.30 (column 3). The same η_{sp}^0 values for each polymer sample both in good and θ solvents are double logarithmically plotted against polymer concentration, c (gm/dl) in Figs. 3.10 to 3.13. Figs. 3.10 and 3.11 show double logarithmic plots of η_{sp}^0 vs. c for polychloroprene samples in benzene and cyclohexane solutions at 45.5°C , as well as benzene and butanone solutions at 25°C respectively, while Figs. 3.12 and 3.13 show the same plots for polybutadiene samples in

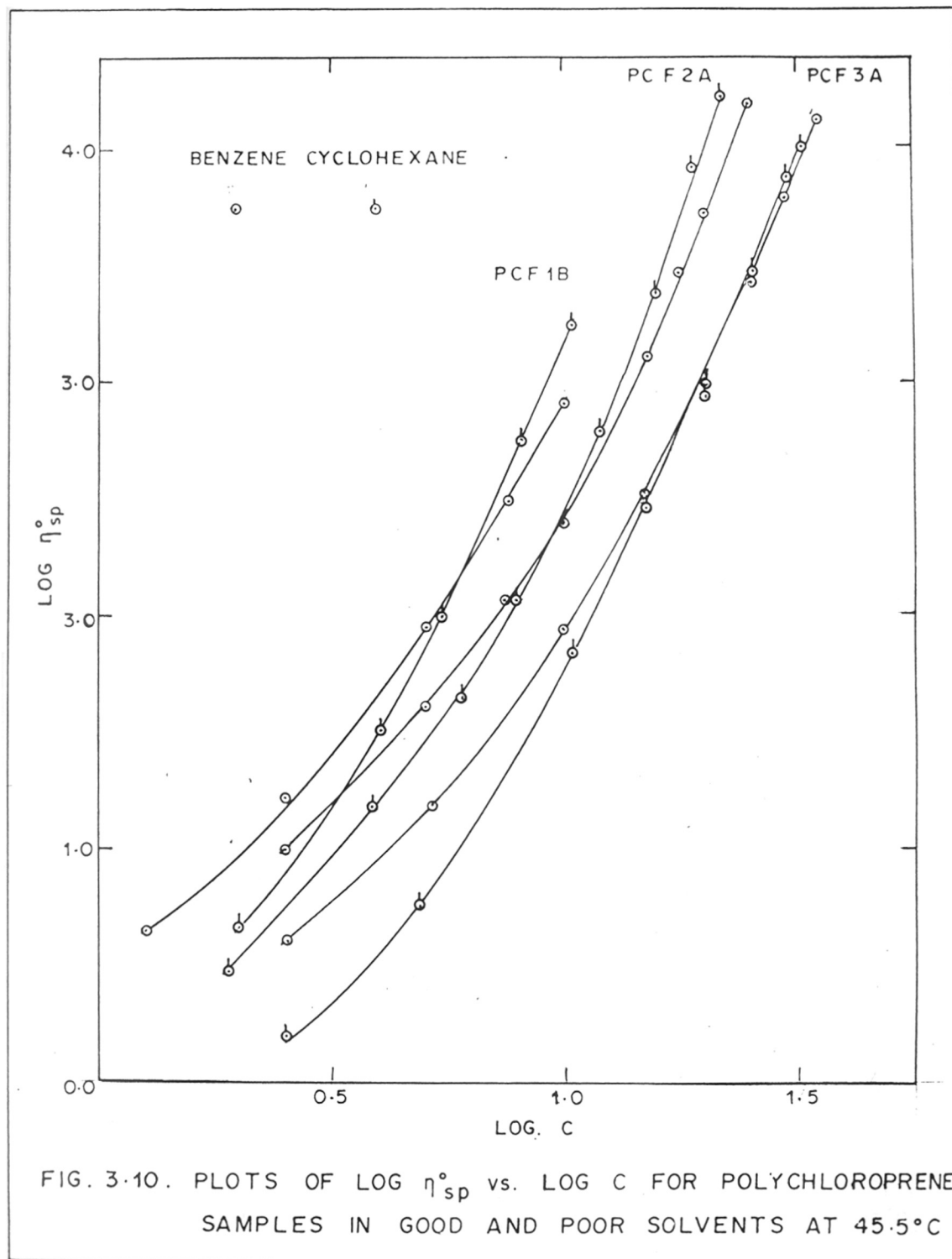


FIG. 3-10. PLOTS OF $\text{LOG } \eta_{sp}^{\circ}$ vs. $\text{LOG } C$ FOR POLYCHLOROPRENE SAMPLES IN GOOD AND POOR SOLVENTS AT 45.5°C

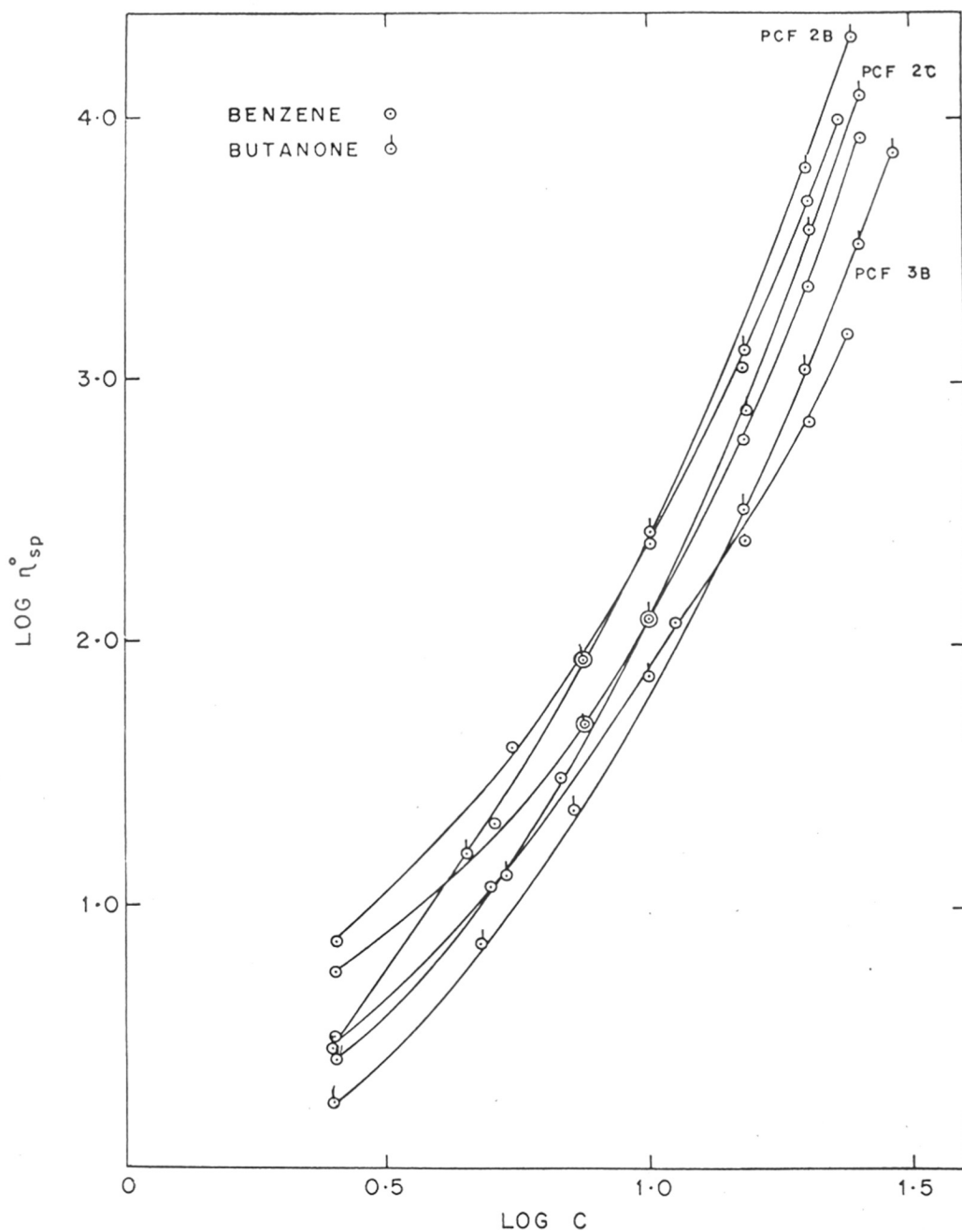


FIG. 3-11. PLOTS OF $\text{LOG } \eta_{sp}^{\circ}$ vs. $\text{LOG } C$ FOR POLYCHLOROPRENE SAMPLES IN GOOD AND POOR SOLVENTS, AT 25°C

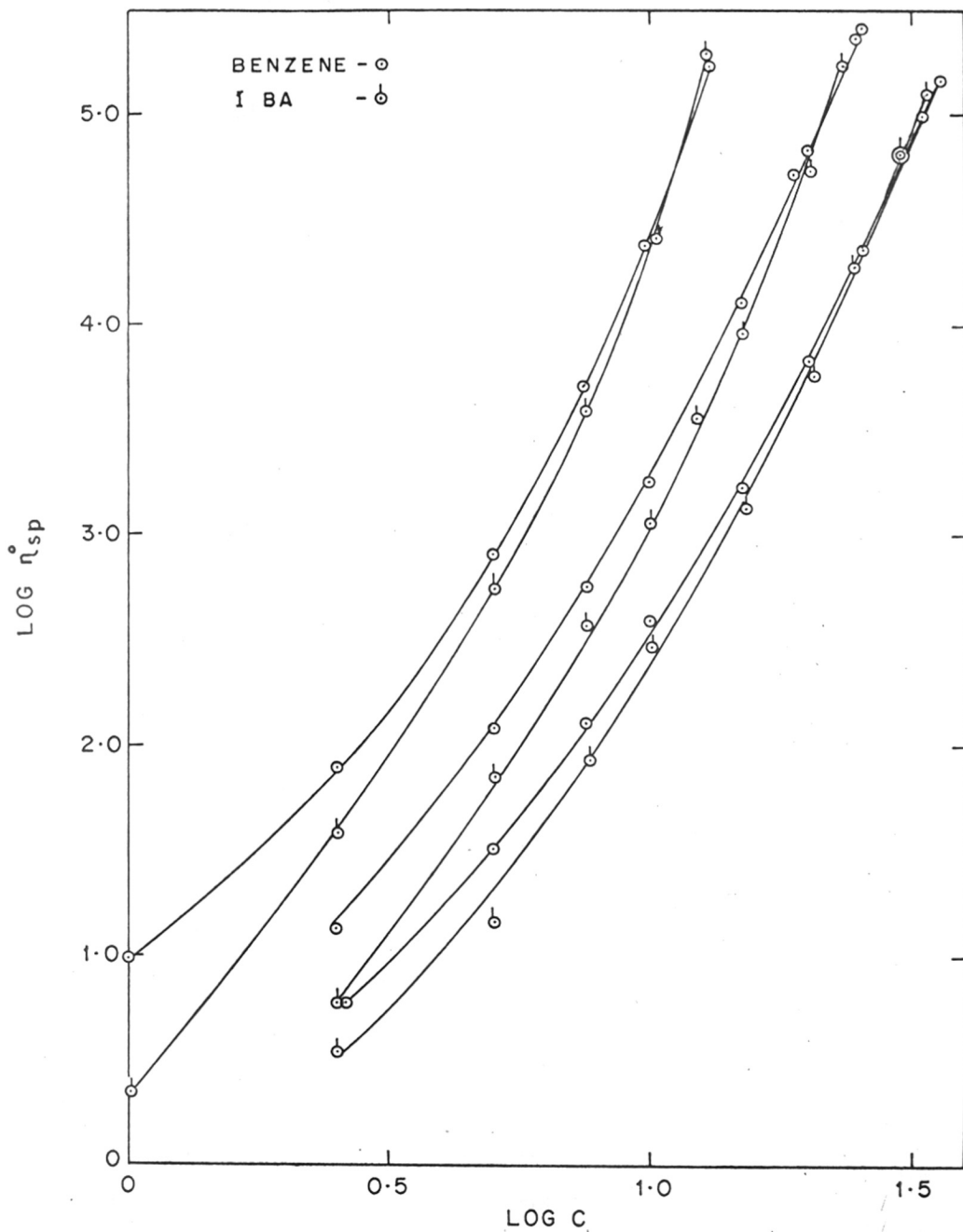


FIG. 3-12 : PLOTS OF $\text{LOG } \eta_{sp}$ vs. $\text{LOG } C$ FOR POLBUTADIENE SAMPLES IN GOOD AND POOR SOLVENTS (BENZENE-I BA)

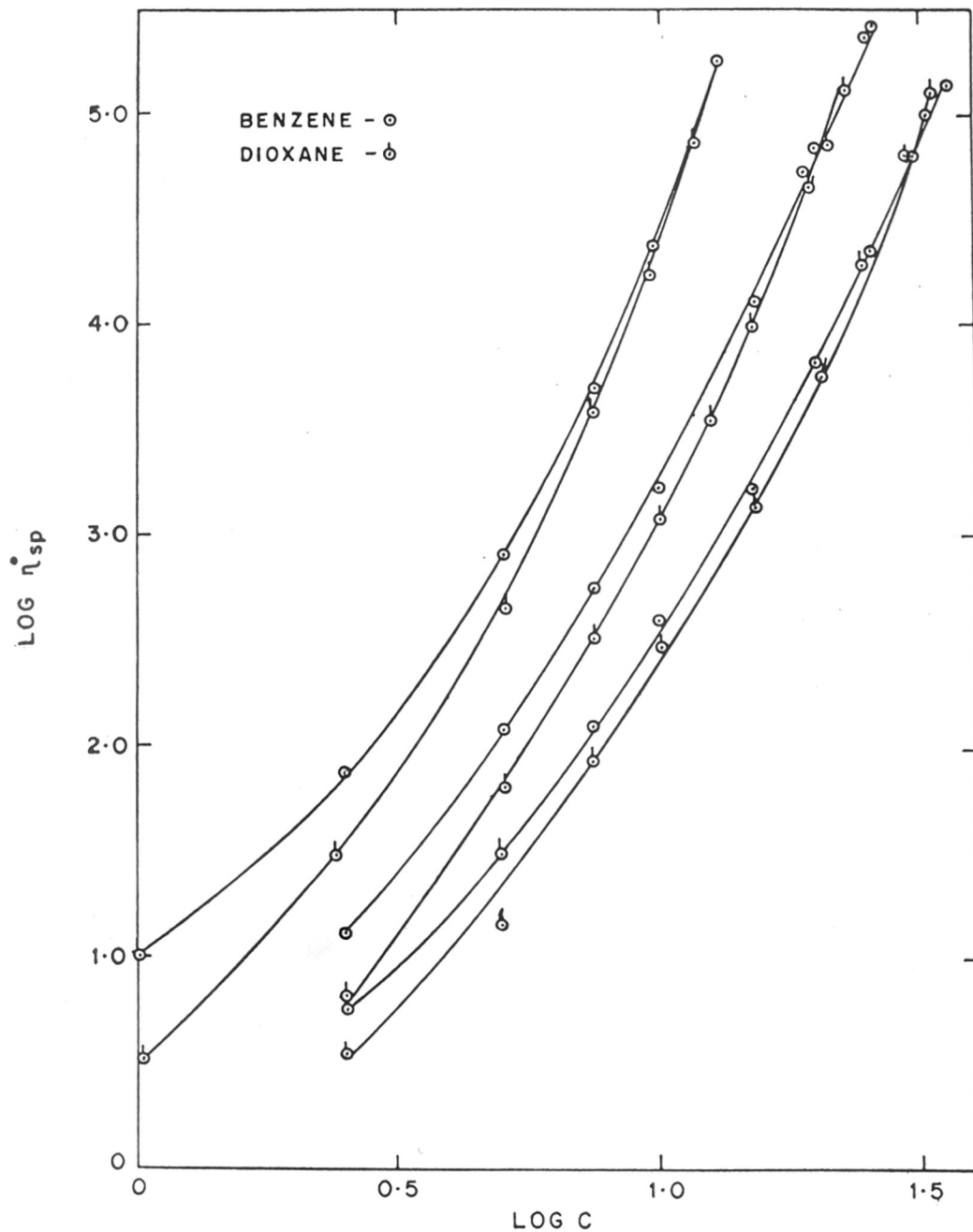


FIG.3.13: PLOTS OF LOG η_{sp}° vs. LOG C FOR POLYBUTADIENE SAMPLES IN GOOD AND POOR SOLVENTS (BENZENE-DIOXANE)

benzene and dioxane solutions, as well as benzene and isobutyl acetate solutions respectively. In case of polybutadiene, the data obtained at 20.5°C for benzene solutions have been used for comparison with those of both dioxane and isobutyl acetate solutions measured at 20.2°C and 20.5°C respectively. (The difference between the data obtained at 20.2° and 20.5°C in benzene solution is very small and hence neglected). In the higher concentration region, the η_{sp}^0 values in θ solvents are higher than those obtained in good solvents, whereas in the moderately concentrated region (the so-called Rouse region) the values are just opposite in θ and good solvents. It may be pointed out that the viscosity cross over in θ solvents for polybutadiene samples is not as sharp as is found in polychloroprene samples and that cross over too has taken place in the concentration region of 11.7 to 31.6% polymer which is comparatively higher than that of polychloroprene samples (6.05 to 21.0% polymer) (Table 3.1). It may be recalled that the relative viscosity of polyisobutylene⁶⁸ (a non-polar polymer with flexible chain) showed same values at equiconcentrated solutions in good and θ solvents, whereas in polyvinyl acetate⁶⁵, polystyrene^{43,62,63,66}

Table 3.1

Cross over point concentration and viscosity for
 polychloroprene and polybutadiene samples in good
 and θ solvent systems

Sample	Solvent system	Cross over point conc. c_{cross} (gm/dl)	Cross over point viscosity $\eta^{\circ}_{\text{cross}}$ (Poise)		$M c_{\text{cross}} \times 10^5$
			good solvent	θ solvent	
PCF1B	Benzene- cyclohexane	6.03	0.692	0.955	29.24
PCF2A		10.5	1.64	2.40	28.24
PCF3A		21.1	5.89	7.59	23.42
PCF2B	Benzene-butanone	8.71	0.759	0.549	14.63
PCF2C		10.0	0.794	0.501	14.40
PCF3B		13.2	0.912	0.759	13.07
PB2F1	Benzene-IBA	11.7	520	554	72.19
PB2F2		20.4	520	554	53.24
PB2F3		31.6	520	554	48.66
PB2F1	Benzene-dioxane	11.6		858	70.95
PB2F2		20.4		858	53.24
PB2F3		30.9		858	47.59

and poly(methyl methacrylate)^{62,63,69} (all polar polymers) the relative viscosities in a θ solvent cross over and become somewhat higher than good solvent values with cross over point concentrations respectively $> 35\%$ polymer, in the range of 15-30% polymer and in the range of 5-7% polymer. The reversal of η_{sp}^0 is generally found in the higher concentration range where the values of radius of gyration in good and poor solvents become almost identical¹⁰⁰⁻¹⁰³. Hence the difference of the radius of gyration is not the cause for the reversal of η_{sp}^0 in concentrated solutions. Williams and Gandhi^{62,63} have explained this solvent effect in terms of polymer aggregation in poor solvents. It may be pointed out that Isona and Nagasawa¹⁰⁴ have explained this phenomena that the strength of entanglement coupling in poor solvent is higher than in good solvent. However, the data present at hand suggest some relationship between viscosity cross over in θ solvent and polymer polarity supporting the idea of enhanced intermolecular association in poor solvents. In this connection it may be pointed out that Vinogradov and coworkers⁷¹ has emphasized that a dependence between glass transition temperature, T_g of the undiluted polymer and hence with T_g for the polymer-solvent mixture

and the viscosity cross over in θ solvent might develop as free draining behaviour is approached at higher concentration, since the viscosity must lose its direct proportionality to solvent viscosity and become proportional instead to a local frictional coefficient ζ^0 . The value of ζ^0 depends on the nature of both solvent and polymer since both influence the free volume and glass temperature of the mixture. Graessley⁷⁰ has also supported this idea. The glass transition of most solvents is well below the room temperature. In polyisobutylene, the T_g for its solution probably remains relatively constant and always well below the room temperature because T_g for pure polyisobutylene is so low ($T_g = -70^\circ\text{C}$). In case of polyvinyl acetate ($T_g = 30^\circ\text{C}$), polystyrene ($T_g = 95^\circ\text{C}$) and poly(methyl methacrylate) ($T_g = 100^\circ\text{C}$), the T_g for their solutions must rise with increasing concentration (all the undiluted polymers have T_g values above the room temperature). The viscosity-concentration curves for solutions of polymers which are in a glassy state at the experimental temperature are much steeper. The approach to a glassy state with an increase of concentration results a sharp rise in viscosity in such a solution. In the

present work, the undiluted polybutadiene has T_g very low (-90°C) and in polybutadiene solution, T_g probably remains relatively constant and always well below room temperature similar to that of the solutions of non-polar polyisobutylene samples. However, the effect for polar polychloroprene ($T_g = -50^{\circ}\text{C}$) should be larger because T_g for its solution will rise somewhat with increasing concentration as ϕ° for polar polymer will be different than that of the non-polar one.

3.4.1 Relation Between Viscosity Cross Over and Entanglement Composition

The cross over point concentration for polychloroprene samples and polybutadiene samples and their corresponding viscosity in both good and θ solvents are given in Table 3.1. It is observed that viscosities at cross over points for polychloroprene samples are much lower than those of polybutadiene samples. Since the molecular weights for polychloroprene samples used in benzene-butanone system are not widely apart, the cross over point viscosities for these samples are accordingly close to each other. From Fig. 3.10 the concentrations for cross over points for PCF1B, PCF2A and PCF3A samples have been obtained as 6.03, 10.5 and 21.1 gm/dl respectively. The same values for PCF2B, PCF2C and PCF3B samples have been obtained as (Fig. 3.11) 8.71, 10.0 and 13.2 gm/dl respectively. In case of polychloroprene, there are indications from our data that at the cross over point concentration

the onset of entanglement starts (the composite curve (Figs. 3.4 and 3.5) starts exactly from the cross over point concentration in each solvent system) and from this concentration the entanglement begins to play a role in the viscosity. In case of polybutadiene (Figs. 3.12 and 3.13), as pointed out earlier that the viscosity cross over in θ solvents is not as sharp as it is found in case of polychloroprene samples. The concentrations for cross over points for PB2F1, PB2F2 and PB2F3 in benzene-isobutyl acetate system (Fig. 3.12) have been obtained as 11.7, 20.4 and 31.6 gm/dl respectively. The same values for PB2F1, PB2F2 and PB2F3 in benzene-dioxane system (Fig. 3.13) have been obtained as 11.5, 20.4 and 30.9 gm/dl respectively. From the composite curves in Figs. 3.6 and 3.7 it is observed that the data for c_{cross} (denoted by parentheses) are deep inside the composite curve in the higher concentration region, and not at the starting points from where the data deviate from the composite curve represented by dashed lines. This implies that the quasi-network formation (entanglement) is higher in polybutadiene solution than in polychloroprene solution. If the polymer concentration and molecular weight dependence of η^0 for polybutadiene sample is determined by the mechanism similar to the

one in polychloroprene samples, then the polybutadiene solutions though show greater viscosity than that of the polychloroprene solutions at the corresponding concentrations are in the Rouse region and not in entanglement region.

The dependence of cross over point concentration, c_{cross} with molecular weight for polychloroprene and polybutadiene samples are shown in Figs. 3.14 and 3.15 respectively. Two separate straight lines (instead of one) almost parallel to each other were obtained with our polychloroprene data (Fig. 3.14). From the figure it is clearly seen that the molecular weight is proportional to -1.20 power of c_{cross} . It may be pointed out that similar to our results, Bueche and coworkers¹⁰⁵ observed that the entanglement molecular weight, M_e was proportional to the -1.20 power of the concentration in case of poly(methyl methacrylate)-diethyl phthalate system and the data obtained from different solvents were fitted on a single curve. As pointed out earlier that in polychloroprene the measurements were taken at two different temperatures (25° and 45.5°C) in two systems, hence probably the use of two temperatures is the cause for this discrepancy. On the other hand, in case of polybutadiene (Fig. 3.15),

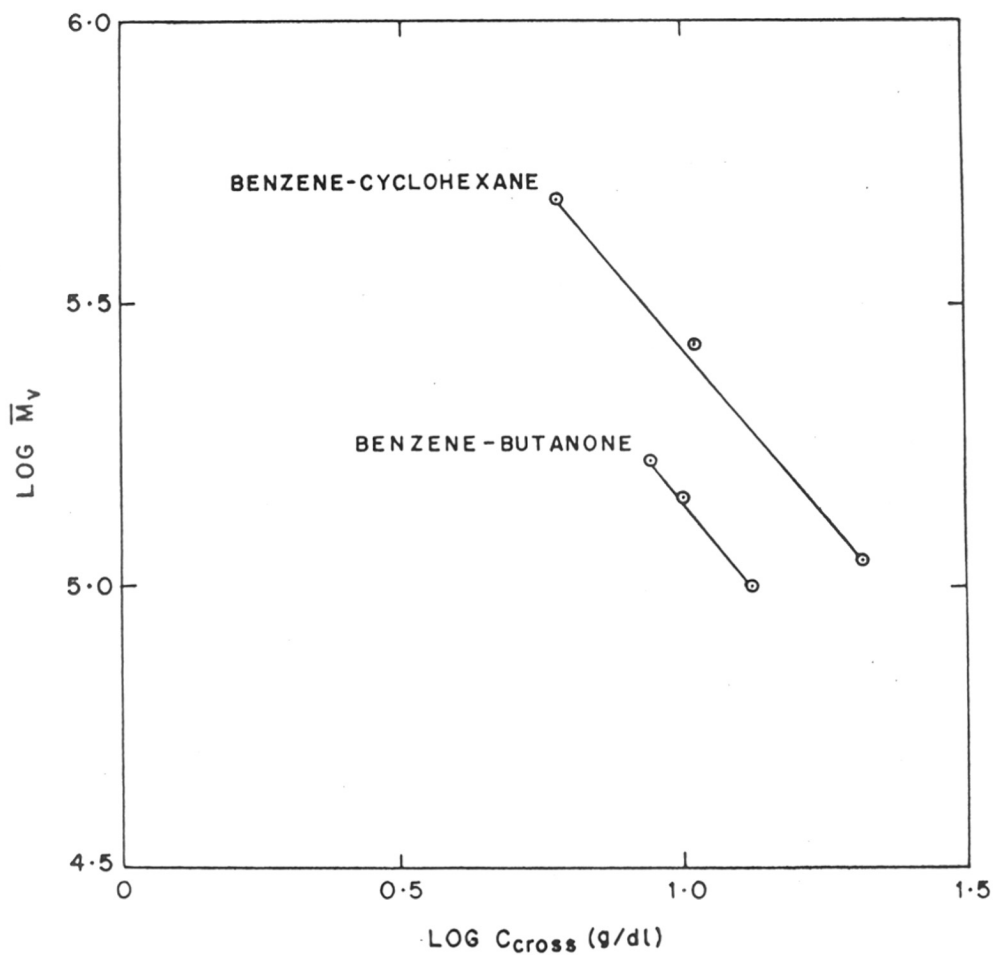


FIG.3-14: PLOTS OF $\text{LOG } \bar{M}_v$ vs. $\text{LOG } C_{\text{cross}}$ FOR POLYCHLOROPRENE SAMPLES IN GOOD AND POOR SOLVENTS.

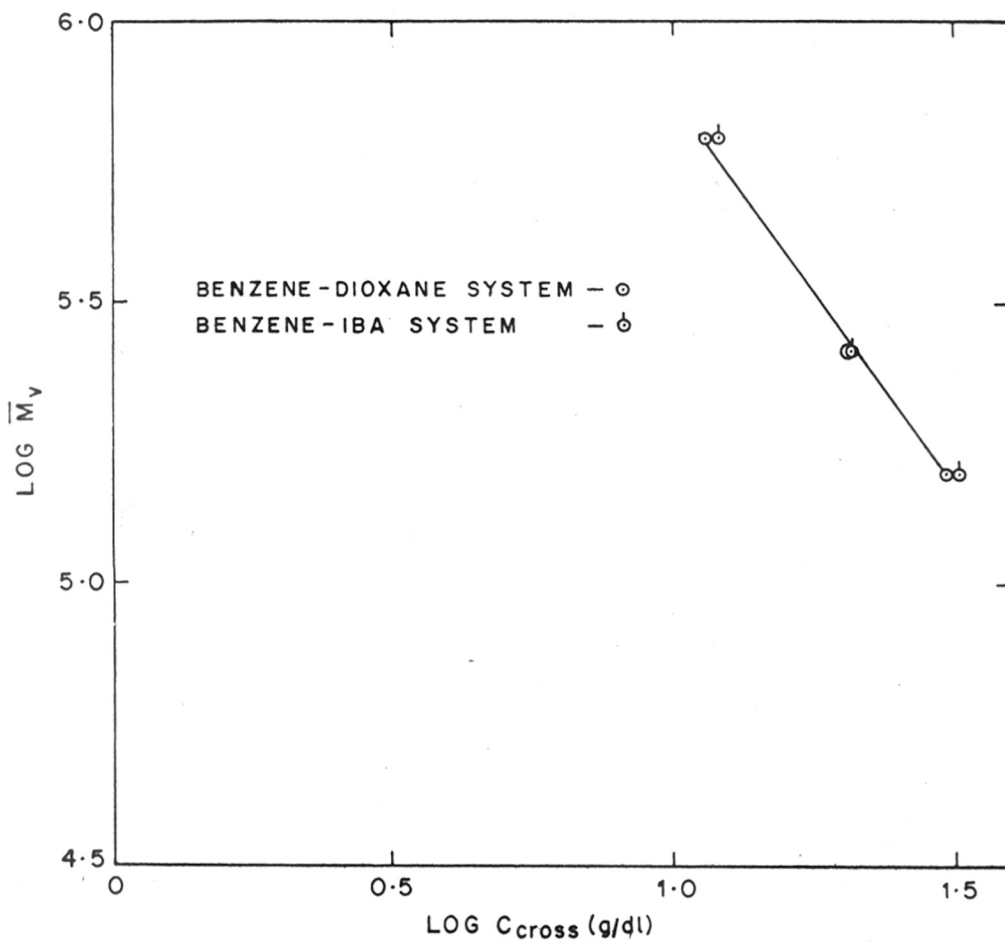


FIG. 3.15 : PLOTS OF $\text{LOG } \bar{M}_v$ vs. $\text{LOG } C_{\text{cross}}$ FOR POLYBUTADIENE SAMPLES IN GOOD AND POOR SOLVENTS.

it is observed that the molecular weight, M is proportional to -1.4 power of c_{cross} and in contrast to polychloroprene, the data obtained for polybutadiene from two systems, benzene-dioxane and benzene-IBA, are fitted in one curve. Here in both the systems, the temperatures at which the measurements were taken, were nearly the same (20.2°C and 20.5°C).

Generally the characteristic entanglement compositions are developed from the abrupt changes in the slope in the plots of $\log \eta^0$ vs. $\log c$, as well as $\log M$. If the onset point for the bulk polymer of density ζ is M^* , the estimate for the onset of entanglement in solution has been recommended by Porter and Johnson¹⁰⁶ as $c_{\text{ent}} M = c M_{\text{ent}} = \zeta M^*$. However, this scheme totally ignores the effect of the solvents. For a number of polar and non-polar polymers it was found that the characteristic entanglement composition, $(Mc)_{\text{ent}}$ was essentially constant over a range of concentrations and molecular weights¹⁰⁷. If we assume that the onset of entanglement (or reptation) has started at the cross over point concentration, then it is expected that (Mc_{cross}) values would be constant. It may be pointed out that the chain motion in the presence of restrains due to interchain entanglements

is equivalent to reptation of a chain inside a tube of diameter d formed by nearby chains^{3,5,6,27}. The values for (Mc_{cross}) for polychloroprene samples and polybutadiene samples over a wide range of concentrations and molecular weights in each system are given in Table 3.1 (column 6). In case of polychloroprene, the (Mc_{cross}) values are fairly constant over a range of concentrations and molecular weights in each system (e.g. $(Mc_{\text{cross}}) \sim 28.00 \times 10^5$ for polychloroprene-benzene-cyclohexane system and $(Mc_{\text{cross}}) \sim 14.00 \times 10^5$ for polychloroprene-benzene-butanone system) indicating that the onset of entanglement has begun at the cross over point concentration. However this entanglement composition is not independent of solvent system in the polychloroprene samples. Since two different temperatures (45.5° and 25°C) are involved in two systems it may be probable that the constancy of (Mc_{cross}) in the solvent systems is not independent of temperature at which the experiments have been carried out. Further data on this line will give an insight into this direction.

On the other hand, it is observed that in case of polybutadiene, the (Mc_{cross}) values are fairly

constant ($\sim 51.0 \times 10^5$) only in case of two samples (PB2F2 and PB2F3) of low molecular weights and the values are independent of the solvent systems (polybutadiene-benzene-dioxane and polybutadiene-benzene-isobutyl acetate) used. Here in both the systems nearly the same temperature (20.2° and 20.5°C) has been used.

3.5 Correlation of Viscosity Data

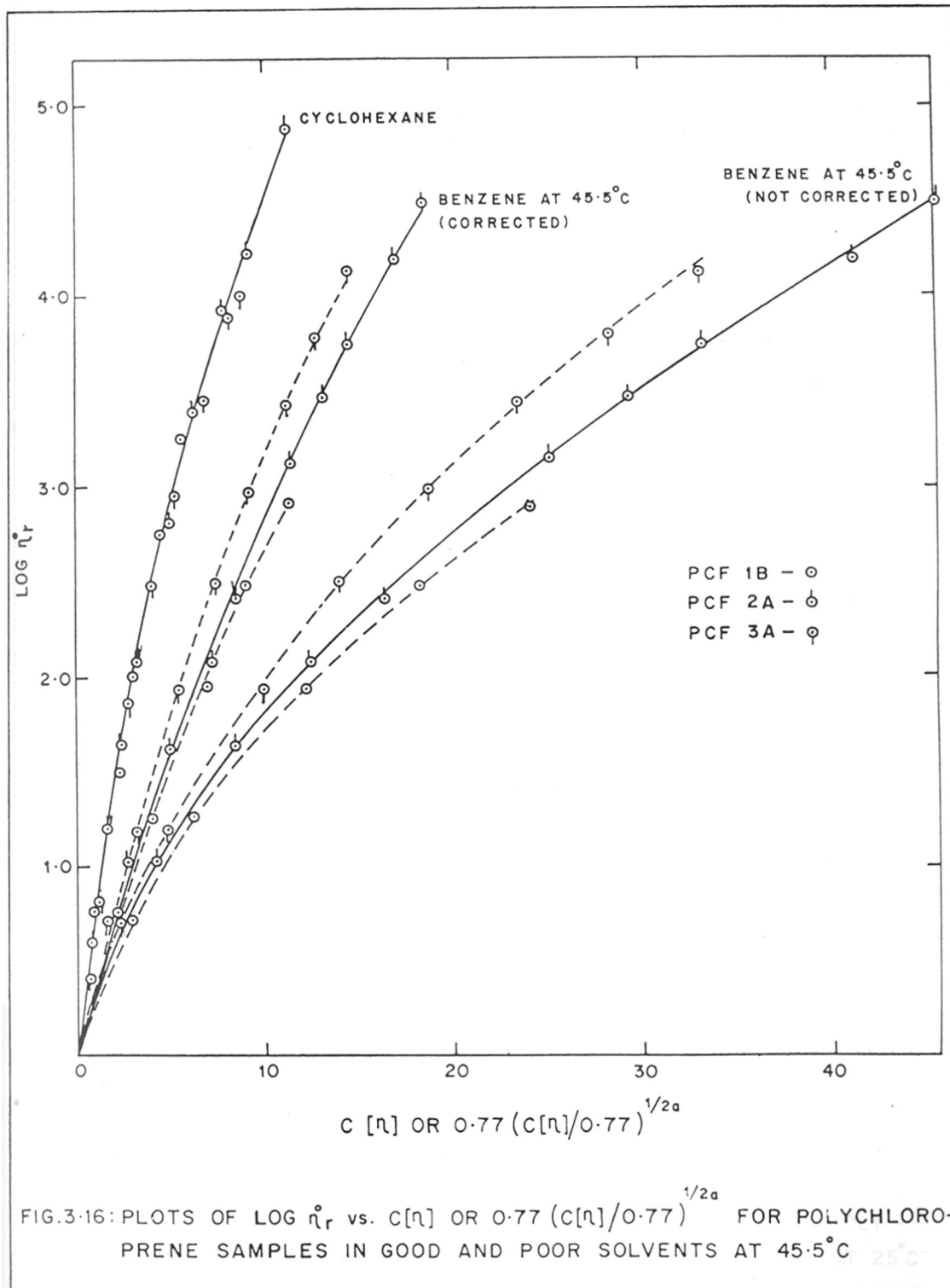
3.5.1 Method of Graessley

Several relations have been used to correlate the viscosity data for moderately concentrated solutions. The effect of solvent and concentration on chain dimensions are reflected in viscoelastic behaviour. In dilute solutions where the intrinsic viscosity, $[\eta]$ depends directly on chain dimension, the correspondence is clear^{108,109}. At moderate concentrations the viscosity is controlled primarily by the extent of coil overlap as characterized by the product $c[\eta]$ ^{70,88}. Graessley⁸⁹ recently has proposed a method for correlating viscometric properties in the semidilute region which takes into account the contraction of coil dimensions with concentration at good solvent. Since in semidilute solutions relative viscosity is

a function of coil overlap (measured in a θ solvent by the product $c[\eta]_{\theta}$ at all concentrations since coil dimensions do not change), the correlating variable, $c[\eta]$ in good solvents should be corrected for coil contraction at each concentration. The appropriate correlating variable for linear chain molecules has been derived by Graessley⁸⁹ as $0.77 \left(\frac{c[\eta]}{0.77} \right)^{1/2a}$, where a is the exponent of Mark-Houwink relation. The correlating variable, however, reduces to $c[\eta]$ in the θ solvent where the exponent $a = 0.5$.

Polychloroprene

The plots of relative viscosity, η_r° of polychloroprene samples as a function of the appropriate correlating variable are shown in Figs. 3.16 and 3.17 for benzene (45.5°C) and cyclohexane solutions, and benzene (25°C) and butanone solutions respectively. The values of exponent a for polychloroprene in benzene solution at 45.5°C and 25°C have been taken as 0.64 and 0.62 respectively. For comparison, the plots of relative viscosity, η_r° versus the correlating variable, $c[\eta]$ in good solvent (without correction for change of coil dimension with concentration) has been shown on the same graph. In good solvents,



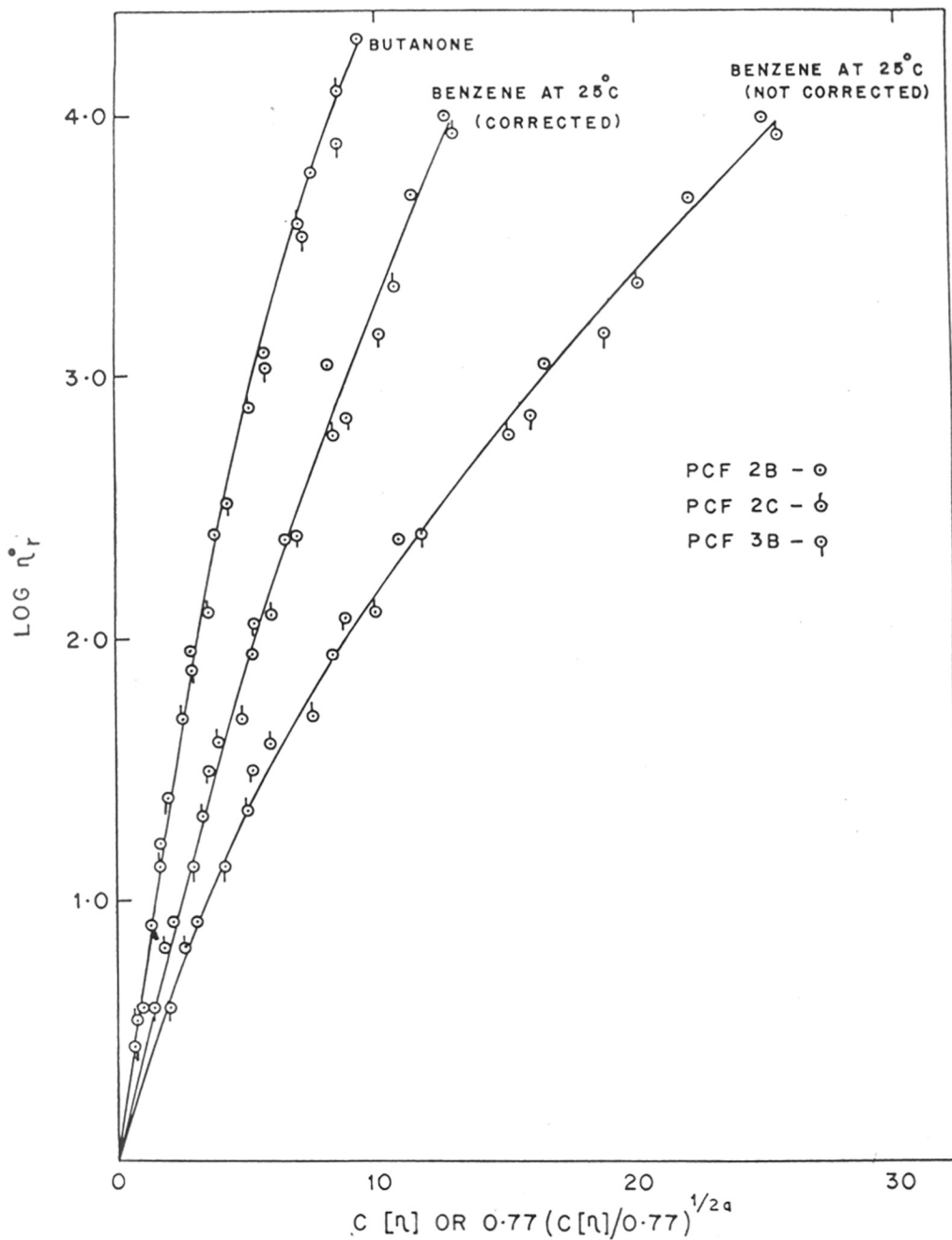
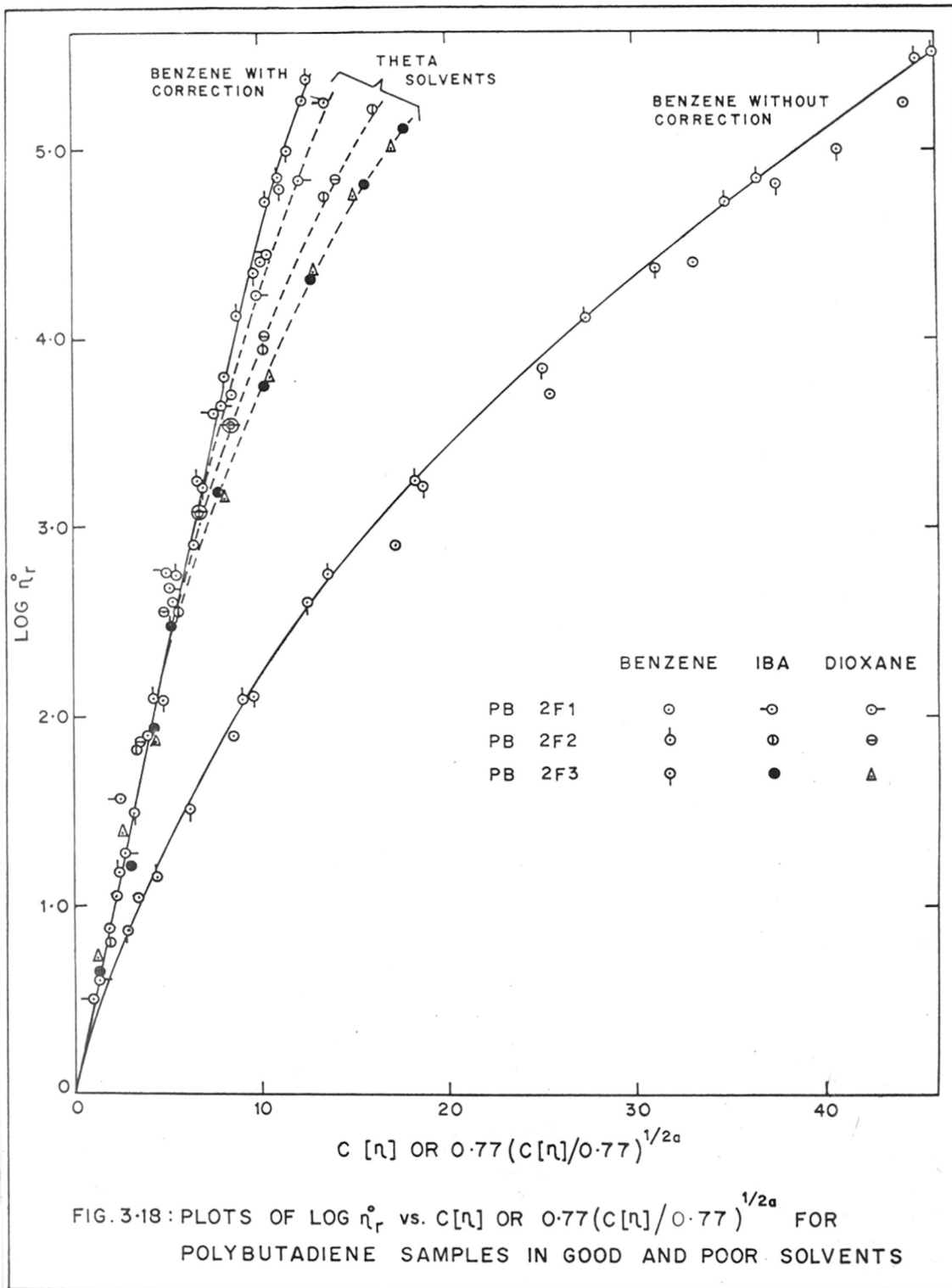


FIG. 3-17: PLOTS OF $\text{LOG } \eta'_r$ vs. $C[\eta]$ OR $0.77(C[\eta]/0.77)^{1/2a}$ FOR POLY-CHLOROPRENE SAMPLES IN GOOD AND POOR SOLVENTS AT 25°C

especially in benzene at 45.5°C , the relative viscosity increases less rapidly with $c [\eta]$ compared to that in θ solvents and small but systematic differences appear for samples of different molecular weights. It may be pointed out that Graessley observed small but systematic differences⁸⁹ similar to our results in the data⁴ of polystyrene samples of different molecular weights in toluene. The most important point that emerges from this observation is that the appropriate correction for variations in chain dimensions with concentration has positively moved the correlations for θ and good solvents closer to a common curve but it has not been able to eliminate the differences between the data completely.

Polybutadiene

Similar plots of relative viscosity as a function of appropriate correlating variable for polybutadiene samples of different molecular weights in both good and θ solvents are shown in Fig. 3.18. The value of the exponent for polybutadiene in benzene solution at 20.5°C has been taken as 0.73 and in isobutyl acetate (20.5°C) and dioxane (20.2°C) as 0.5. For comparison, the plots of relative



viscosity versus the uncorrected correlating variable, $c[\eta]$ in benzene (good solvent) has been shown on the same graph (Fig. 3.18). In θ solvents the scatter of data at the higher concentration was such that they can be fitted in three different curves (shown by dashed lines) instead of a single one. It is not understood at present why the three samples yielded three separate curves instead of a single one. However, in benzene (good solvent), the deviations of the data was very small, and only a single curve has been drawn for three samples. In good solvent, similar to the results in polychloroprene, the relative viscosity increases less rapidly with $c[\eta]$ compared to that in θ solvents. It may be pointed out that since the three polybutadiene samples have produced three different curves instead of a single one, especially at higher concentration region in θ solvents, the superposition of data obtained in benzene (good solvent) and θ solvents (IBA and dioxane) has become somewhat irrelevant. However, the curve for benzene obtained after correction for chain contraction in concentrated region was found to be exactly fitting with the curve obtained for the θ solvents in the lower concentration region, while

at the higher concentration region, it has moved away slightly from the curves (three) obtained in θ solvents, after crossing them. A slight over estimation of data by this correction seems to have been effected.

3.5.2 Method of Dreval and coworkers

Another correlation of η° which is connected to $c[\eta]$ may be considered here also. It is well known that in very dilute solution the viscosity tends to the limiting behaviour

$$\eta_r^{\circ} = \exp(c[\eta]) \quad (3.1)$$

and intrinsic viscosity, $[\eta]$ with the Flory-Fox equation is given as $[\eta] = \phi (\bar{S}^2)^{3/2} / M$, where $\phi \approx 2.5 \times 10^{23}$ (c.g.s. units) and $(\bar{S}^2)^{1/2}$ is the root mean square radius of gyration. In terms of $[\eta]$, the overlap concentration, c^* at moderately concentrated solution is given as

$$c^* = \frac{6^{3/2} \phi}{8 N_a} \frac{1}{[\eta]} = \frac{0.77}{[\eta]} \quad (3.2)$$

in which N_a is the Avogadro's number.

To correlate the viscometric data for moderately concentrated solutions, Simha and coworkers¹⁰⁹ have

used a relation of the form (for $\eta_r^0 \gg 1$)

$$\eta_r^0 = c[\eta] P(cM^\epsilon) \quad (3.3)$$

where ϵ is often equal to $d \ln [\eta] / d \ln M$. If it is obtained precisely then Eq. (3.2) reduces to

$$\eta_r^0 = H c[\eta] \quad (3.4)$$

which emphasizes the role of chain dimensions in dilute solutions (with screening length \approx root mean square radius of gyration) in the correlation of η^0 with c and M^{110} . Hence Eq. (3.4) may be considered as a generalization of Eq. (3.1). One variation of Eq. (3.4) is the Martin's relation

$$\eta_r^0 = 1 + c[\eta] \exp(K'_M c[\eta])$$

or

$$\eta_{sp}^0 / (c[\eta]) = \bar{\eta} = \exp(K'_M c[\eta]) \quad (3.5)$$

Dreval and coworkers⁸⁸ have used this Martin relation to correlate the viscosity data in moderately concentrated solution in which a plot of $\log [\eta_{sp}^0 / (c[\eta])]$ vs. $c[\eta]$ produced a single curve for samples of various molecular weights in a single good solvent

over the entire concentration range. However, a similar plot of $\log [\eta_{sp}^0 / (c [\eta])]$ as a function of concentration, c was proposed by Gandhi and Williams^{62,63} but this produced separate curves in an ordered way as a function of solvent power. The data for $c [\eta]$ and $\bar{\eta}$ i.e. $[\eta_{sp}^0 / (c [\eta])]$ for polychloroprene and polybutadiene samples are given in Tables 2.10 to 2.30 (columns 4 and 5).

Polychloroprene

The plots of $\log [\eta_{sp}^0 / (c [\eta])]$ vs. $c [\eta]$ for polychloroprene samples in good and θ solvents are shown in Figs. 3.19 and 3.20 respectively. As expected the data in good solvents (benzene at two different temperatures (25° and 45.5°C) are considered here as two different solvents) are fitted in two separate curves according to their solvent power (the coil dimensions vary according to their solvent power), whereas the data taken in poor solvents (butanone and cyclohexane) are fitted in a single curve as the different θ solvents are considered to have the similar solvent power, where the chain dimensions remain the same. The intrinsic viscosity, $[\eta]_{\theta}$ of polychloroprene in two θ solvents, cyclohexane and butanone, was proportional to $M^{0.50}$.

The solvent solute interaction constant, K_M obtained from the Martin equation (Eq. 3.5) has been used to normalize the dimensionless concentration, $c[\eta]$ so as to move the correlations for Θ and good solvents to a common curve. It may be pointed out that the Huggins constant, K_H is theoretically equal to Martin constant, K'_M and K_M is taken as $K'_M/2.303$. The K_M was determined from the initial slope of $\log \bar{\eta}$ vs. $c[\eta]$ curves as a rheological measure of interactions in dilute solutions. There was a small but systematic difference of the data (Fig. 3.19) for three polychloroprene samples of different molecular weights in benzene at 45.5°C , so three different K_M values (instead of one) were determined from the curves. This scatter of data may be due to large differences of molecular weights among the samples. However, for polychloroprene samples in benzene at 25°C , only one value for K_M was obtained as the deviation of the data was very small and only a single curve was drawn with the data (Fig. 3.20). The values for K_M obtained at different solvents are listed in Table 3.2. In all cases the normalization of the correlating variable, $c[\eta]$ with Martin constant, K_M reduced all experimental

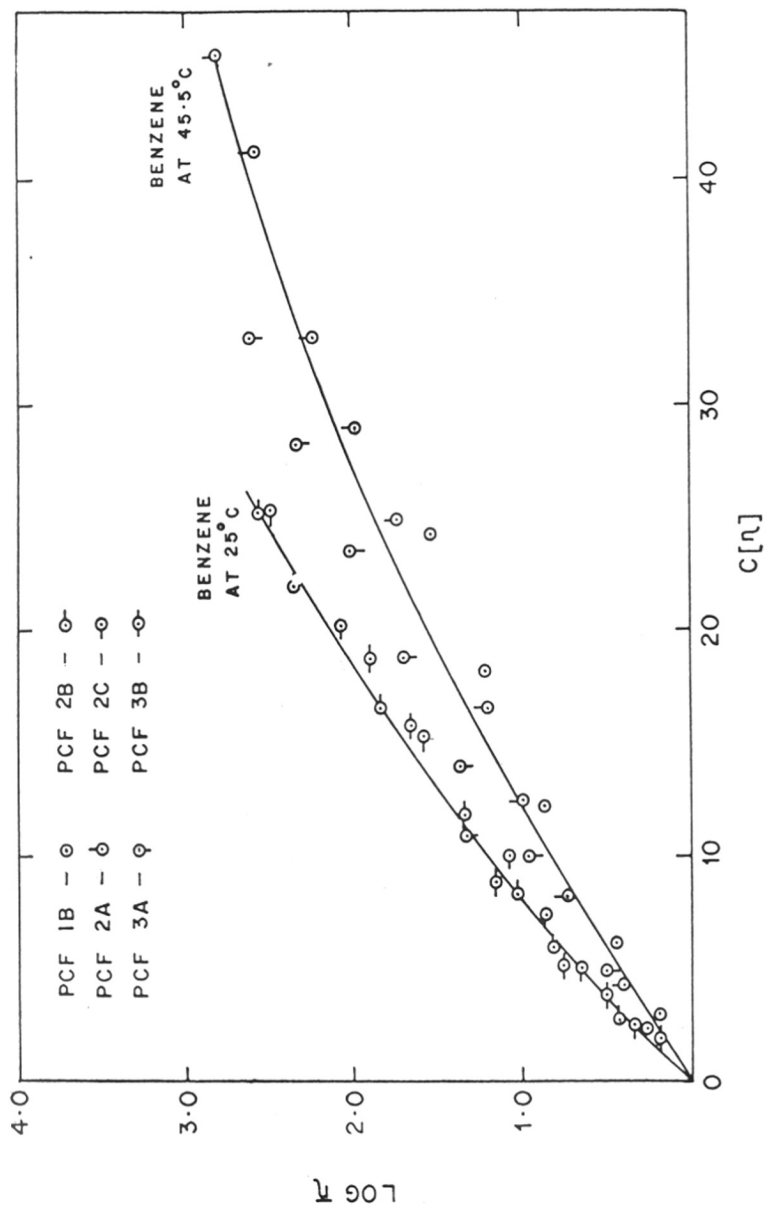


FIG. 3.19: PLOTS OF $\text{LOG } \bar{\eta}$ vs. $\bar{c}[\eta]$ FOR POLYCHLOROPRENE SAMPLES IN DIFFERENT GOOD SOLVENTS.

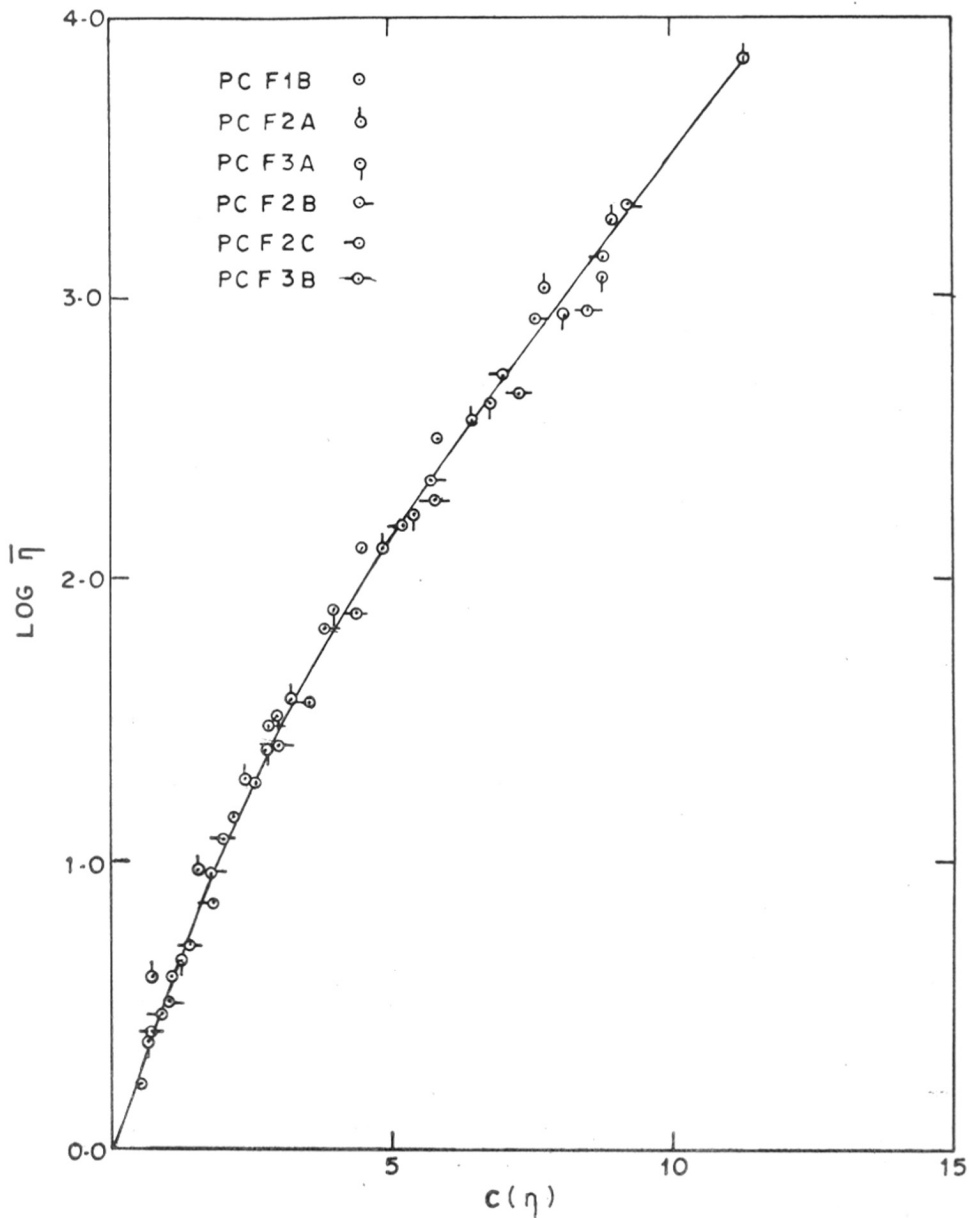


FIG. 3.20. PLOTS OF $\text{LOG } \bar{\eta}$ vs $c(\eta)$ FOR POLYCHLOROPRENE SAMPLES IN CYCLOHEXANE AND BUTANONE SOLUTIONS

Table 3.2

The values of Martin constant, K_M and expansion factor α^3 for polychloroprene-solvent systems.

Sample	Solvent, Temperature (°C)	K_M	$\alpha^3 = \frac{[\eta]}{[\eta]_\theta}$
PCF1B	Benzene, 45.5	0.071	4.32
PCF2A		0.085	4.05
PCF3A		0.099	3.48
PCF2B, PCF2C, PCF3B	Benzene, 25	0.127	2.89, 2.86, 2.72
PCF1B, PCF2A, PCF3A	Cyclohexane, 45.5	0.497	1.0
PCF2B, PCF2C, PCF3B	Butanone, 25	0.497	1.0

data for each polymer sample to the master curve as shown in Fig. 3.21. The zero shear viscosity master curve as obtained with our experimental data for polychloroprene samples by plotting $\log \bar{\eta}$ vs. $K_M c[\eta]$ is valid for the entire concentration range independent of molecular weight and nature of solvent. The introduction of Martin constant, K_M allows one to take into account effectively the flexibility of the macromolecular chain and the polymer solvent interaction. From Table 3.2 it is observed that as the quality of the solvent deteriorates (becomes poor), the quantity K_M and consequently the viscosity of the solution becomes greater. The Martin constant, K_M can be correlated with different thermodynamic properties of polymer solutions particularly with the expansion factor, α of a linear chain polymer coil. The values for α^3 have been determined as the ratio of intrinsic viscosity, $[\eta]$ at a given solvent to that in a θ solvent. The plots of K_M as a function of expansion factor is shown in Fig. 3.22. The increase in expansion factor is accompanied with the decrease of K_M . The normalization of the correlating variable, $c[\eta]$ with K_M hence in effect may be to make a correction of chain dimension related to expansion factor.

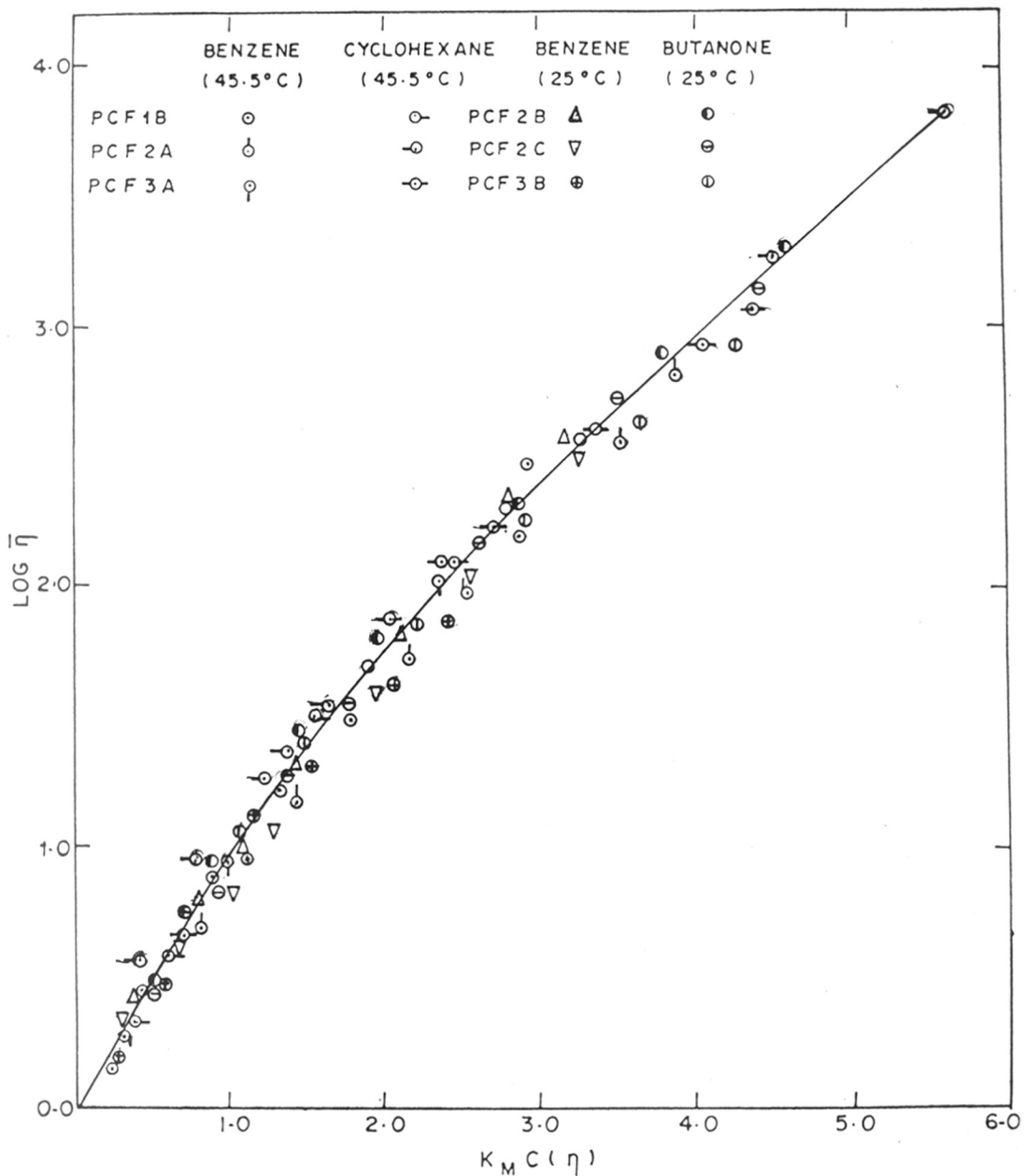


FIG. 3-21. PLOTS OF $\text{LOG } \bar{\eta}$ vs $K_M C(\eta)$ FOR POLYCHLOROFRENE SAMPLES IN GOOD AND POOR SOLVENTS

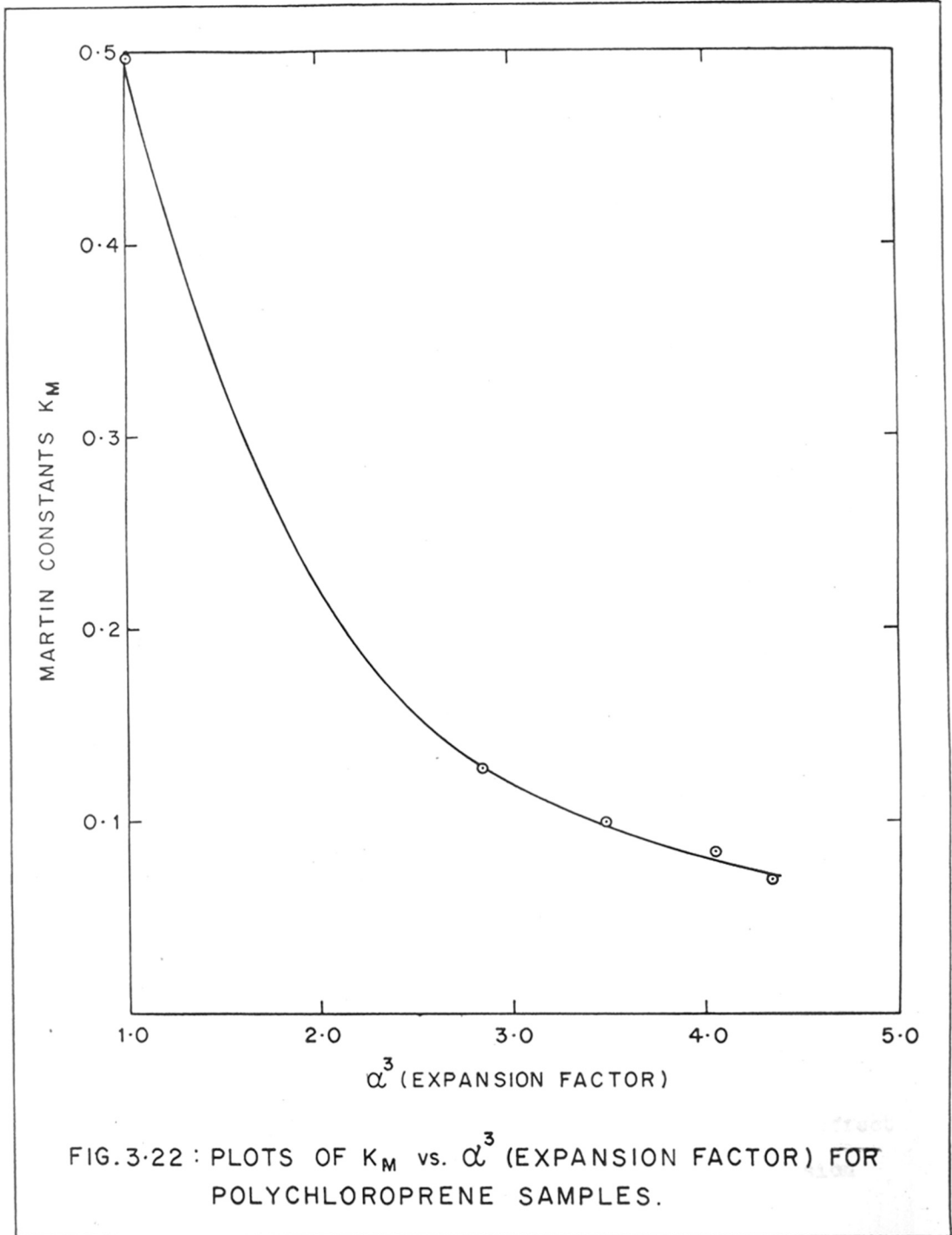


FIG.3-22 : PLOTS OF K_M vs. α^3 (EXPANSION FACTOR) FOR POLYCHLOROPRENE SAMPLES.

In conclusion it may be stated that in case of polar polymer polychloroprene the appropriate correction of the correlating variable, $c[\eta]$ by the method given by Graessley for the contraction of coil dimension with concentration in good solvents no doubt improves the correlation, but it does not eliminate completely the difference between the data obtained in good and θ solvents. Further this method does not account for the increased deviations with increase of molecular weight which appeared in good solvent correlation⁸⁹.

On the other hand, the correlation of the data by the method given by Dreval and coworkers (plots of $\log \bar{\eta}$ vs. $c[\eta]$) produced a single curve for solutions of polychloroprene samples in two different θ solvents, whereas in good solvents separate curves for each solvent was produced. However, the normalization of the reduced concentration, $c[\eta]$ by Martin constant, K_M eliminated completely all the differences between the data obtained at θ and good solvents. K_M can be correlated with the expansion factor, α of a polymer coil. The normalization of the correlating variable, $c[\eta]$ with K_M hence in effect is to make a suitable correction for chain dimension

characterized by the expansion factor. This method has no doubt yielded better correlation of the data for polychloroprene samples than the previous one.

Polybutadiene

The plots of $\log [\eta_{sp}^0 / (c [\eta])]$ as a function of the correlating variable, $c [\eta]$ for polybutadiene samples in good and θ solvents are shown in Figs. 3.23 and 3.24 respectively. Similar to our results for polychloroprene, the data taken in good solvent (benzene at 20.5°C) for three samples are fitted in a single curve, while the data taken in poor solvents (IBA and dioxane) for three polymer samples of different molecular weights are fitted in three separate curves which is certainly an observation of very different in nature. Since the intrinsic viscosity, $[\eta]_{\theta}$ of the polymer in two θ solvents (dioxane and IBA) was proportional to $M^{0.5}$ and since the two θ solvents are considered to have the similar solvent power, it is not understood why the plots yielded three separate curves instead of a single one, in the present case. However, the data for two θ solvents for each sample are fitted in one curve. The Martin constant, K_M was determined in this case

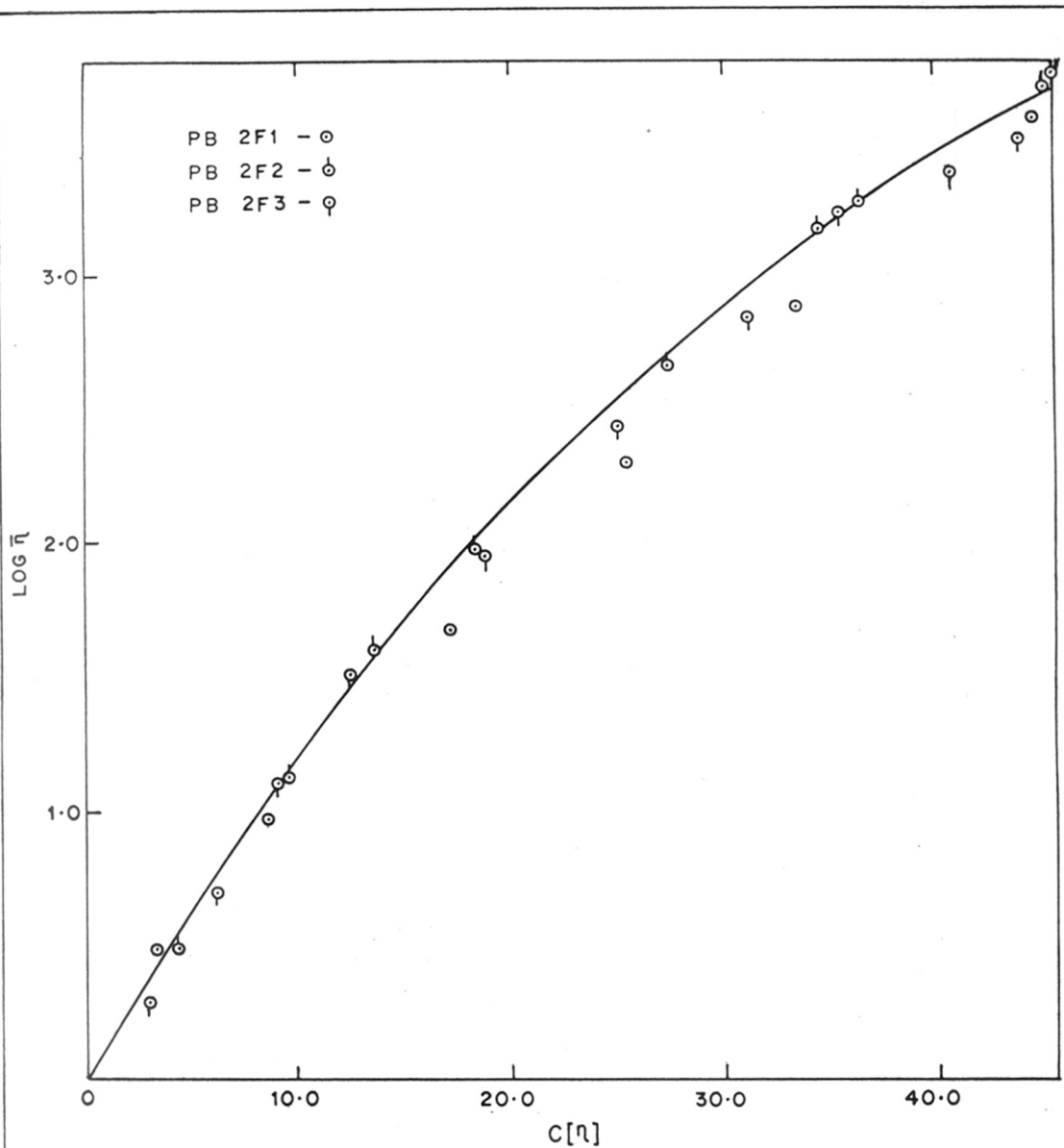


FIG.3.23: PLOTS OF $\text{LOG } \bar{\eta}$ vs. $C[\eta]$ FOR POLYBUTADIENE SAMPLES IN GOOD SOLVENTS (BENZENE)

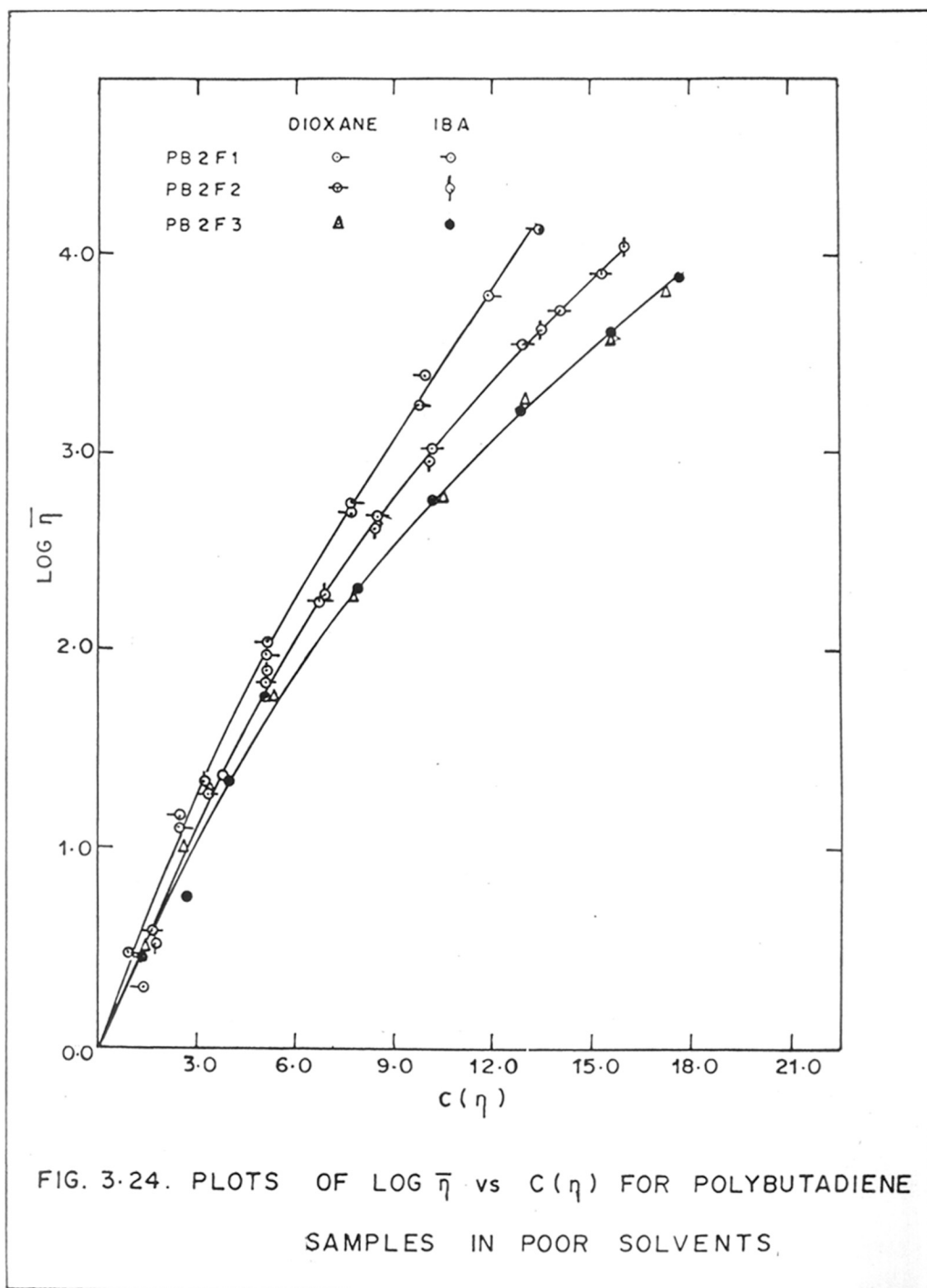


FIG. 3.24. PLOTS OF $\log \bar{\eta}$ vs $c(\eta)$ FOR POLYBUTADIENE SAMPLES IN POOR SOLVENTS.

also from the initial slope of $\log \bar{\eta}$ vs. $c[\eta]$ curves and K_M has been obtained as $K_M'/2.303$. Since three separate curves were obtained for three samples in θ solvents, three different values of K_M have been obtained for them, whereas in benzene only one K_M value has been obtained since the data are fitted in a single curve. The values of K_M obtained for different samples in good and poor solvents are listed in Table 3.3. It is observed that as the solvent becomes poor, the value of K_M increases. These K_M values have been used to normalize the correlating variable, $c[\eta]$ so as to move the correlations for θ and good solvents to a common curve. The plots of $\log \bar{\eta}$ vs. $K_M c[\eta]$ for all the samples in good and θ solvents are shown in Fig. 3.25. It is observed from the figure that the normalization of the correlating variable, $c[\eta]$ with Martin constant, K_M reduced all experimental data for the three polymer samples of different molecular weights in different solvents to the master curve. This zero shear viscosity master curve is valid for entire range of concentration independent of molecular weight and nature of solvents.

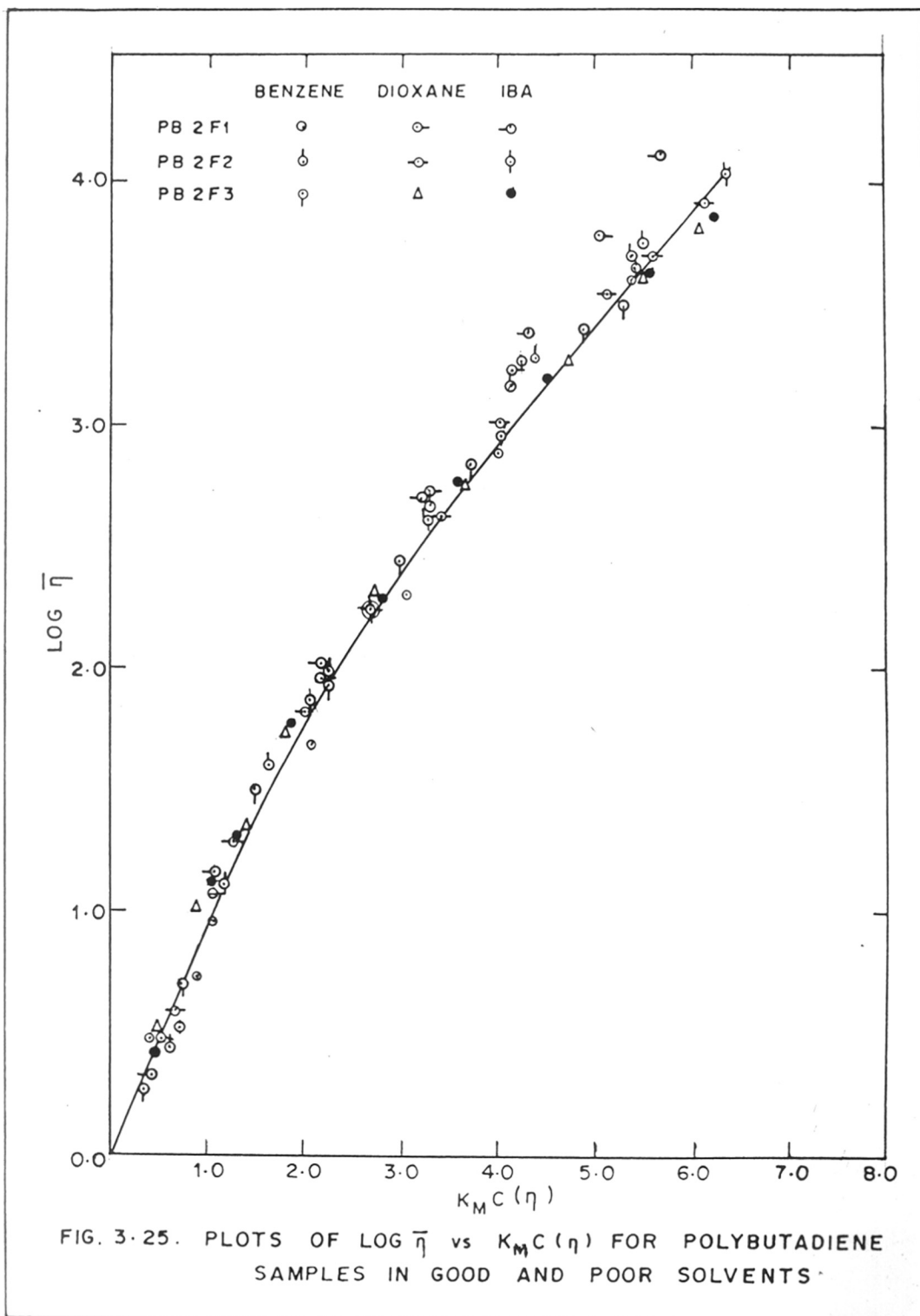


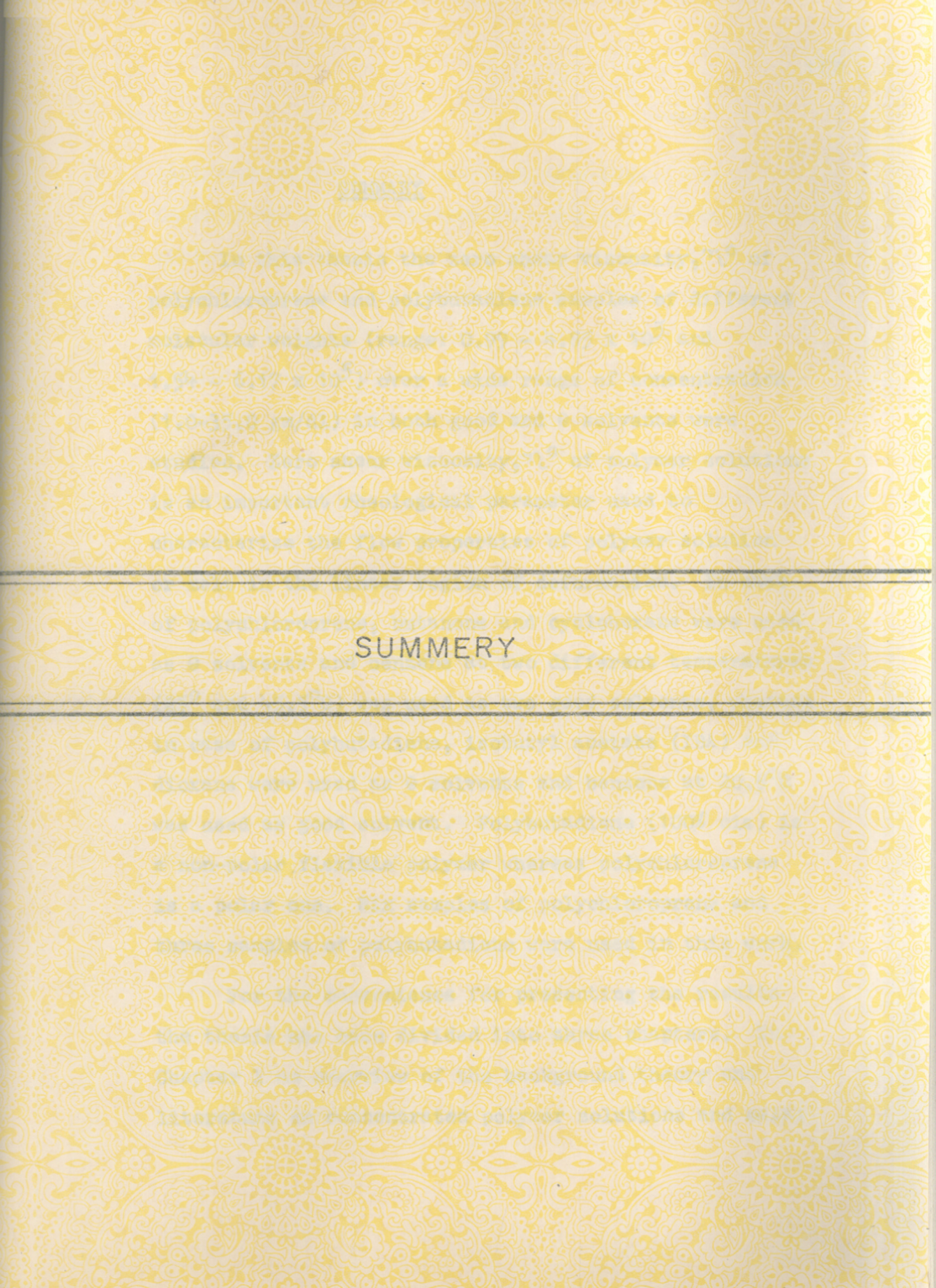
Table 3.3

Values of Martin constant, K_M for polybutadiene samples in good and poor solvents

Sample	Solvent, Temperature (°C)	K_M
PB2F1, PB2F2, PB2F3	Benzene, 20.5	0.120
PB2F1	IBA, 20.5 and Dioxane, 20.2	0.424
PB2F2		0.398
PB2F3		0.352

In conclusion it may be stated that the correlation of the data by the method given by Dreval and coworkers (plot of $\log \bar{\eta}$ vs. $c[\eta]$) produced a single curve with comparatively less scatter of data than that of polychloroprene samples in benzene (good solvent), whereas in θ solvents though the data for two θ solvents were fitted into a single curve for each polymer sample but three separate curves (instead of a single one) were obtained for three polybutadiene samples. However, the normalization of the correlating variable, $c[\eta]$ by Martin constant, K_M eliminated completely all the differences between the data obtained for three samples in good and θ solvents.

On the other hand, the appropriate correction of the correlating variable, $c[\eta]$ by the method given by Graessley for contraction of coil dimension with concentration in good solvents has moved the correlation for θ and good solvents to a common curve especially in lower concentration region, but at higher concentration region, an over estimation of data by this correction seems to have been effected. The correlation of data by either of the two methods seems to be possible in case of non-polar flexible polymer, polybutadiene.



SUMMERY

SUMMARY

In this thesis the zero shear viscosity, η^0 of polychloroprene and polybutadiene samples of different molecular weights (range: $0.99 - 4.85 \times 10^5$ and $1.54 - 6.17 \times 10^5$) over a wide range of concentration (1.0-35.0 gm/dl) in both good and θ solvents were studied. Zero shear viscosity, η^0 of polymer solutions is an important rheological parameter used to characterize the flow properties of polymer solution or melt in the linear region of deformation. In case of polychloroprene, butanone and cyclohexane were used as θ solvents and benzene at two different temperatures (25° and 45.5°C) was used as two good solvents, whereas in case of polybutadiene, isobutyl acetate (IBA) and dioxane were used as θ solvents and benzene at 20.5°C was used as good solvent. Polybutadiene (100% cis) is a non-polar flexible polymer whereas polychloroprene is a polar one. Six samples of polychloroprene and three samples of polybutadiene were used in this work.

For the convenience for presenting the results the thesis has been divided into three chapters. In Chapter I an overview of the background theory and literature on concentrated polymer solutions and melts

pertinent to this work has been described. The description of the experiments and results have been given in Chapter II. The zero shear viscosity of concentrated polymer solutions was measured by means of a Brookfield LVT viscometer and the solvents and dilute solutions (5% or below) with a Maron-type capillary viscometer with continuously varying pressure head. Purification and fractionation of the polymers were done with utmost care. The molecular weights of the polymer samples were measured with light scattering method and the $[\eta] - \bar{M}_w$ relation was determined by comparing the molecular weights, \bar{M}_w with intrinsic viscosity, $[\eta]$ measured with various solvents. The preparation of solutions was made by mixing the weighed amounts of the polymer and the solvent and the relations of apparent specific volumes, V_p and V_s of the polymer and solvent respectively were used to calculate the concentration (gm/dl) of solution.

In Chapter III the discussion of the results has been presented. The zero shear viscosity for all the polymer samples studied is strongly dependent on concentration. The slope of $d \log \eta^0 / d \log c$ becomes steeper with increasing concentration as entanglement of polymer chains and cross linkings are increased with

increasing concentration. Superposition of viscosity data for the samples of the two polymers, polychloroprene and polybutadiene, has been made so as to give a single composite curve for each solvent (good and poor) by shifting them vertically by a factor $(M^0/M)^{3.4}$, where M^0 represents the molecular weight of the reference sample. The superposition was not successful, however, over the entire range of concentration. The shift factor is found to be exactly proportional to $M^{3.4}$ in the higher concentration region for both the polymers. The results indicate that the relation $\eta^0 \propto M^{3.4}$ was obeyed by the data obtained from both polychloroprene samples and polybutadiene samples. The relation that the relative viscosity, η_r^0 is a single function of $c^5 M^{3.4}$ was examined with the data obtained from samples of the two polymers. In case of polybutadiene, the double logarithmic plots of η_r^0 as a function of $c^5 M^{3.4}$ yielded a single composite curve approximating a straight line with slope of unity at the higher values of the variables. The results indicate that over a considerable range of the variables (concentration and molecular weight) at a constant temperature the relative viscosity is a single function of $c^5 M^{3.4}$. However in case of polychloroprene samples the same plots of η_r^0 vs. $c^5 M^{3.4}$ in good and θ solvents yielded two separate curves

parallel to each other. The data taken in benzene and butanone solutions at 25°C were fitted in one curve and the data for benzene and cyclohexane solutions at 45.5°C were fitted in another one. Each curve at the higher values of the variables produced a straight line with slope of unity. Since the data taken at two different temperatures (25°C and 45.5°C) are fitted in two separate curves, the discrepancy is probably due to two temperatures used for measurements.

The zero shear specific viscosity, η_{sp}^0 in θ solvents at the higher concentration region is found to be higher compared to the values obtained in good solvents. In case of polybutadiene samples, the viscosity cross over in θ solvents is not as sharp as is found in case of polychloroprene samples and that cross over too has taken place in the range of concentration of 11.7 - 31.6% polymer which is comparatively higher than that of polychloroprene samples (6.05-21.0% polymer). The result supports the idea that there exists a relationship between viscosity cross over and polymer polarity supporting the idea of enhanced intermolecular association in poor solvents. Further the result supports another idea given by Vinogradov and coworkers that a dependence between glass transition

temperature, T_g for the polymer solvent mixture and viscosity cross over in poor solvent might develop as free draining behaviour is approached at higher concentration, since the viscosity must lose its direct proportionality to solvent viscosity and become proportional instead to a local frictional coefficient, ζ^0 . The value of ζ^0 depends on the nature of both solvent and polymer since both influence the free volume and glass temperature of the mixture. The glass temperature of most solvents is well below room temperature. In polybutadiene solutions T_g probably remains relatively constant and always well below room temperature because T_g for pure polybutadiene is so low ($T_g = -90^\circ\text{C}$). The effect for polychloroprene ($T_g = -50^\circ\text{C}$) should be larger because T_g for its solution must rise somewhat with increasing concentration since the ζ^0 for the polar polymer will be different than that of the non-polar one.

There are indications from the data for polychloroprene samples that at the cross over point concentration, c_{cross} the onset of entanglement begins and from this concentration the entanglement begins to play a role to the viscosity. In case of polybutadiene the data for c_{cross} are found deep inside the composite curve in the higher concentration region and not at the starting points from where the data deviate from the

composite curve as is found in case of polychloroprene. This implies that the quasi-network formation (entanglement) is higher in polybutadiene solutions than in polychloroprene solutions. If the polymer concentration and molecular weight dependence of η^0 for polybutadiene samples is determined by the mechanism similar to the one in polychloroprene samples, then the polybutadiene samples though show greater viscosity than that of the polychloroprene samples at the corresponding concentration are in the Rouse region and not in the entanglement region.

The cross over point concentration, c_{cross} is dependent on the molecular weight of the samples. In case of polychloroprene, the molecular weight, M is proportional to -1.20 power of c_{cross} but the data obtained from two solvent systems (benzene-cyclohexane and benzene-butanone) yielded two separate curves instead of a single one. As pointed out earlier that in polychloroprene solutions the measurements were taken at two different temperatures (45.5° and 25°C), hence temperature probably is the reason for this discrepancy. However, in case of polybutadiene, the molecular weight was found to be proportional to -1.4 power of c_{cross} and in contrast to polychloroprene, the data obtained

from two solvent systems (benzene-dioxane and benzene-IBA) were fitted in one single curve. Here in both the systems the temperature at which the measurements were taken, were nearly the same (20.2° and 20.5°C). Further in case of polychloroprene, the ($M_{c_{\text{cross}}}$) values are fairly constant over a wide range of concentrations and molecular weights in each solvent system (e.g., ($M_{c_{\text{cross}}}$) $\sim 28.00 \times 10^5$ for polychloroprene-benzene-cyclohexane system and ($M_{c_{\text{cross}}}$) $\sim 14.00 \times 10^5$ for polychloroprene-benzene-butanone system) indicating that the onset of entanglement (where the polymer chain diffuse freely by reptation) has began at the cross over point concentration. However, the entanglement composition is not independent of solvent system (probably the reason for this discrepancy is the two different temperatures at which the measurements were taken in two solvent systems). On the other hand it is observed that in case of polybutadiene the ($M_{c_{\text{cross}}}$) values are somewhat constant ($\sim 51.00 \times 10^5$) only in case of two samples of lower molecular weights (PB2F2 and PB2F3) and the values are independent of the solvent systems (polybutadiene-benzene-IBA and polybutadiene-benzene-dioxane) used as the temperature for measurements in both the systems here is nearly the same.

In order to correlate the viscosity data obtained at good and poor solvents, two methods, one given by Graessley and the other given by Dreval and coworkers involving the correlating variable, $c[\eta]$ were considered. In the former method the contraction of dimension of chains with concentration in good solvent has been accounted, whereas in the second method, the correlating variable, $c[\eta]$ has been normalized by the Martin constant, K_M which is related to the flexibility of macromolecular chain and polymer solvent interaction. Since in semi-dilute solutions relative viscosity is a function of coil overlap, the correlating variable, $c[\eta]$ in good solvent should be corrected for coil contraction at each concentration. The appropriate correlating variable which takes into account the contraction of coil dimensions with concentration at good solvent has been derived by Graessley as $0.77 \left(\frac{c[\eta]}{0.77}\right)^{1/2a}$ (a is the exponent of Mark-Hauwink relation). When the exponent $a = 0.5$, the appropriate correlating variable reduces to $c[\eta]$ in θ solvent. In case of polychloroprene in good solvents, especially in benzene at 45.5°C the relative viscosity, η_r° increases less rapidly with $c[\eta]$ compared to that of in θ solvents. The most important

point that emerges from the polychloroprene results is that the appropriate correction for variation in chain dimensions with concentration has positively moved the correlations for Θ and good solvents closer to a common curve but it has not been able to eliminate the differences between the data completely.

In polybutadiene the plots of relative viscosity, η_r^0 as a function of correlating variable, $c[\eta]$ in Θ solvents produced three separate curves for three polymer samples, instead of a single one as was obtained in case of polychloroprene samples, which is rather unusual. However in benzene (good solvent) only one curve was obtained for the same polybutadiene samples having different molecular weights. Here in this case the appropriate correction of correlating variable for chain contraction in concentrated region in good solvent moved the data to a common curve especially in the lower concentration region, but at the higher concentration region a slight over estimation of data seems to have been effected.

In the method given by Dreval and coworkers for the correlation of viscosity data in good and poor solvents, Martin relation, $\eta_{sp}^0/(c[\eta]) = \bar{\eta} = \exp K_M' (c[\eta])$ has been used. In case of polychloroprene the plots of $\log \bar{\eta}$ as a function of correlating variable, $c[\eta]$

produced a single curve in two different θ solvents (butanone and dioxane) over the entire concentration region, but in case of two good solvents (benzene at 25° and benzene at 45.5°C were considered as two good solvents) the similar plots yielded, instead of one, two separate curves. However, the normalization of the correlating variable, $c[\eta]$ by Martin constant, K_M (which is equal to $K_M^1 / 2.303$) which is related to the flexibility of macromolecular chain and polymer-solvent interaction, reduced all data of the six polychloroprene samples to a common curve. This zero shear viscosity master curve is valid for entire range of concentration independent of molecular weight and nature of solvents. K_M can be correlated with the expansion factor, α of a polymer coil. The increase in expansion factor is accompanied with the decrease of K_M . The normalization of the correlating variable $c[\eta]$ with K_M hence in effect may be to make a correction of chain diminution related to expansion factor. This method has no doubt yielded a better correlation of the data in good and poor solvents for polychloroprene samples than the previous one.

In case of polybutadiene, the plots of $\log \bar{\eta}$ as a function of correlating variable, $c[\eta]$ yielded

a single curve for three samples in good solvent, benzene but in poor solvents (dioxane and IBA) the same plots yielded three separate curves for three polymer samples instead of a single one, the reason for which is not known at present. However, the normalization of the correlating variable, $c[\eta]$ by Martin constant, K_M eliminated completely all the differences between the data obtained for the three samples in both good and poor solvents. This zero shear master curve is valid for entire concentration range independent of molecular weights and nature of solvents. The correlation of data by either of the two methods seems to be possible in case of non-polar flexible polymer, polybutadiene.



REFERENCES

REFERENCES

1. Onogi, S., Masuda, T., Miyanago, N. and Kimura, Y., *J. Polym. Sci., Part A-2*, 5, 899 (1967).
2. Berry, G.C. and Fox, T.G., *Adv. Polym. Sci.*, 5, 261 (1968).
3. de Gennes, P.G., *J. Chem. Phys.*, 55, 572 (1971).
4. Utracki, L.A. and Simha, R., *Rheol. Acta*, 12, 455 (1973).
5. Doi, M. and Edwards, S.F., *J. Chem. Soc., Faraday Trans. II*, 74, 1789, 1802, 1818 (1978).
6. Klein, J., *Macromolecules*, 11, 852 (1978).
7. Doi, M., *Polym. Prepr. Amer. Chem. Soc., Div. Polym. Chem.*, 22, 100 (1981).
8. Pearson, D.S., Mera, A. and Rocheforts, W.E., *Polym. Prepr. Amer. Chem. Soc., Div. Polym. Chem.*, 22, 102 (1981).
9. Jamieson, A.M. and Telford, D., *Macromolecules*, 15, 1329 (1982).
10. Doi, M., *J. Polym. Sci. Polym. Lett. Ed.*, 19, 265 (1981).
11. de Gennes, P.G., Scaling Concept in Polymer Physics, Cornell University Press, 1979.
12. Busse, W.F., *J. Phys. Chem.*, 36, 2862 (1932).
13. Treloar, L.R.G., *Trans. Faraday Soc.*, 36, 538 (1940).
14. Mark, H. and Tobolsky, A.V., Physical Chemistry of High Polymeric Systems, Interscience, New York, 1950, Chapter 5, p. 344.
15. Andrews, R.D. and Tobolsky, A.V., *J. Polym. Sci.*, 2, 224 (1951).
16. Bueche, F., *J. Chem. Phys.*, 20, 1959 (1952).

17. Bueche, F., Physical Properties of Polymers, Interscience, N.Y., 1962.
18. Ferry, J.D., Viscoelastic Properties of Polymers, John Wiley & Sons, Inc., New York, Third Edition, 1980, p. 245.
19. Landel, R.F., Berge, J.W. and Ferry, J.D., J. Colloid Sci., 12, 400 (1957).
20. Helders, F.E., Ferry, J.D., Markovitz, H. and Zapas, L.J., J. Phys. Chem., 60, 1575 (1956).
21. Meyer, H.H., Pfeiffer, W.F. and Ferry, J.D., Biopolym., 2, 123 (1967).
22. Tschsegl, N.W. and Ferry, J.D., J. Amer. Chem.Soc., 86, 1474 (1964).
23. Saunders, P.R., Stern, D.M., Kurath, S.F., Sakoonkin, C. and Ferry, J.D., J. Colloid Sci., 14, 222 (1959).
24. Edwards, S.F., Proc. Phys. Soc., 92, 9 (1967).
25. de Gennes, P.G., Macromolecules, 9, 587 (1976).
26. de Gennes, P.G., Macromolecules, 9, 594 (1976).
27. Graessley, W.W., J. Polym. Sci., Polym. Phys. Ed., 18, 27 (1980).
28. Ferry, J.D., Viscoelastic Properties of Polymers, John Wiley & Sons, Inc., Third Edition, New York, 1980, p. 486.
29. Merker, R.L., J. Polym. Sci., 22, 353 (1956).
30. Bueche, F., J. Appl. Phys., 26, 738 (1955).
31. Takemura, T., J. Polym. Sci., 28, 185 (1958).
32. Bueche, F., J. Chem. Phys., 25, 599 (1956).
33. Bueche, F., J. Appl. Phys., 24, 423 (1953).

34. Ferry, J.D., Viscoelastic Properties of Polymers, John Wiley & Sons, Inc., New York, Second Edition, 1961, p. 192.
35. Ferry, J.D., Landel, R.F. and Williams, M.L., J. Appl. Phys., 26, 359 (1955).
36. Newlin, T.E., Lovell, S.E., Saunders, P.R. and Ferry, J.D., J. Colloid Sci., 17, 10 (1962).
37. Bueche, F., J. Chem. Phys., 22, 603 (1954).
38. Fixman, M. and Peterson, J.M., J. Amer. Chem. Soc., 86, 3524 (1964).
39. Onogi, S., Kobayashi, T., Kojima, Y. and Taniguchi, Y., J. Appl. Polym. Sci., 7, 847 (1963).
40. Fixman, M., Paper submitted at the Symposium on "Thermodynamics and Mechanics of Polymer Systems" New York, Academy of Science, May 27, 1960.
41. Fujita, H. and Malkawa, E., J. Phys. Chem., 66, 1053 (1963).
42. Cornet, C.F., Polymer (London), 6, 373 (1965).
43. Ferry, J.D., Grandine, L.D. and Udy, D.C., J. Colloid Sci., 8, 529 (1953).
44. Flory, P.J., J. Amer. Chem. Soc., 62, 1057 (1940).
45. Fox, T.G. and Loshaek, S., J. Appl. Phys., 26, 1080 (1955).
46. Boon, J., Challa, G. and Hermans, P.H., Macromol. Chem., 74, 129 (1964).
47. Busse, W.F. and Longworth, R., J. Polym. Sci., 58, 49 (1962).
48. Onogi, S., Masuda, T. and Kitagawa, K., Macromolecules, 3, 109 (1970).
49. Stratton, R.T., J. Colloid Interface Sci., 22, 517 (1966).
50. Fujimoto, T., Ozaki, N. and Nagasawa, M., J. Polym. Sci., A-2, 6, 129 (1968).

51. Peticolas, W.L. and Watkins, J.M., *J. Amer. Chem. Soc.*, 79, 5083 (1957).
52. Charlesby, A., *J. Polym. Sci.*, 17, 379 (1955).
53. Moore, L.D., *J. Polym. Sci.*, 36, 155 (1959).
54. Kraus, G. and Gruver, J.R., *J. Polym. Sci.*, A 3, 105 (1965).
55. Kraus, G. and Gruver, J.R., *J. Appl. Polym. Sci.*, 9, 739 (1965).
56. Graessley, W.W., Masuda, T., Roovers, J.E.L. and Hadjichristidis, N., *Macromolecules*, 9, 127 (1976).
57. Glasstone, S., Laidler, K.J. and Eyring, H., *The Theory of Rate Processes*, New York, McGraw-Hill, 1941.
58. Eyring, H., *J. Chem. Phys.*, 4, 283 (1936).
59. Schott, H., *J. Appl. Polym. Sci.*, 6, S 29 (1962).
60. Litovitz, T.A. and McDuffie, G.E., *J. Chem. Phys.*, 39, 729 (1963).
61. Williams, M.L., Landel, R.F. and Ferry, J.D., *J. Amer. Chem. Soc.*, 77, 3701 (1955).
62. Gandhi, K.S. and Williams, M.C., *J. Polym. Sci.*, C35, 211 (1971).
63. Gandhi, K.S. and Williams, M.C., *J. Appl. Polym. Sci.*, 16, 2721 (1972).
64. Dreval, V. Ye., Tager, A.A. and Fomina, A.S., *Polymer Sci., U.S.S.R.*, 5, 495 (1964).
65. Ferry, J.D., Foster, E.L., Browning, G.V. and Sawyer, W.M., *J. Colloid Sci.*, 6, 377 (1951).
66. Simha, R. and Zakin, J.L., *J. Colloid Sci.*, 17, 270 (1962).
67. Quadrat, O. and Podnecka, J., *Collection Czech. Chem. Commun.*, 37, 2402 (1972).

68. Johnson, M.F., Evans, W.W., Jordan, I. and Ferry, J.D.,
J. Colloid Sci., 2, 498 (1952).
69. Toms, B.A. and Strawbridge, D.J., *Trans. Faraday Soc.*,
49, 1225 (1953).
70. Graessley, W.W., *Adv. Polym. Sci.*, 16, 1 (1974).
71. Dreval, V. Ye., Malkin, A. Ya., Vinogradov, G.V. and Tager,
Eur. Polym. J., 9, 85 (1973). A.A.,
72. Masuda, T., Toda, N., Aoto, Y. and Onogi, S.,
Polym. J. (Japan), 3, 315 (1972).
73. Spencer, R.S. and Dillon, R.E., *J. Colloid Sci.*,
3, 163 (1948).
74. Kataoka, T. and Veda, S., *J. Appl. Polym. Sci.*,
12, 939 (1968).
75. Ferry, J.D., *J. Amer. Chem. Soc.*, 64, 1330 (1942).
76. Cross, M.M., *Eur. Polym. J.*, 2, 299 (1966).
77. Rudin, A. and Chee, K.K., *Macromolecules*, 6, 613 (1973).
78. Ballauff, M., Kramer, H. and Wolf, B.A.,
J. Polym. Sci., Polym. Phys., Ed., 21, 1205 (1983).
79. Asbeck, W.K., Laiderman, D.D., Van Loo, M.,
J. Colloid Sci., 2, 306 (1952).
80. Bagley, E.B. and West, D.C., *J. Appl. Phys.*,
29, 1511 (1958).
81. Schreiber, H.P., Bagley, E.B. and West, D.C.,
Polymer, 4, 355 (1963).
82. Sabia, R., *J. Appl. Polym. Sci.*, 8, 1053 (1964).
83. Chinai, S.A. and Schneider, W.C., *J. Polym. Sci.*,
A 3, 1359 (1965).
84. Panov, Yu. N., Nordleck, K.E. and Frenkel, S. Ya.,
Vysokomolekul Soedin, 6, 47 (1964).
85. Rudd, J.F., *J. Polym. Sci.*, 60, S 7 (1962).

86. Edelman, K., Kolloid-Z., 145, 92 (1955).
87. Passaglia, E., Yang, J.P. and Wegemer, N.J., J. Polym. Sci., 47, 333 (1960).
88. Dreval, V.E., Malkin, A. Ya. and Botvinnik, G.C. J. Polym. Sci., Polym. Phys. Ed., 11, 1055 (1973).
89. Graessley, W.W., Polymer, 21, 258 (1980).
90. Solutions to Sticky Problems, Brookfield Engineering Laboratories, Inc., Stoughton, Mass., U.S.A.
91. Van Wazer, J.R., Lyons, J.W., Kim, K.Y. and Colwell, R.E., Viscosity and Flow Measurement. A Laboratory Handbook of Rheology, Interscience Publishers, New York, 1963, p. 57.
92. Instruction Manual, Brookfield Synchro-Lectric Viscometer, Brookfield Engineering Laboratories, Inc., Stoughton, Mass., U.S.A.
93. Collins, E.A., Bares, J. and Billmeyer, F.W., Experiments in Polymer Science, Wiley Interscience, New York, 1973, p. 276.
94. Van Wazer, J.R., Lyons, J.W., Kim, K.Y. and Colwell, R.E., Viscosity and Flow Measurements. A Laboratory Handbook of Rheology, Interscience Publishers, New York, 1963, p. 142.
95. Maron, S.H., Krieger, I.M. and Sisko, A.W., J. Appl. Phys., 25, 971 (1954).
96. Krieger, I.M. and Maron, S.H., J. Appl. Phys., 25, 72 (1954).
97. Brandrup, J. and Immergut, E.H., Polymer Handbook, John Wiley, New York, 1975, pp. IV-157, 159; IV-6.
98. Stacy, K.A., Light Scattering in Physical Chemistry, Butterworths, 1950, p. 103.
99. Cooper, W.G., Eaves, D.E. and Vaughan, G., J. Polym. Sci., 59, 241 (1962).
100. Cotton, J.P., Decker, D., Benoit, H., Farnoux, B., Huggins, J., Jannink, G., Ober, R., Picot, C. and Cloizeaux, J. des Macromolecules, 7, 863 (1974).

101. Daoud, M., Cotton, J.P., Farnoux, B., Jannink, G., Sarma, G., Benoit, H., Duplessix, R., Picot, C. and de Gennes, P.G., *Macromolecules*, 8, 804 (1975).
102. Hayashi, H., Hamada, F. and Nakajima, A., *Macromol. Chem.*, 178, 827 (1977).
103. Hayashi, H., Hamada, F. and Nakajima, A., *Polymer*, 18, 638 (1977).
104. Isono, Y. and Nagasawa, M., *Macromolecules*, 13, 862 (1980).
105. Bueche, F., Coven, C.J. and Kinzig, B.J., *J. Chem. Phys.*, 19, 128 (1963).
106. Porter, R.S. and Johnson, J.F., *Chem. Rev.*, 66, 1 (1966).
107. Fetters, L.J., *J. Res. Natl. Bur. Stand.*, 69A, 33 (1965).
108. Yamakawa, H., Modern Theory of Polymer Solutions, Harper and Row, New York, 1971.
109. Simha, R. and Utracki, L., *J. Polym. Sci.*, Part A-2, 5, 853 (1967).
110. Hager, B.L. and Berry, G.C., *J. Polym. Sci.*, Polym. Phys. Ed., 20, 911 (1982).

Effect of Solvent, Concentration, and Molecular Weight on the Rheological Properties of Polymer Solutions*

PHANIBHUSAN ROY-CHOWDHURY and VIVEK D. DEUSKAR,
National Chemical Laboratory, Poona 411008, India

Synopsis

The zero-shear viscosity η^0 of polychloroprene samples of different molecular weights over a wide range of concentration in good and poor solvents has been studied. Butanone and cyclohexane were used as θ solvents and benzene at two different temperatures (25 and 45.5°C) was used as two good solvents. The zero shear specific viscosity η_{sp}^0 in θ solvents at the high concentration region is found to be higher compared to the values obtained in good solvents, whereas in a moderately concentrated region the values are just opposite in θ and good solvents. The high values of specific viscosity in poor solvent at the concentrated region have been explained as due to the fact that the efficiency of entanglements is much bigger in θ solvent than in good solvent. There are indications from our data that, at the crossover point concentration, the onset of entanglements begins, and from this concentration the entanglement begins to play a role in the viscosity. The superposition of viscosity data for each solvent was carried out by shifting vertically the curve along $\log \eta^0$ axis at constant concentration by a factor $(M/M^0)^{3.4}$, where M^0 is the molecular weight of the reference sample. The shift factor was found to be exactly proportional to $M^{3.4}$ in the range of higher concentration (beyond the crossover point concentration) and approximately to M in the lower concentration range (below the crossover point concentration). This showed that the relation $\eta^0 \propto M^{3.4}$ was obeyed by the present data. To correlate the viscosity data obtained at good and θ solvents, the method as given by Graessley has been employed, which has taken into account the contraction of dimensions of chains with concentration in good solvents. It has been observed that, though this approximate correction for variation of chain dimensions on correlating variable, $C[\eta]$, has moved the correlations for θ and good solvents closer to a common curve, complete superposition of data has not been effected by this correction. On the other hand, the correlation of the data by the method given by Dreval and co-workers showed the plot of $\log\{\eta_{sp}^0/(C[\eta])\}$ vs. $C[\eta]$ produced a single curve for solutions of polychloroprene samples in two different θ solvents (butanone and cyclohexane) over the entire concentration range. But in the case of good solvents (benzene at 25°C and benzene at 45.5°C) the similar plots yielded, instead of one, two curves. However, the normalization of the correlating variable, $C[\eta]$, by the Martin constant K_M , which is related to the flexibility of macromolecular chain and polymer-solvent interaction, reduced all data of the polymer samples to a common curve. This zero-shear viscosity master curve is valid for the entire range of concentration independent of molecular weight and the nature of solvents.

INTRODUCTION

The zero-shear viscosity η^0 of polymer solutions is an important rheological parameter used to characterize the flow properties of polymer solution or melt in the linear region of deformation. Several factors such as the concentration of the solution, its temperature, the molecular weight and molecular structure of the polymer, and the nature of the solvent are responsible for the viscosity of polymer solutions. Many endeavors have been made for many years to correlate

* Communication No. 3097 from National Chemical Laboratory, Poona, India.

the data for zero-shear viscosity of polymer solutions obtained at different concentrations (high and low), molecular weights, and solvents.¹⁻¹⁰ Most recently molecular dynamic models based on reptation in a "tube" formed from entanglement constrains have been successfully compared^{3,5-10} with experimental data in a few cases. In order to explain the discrepancies exhibited by the reptation theory that the terminal relaxation time T_1 and static shear viscosity η^0 are found to depend on the third power of the molecular weight while experiments yields $T_1 \sim \eta^0 \sim M^{3.4}$. Doi¹⁰ has recently proposed a correction applicable for samples of molecular weight of practical importance, which improves the above disagreements.

Dilute solutions usually have polymer concentrations less than 1% by volume, and contributions to properties by one polymer chain are unaffected by other chains. Semidilute solutions are generally 1-10% by volume, and contributions to properties from one chain are affected by the others, though chains are not entangled with one another as they are assumed in concentrated solution. The Newtonian viscosity η^0 for many polymers in bulk and at fixed diluent concentration is observed to increase sharply to a constant 3.4 power dependence on M as the molecular weight of the polymer is exceeded to a critical value M_c . The onset of entanglement or aggregation phenomena can be identified by a rather abrupt change in slope in plots of relative viscosity $\eta_r^0(C)$ vs. concentration C , $\eta_r^0(M)$ vs. molecular weight M , or $\eta_r^0(C,M)$ vs. CM^b . The attainment of C^5 or $M^{3.4}$ behavior is often used to mark "critical" entanglement conditions. When viscosities of solutions in different solvents are compared at the same values of concentration and molecular weight, the most important parameter is the solvent viscosity η_s , to which η^0 of the solution is proportional at moderate concentration.¹¹ This cannot hold as the concentration approaches the undiluted polymer, because all systems must then approach η^0 of the polymer regardless of η_s . In the region of low concentration, the specific viscosity η_{sp}^0 of polymer solutions in poor solvents is found to be lower, but it changes more rapidly with concentration. Therefore, as the concentration increases, the specific viscosity of polymer solutions in a poor solvent may be found higher than in a good solvent.^{12,13} Some observations of ours seem to indicate that, at the crossover point concentration, the onset of entanglements begins, as a result of which from this concentration the entanglement begins to play a role in the viscosity.

In the present paper we report the study of the zero-shear viscosity of polychloroprene samples of different molecular weights over a wide range of concentrations in both good and θ solvents and the probability of constructing a zero-shear viscosity master curve valid for the entire concentration range independent of molecular weight and nature of solvent has been considered. Attempts have been made to correlate the viscosity data of the present work employing the correlating variable $C[\eta]$. The solvent-solute interaction constant K_M , which is related to the flexibility of the macromolecular chain and the polymer-solvent interaction, obtained from the Martin equation, has been used to normalize the correlating variable $C[\eta]$ so as to reduce all experimental data of the polymer samples to a common curve. Further, the method as given by Graessley,¹⁴ which has taken into account the contraction of dimensions of chains with concentration in good solvent, has been employed to correlate the data obtained at good and θ solvents. This approximate correction on correlating variable $C[\eta]$, though, improves the correlations much, but it cannot eliminate

TABLE I
Values of Intrinsic Viscosity and Molecular Weight for the Polychloroprene Samples

Samples	Solvent	Temp (°C)	$[\eta]$ (dL/g)	$\bar{M}_w \times 10^{-5}$
F1B	Benzene	25	2.12	4.85
	Benzene	45.5	2.42	
	Cyclohexane	45.5	0.56	
F2A	Benzene	25	1.47	2.69
	Benzene	45.5	1.66	
	Cyclohexane	45.5	0.41	
F2B	Benzene	25	1.10	1.68
	Butanone	25	0.38	
F2C	Benzene	25	1.00	1.44
	Butanone	25	0.35	
F3A	Benzene	25	0.85	1.11
	Benzene	45.5	0.94	
	Cyclohexane	45.5	0.27	
F3B	Benzene	25	0.79	0.99
	Butanone	25	0.29	

completely the difference between the data obtained at good and θ solvents in the present work.

EXPERIMENTAL

Polychloroprene (Denkachloroprene type M-40) obtained as a gift from Swastic Rubber Products, Ltd., Poona was fractionated from benzene solution at 25°C with the addition of acetone as nonsolvent. Molecular weights of the fractions were calculated from the intrinsic viscosities measured in benzene solution at 25°C. The relation between intrinsic viscosity $\{[\eta](\text{dL/g})\}$ and molecular weight as $[\eta] = 63.28 \times 10^{-5} \bar{M}_w^{0.62}$ was determined in this laboratory using light scattering values of M_w in benzene solution for five polychloroprene fractions (range: $0.88-10.0 \times 10^5$). The viscosity of the solutions were measured with a Ubbelohde capillary viscometer and the intrinsic viscosity $[\eta]$ was determined by extrapolation to infinite dilution according to the relation $\eta_{sp}/C = [\eta] + K'[\eta]^2C$, where K' is the Huggins constant. The data for intrinsic viscosity and molecular weight of the samples used in this work are given in Table I.

The apparent specific volume V_p of the polymer was determined at a number of temperatures above 20°C (20°C, 30°C, 40°C, 50°C, and 60°C) by specific gravity bottle using ethylene glycol as confining liquid, and the apparent specific volume V_s of the solvents, namely, benzene, cyclohexane, and butanone, was determined pycnometrically over the same range of temperature (20–60°C) which were represented by the following equations:

$$V_p \text{ (polychloroprene)} = 0.8230 + 6.36 \times 10^{-4} (\theta - 20^\circ\text{C})$$

$$V_s \text{ (butanone)} = 1.2421 + 17.40 \times 10^{-4} (\theta - 20^\circ\text{C})$$

$$V_s \text{ (cyclohexane)} = 1.2849 + 16.30 \times 10^{-4} (\theta - 20^\circ\text{C})$$

$$V_s \text{ (benzene)} = 1.1386 + 14.28 \times 10^{-4} (\theta - 20^\circ\text{C})$$

where θ is the temperature.

The solutions of higher concentration were prepared by mixing the weighed

TABLE II
Values of Zero-Shear Viscosity η^0 and θ -Temperature for the Solvents

Solvent	Temp (°C)	η^0 (cps)	θ -temp (°C)
Benzene	25	0.598	Good solvent
Benzene	45.5	0.473	Good solvent
Cyclohexane	45.5	0.648	45.5
Butanone	25	0.381	25

amounts of the polymer and the solvent and the relations for V_p and V_s were used to calculate the concentration of the solution (g/dL), assuming that there was no volume change on mixing. However, in higher concentrations (>30%), this assumption is not correct. Dilution was carried out by adding solvents by weight, and polymer concentration was converted to g/dL. Benzene at two different temperatures (25°C and 45.5°C) was used as good solvent, and cyclohexane and butanone were used as θ solvents. The θ temperature of the solvents used in this work is listed in Table II.

The zero shear viscosity η^0 of the polymer solutions was measured by means of a Brookfield LVT Viscometer (manufactured by Brookfield Engineering Laboratories, Inc., Stoughton, Mass.). In this instrument the shear rate and the shear stress are not readily calculated, but the simple approximation that the shear rate is approximately 0.2 times the rpm of the cylinder is useful.^{15,16} The viscosity of the non-Newtonian fluids is dependent on the rate of shear at which they are measured, and the shearing rate depends on the speed at which the spindle rotates. Since the rate of shear is directly proportional to rpm of the spindle at which the measurements are made, the η values taken at different speeds (rpm) were extrapolated to zero for the determination of the zero-shear viscosity in this work.

The Brookfield viscometer was recalibrated with smaller container (cell) made with stainless steel (35 mm diameter) and with this container the measurements were carried out with 63 cc of solution. The cell was kept immersed into a thermostatic water both at $25 \pm 0.02^\circ\text{C}$ and $45.5 \pm 0.02^\circ\text{C}$ temperatures. Only three spindles, nos. 2, 3, and 4, were used. The viscosity of each solution was measured at least with four different speeds and the plot of η vs. speed (rpm) was extrapolated to zero for the determination of zero-shear viscosity. The typical plots of viscosity as a function of speed at which the spindle rotates (i. e., shear rate) corresponding to the highest viscosities and then an order of magnitude of the shear rate for all other concentrations for the sample F2A in benzene and cyclohexane are given in Figures 1 and 2, respectively. Since the flow curves are curvilinear at low shear rate, direct extension of such plots to zero values of the experimental variable is somewhat subjective. However, the same plots of semilog paper converted the data to a somewhat linear form, and subsequent extrapolation to η^0 produced the same results.

The zero-shear viscosity of the solvents was measured by a capillary viscometer with a continuously varying pressure head designed by Maron and co-workers.¹⁷ The water from the thermostatic water baths maintained at $25 \pm 0.02^\circ\text{C}$ and $45.5 \pm 0.02^\circ\text{C}$ temperatures was circulated through the instrument for maintaining the constant temperatures. For Newtonian fluids, the viscosity was calculated

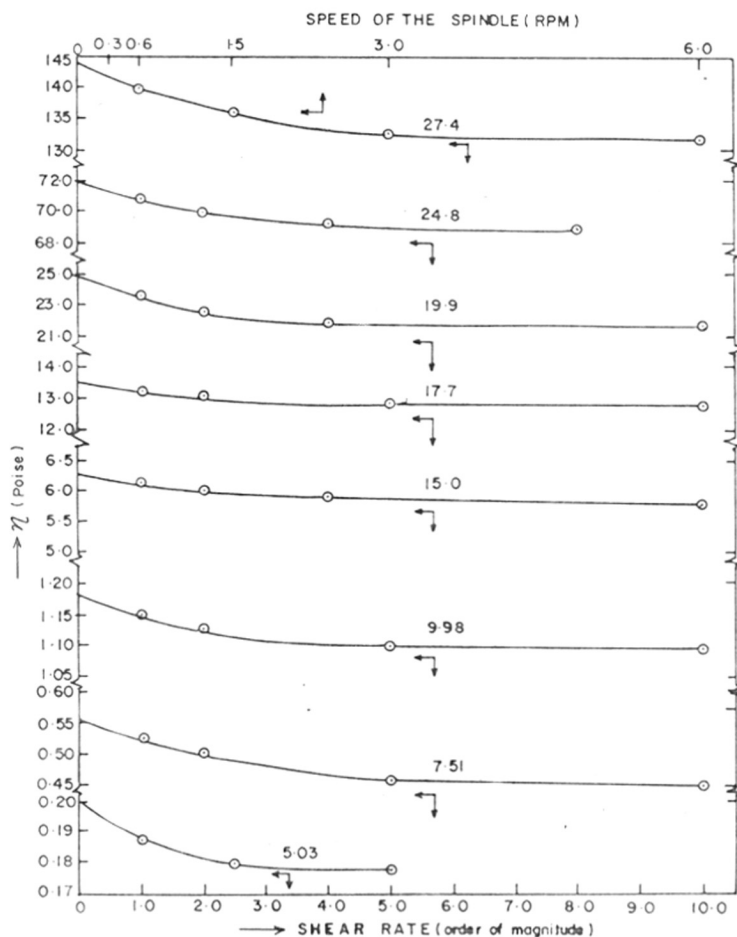


Fig. 1. Plots of viscosity as a function of shear rate (order of magnitude) for polychloroprene sample F2A in benzene for different concentrations at 45.5°C.

by the equation as given below:

$$1/\eta^0 = -(1/B)[d(\log h)/dt] = -m/B$$

where h is the height of the mercury manometer from its equilibrium position and B is the apparatus constant. The solvents used in this work showed Newtonian flow as $d(\log h)/dt$ was constant. However, the zero-shear viscosity for some dilute polymer solutions (below 5%) having non-Newtonian flow was measured with this instrument. The apparent viscosity η_a was calculated by the following equation:

$$1/\eta_a = -(m/B)\{1 + [1/(9.212m^2)](dm/dt)\}$$

The zero shear viscosity was determined by extrapolating the rate of shear to zero. The zero shear viscosity of the solvents are given in Table II.

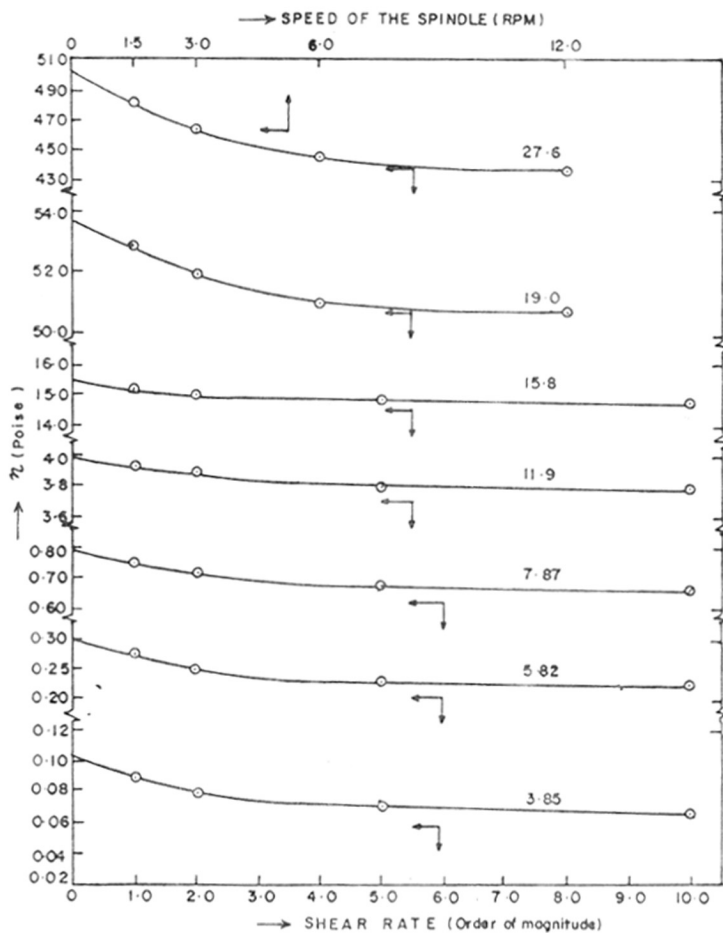


Fig. 2. Plots of viscosity as a function of shear rate (order of magnitude) for polychloroprene sample F2A in cyclohexane for different concentrations at 45.5°C.

RESULTS AND DISCUSSION

The experimental data for viscosity measurements are summarized in Tables III and IV. Table III gives the data for three polychloroprene samples (F1B, F2A, and F3A) in benzene and cyclohexane at 45.5°C, while Table IV gives the data for another three samples (F2B, F2C, and F3B) in butanone and benzene at 25°C. Butanone and cyclohexane were used as poor solvents, while benzene at two temperatures (25°C and 45.5°C) was used as two good solvents. The viscosity data given in Tables III and IV have been plotted as $\log \eta^0$ vs. $\log C$ in Figures 3 and 4. The viscosity is strongly dependent on concentration. The slope $d \log \eta^0 / d \log C$ becomes steeper with increasing concentration as entanglement of polymer chains and crosslinkings are increased with increasing concentration. It is observed that the curves 2 (F2A) and 4 (F2B) in Figure 3 have

TABLE III
 Summary of Results of Zero-Shear Viscosity η^0 for Polychloroprene Samples in Benzene and Cyclohexane at 45.5°C

Sample	Solvent	Concn at 45.5°C (g/dL)	η^0 (P)
F1B	Cyclohexane	2.02	2.91×10^{-2} ^a
		4.05	2.12×10^{-1}
		5.42	6.35×10^{-1}
		8.12	3.63×10^0
		10.4	1.14×10^1
	Benzene	1.26	2.56×10^{-2} ^a
		2.53	8.40×10^{-2} ^a
		5.08	4.25×10^{-1}
		7.57	1.46×10^0
		10.0	3.79×10^0
F2A	Cyclohexane	1.89	2.60×10^{-2} ^a
		3.85	1.03×10^{-1}
		5.82	3.00×10^{-1}
		7.87	7.80×10^{-1}
		11.9	4.00×10^0
		15.8	1.55×10^1
		19.0	5.37×10^1
		21.9	1.07×10^2
		27.6	5.03×10^2
		Benzene	2.55
	5.03		1.99×10^{-1}
	7.51		5.55×10^{-1}
	9.98		1.18×10^0
	15.0		6.22×10^0
	F3A	Cyclohexane	17.7
19.9			2.47×10^1
24.8			7.17×10^1
27.4			1.44×10^2
2.50			2.61×10^{-2} ^a
4.87			7.55×10^{-2} ^a
10.5			4.55×10^{-1}
15.0			2.00×10^0
20.0			5.92×10^0
25.1			1.82×10^1
30.1		4.80×10^1	
32.5		6.65×10^1	
Benzene		2.45	2.41×10^{-2} ^a
		5.19	7.60×10^{-2} ^a
		10.1	4.13×10^{-1}
	15.0	1.54×10^0	
	20.1	4.50×10^0	
	25.1	1.25×10^1	
	30.0	2.80×10^1	
	35.1	6.22×10^1	

^a Viscosity was measured by capillary viscometer with varying pressure head.

crossed each other at the lower concentration range. However, there is no apparent reason for the same. The double logarithmic plots of zero-shear specific viscosity η_{sp}^0 as a function of concentration for each sample both in good and poor solvents are shown in Figures 5 and 6. In the high concentration region, the η_{sp}^0

TABLE IV
Summary of Results of Zero-Shear Viscosity η^0 for Polychloroprene Samples in Benzene and Butanone at 25°C

Samples	Solvent	Concn at 25°C (g/dL)	η^0 (P)
F2B	Butanone	2.51	1.47×10^{-2} a
		4.47	6.40×10^{-2} a
		7.50	3.34×10^{-1}
		10.1	9.90×10^{-1}
		15.0	4.79×10^0
		20.0	2.46×10^1
		24.2	7.60×10^1
	Benzene	2.54	4.94×10^{-2} a
		5.53	2.46×10^{-1}
		7.54	5.25×10^{-1}
		10.0	1.44×10^0
		15.0	6.70×10^0
		20.0	2.95×10^1
		22.9	5.86×10^1
F2C	Butanone	2.62	1.39×10^{-2} a
		5.23	5.20×10^{-2} a
		7.51	1.95×10^{-1}
		10.0	4.90×10^{-1}
		15.0	3.01×10^0
		20.1	1.45×10^1
		25.3	4.72×10^1
	Benzene	2.49	3.96×10^{-2} a
		5.01	1.29×10^{-1}
		7.51	3.00×10^{-1}
		10.0	7.41×10^{-1}
		15.2	3.64×10^0
		20.1	1.35×10^1
		25.4	5.04×10^1
F3B	Butanone	2.52	1.07×10^{-2} a
		4.76	3.10×10^{-2} a
		7.08	9.55×10^{-2} a
		10.0	2.90×10^{-1}
		15.1	1.26×10^0
		20.0	4.18×10^0
		25.1	1.26×10^1
	Benzene	29.5	2.92×10^1
		2.50	2.38×10^{-2} a
		5.07	7.90×10^{-2} a
		6.75	1.90×10^{-1}
		11.2	7.20×10^{-1}
		15.0	1.49×10^0
		20.1	4.15×10^0
23.8	8.90×10^0		

^a Viscosity was measured by capillary viscometer with varying pressure head.

values in θ solvents are higher than those obtained in good solvents, whereas in the moderately concentrated region (the so-called Rouse region) the values are just the opposite in θ and good solvents. These results are in accord with those reported by other authors^{12,13} that the poor solvent η_{sp}^0 increases faster than the good solvent η_{sp}^0 and eventually exceeds it. The reversal of η_{sp}^0 is generally found

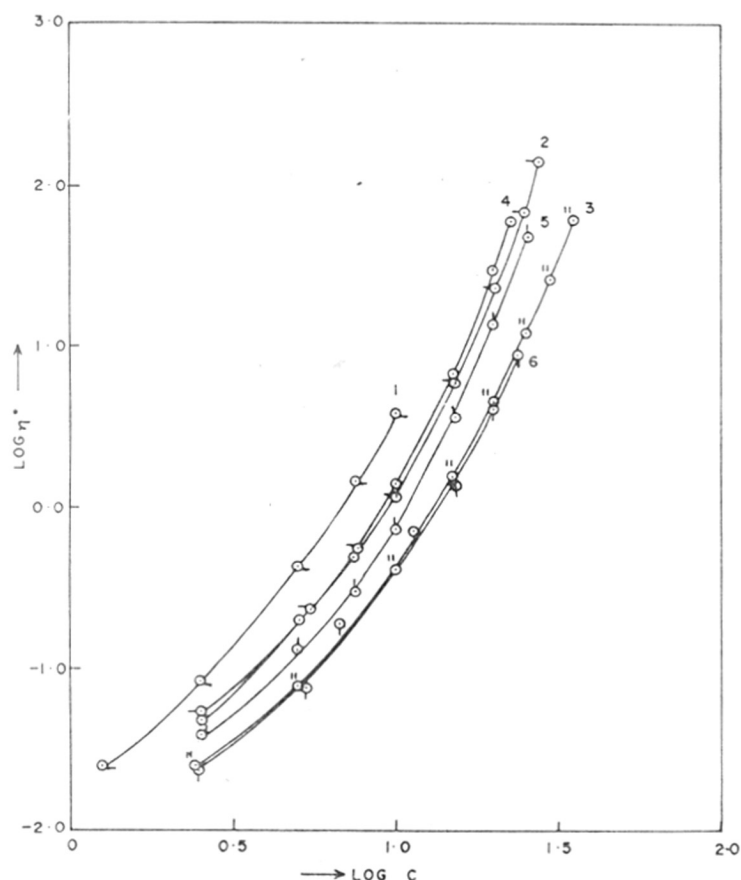


Fig. 3. Plots of $\log \eta^0$ vs. $\log C$ for polychloroprene samples in benzene at 45.5°C: (1) F1B; (2) F2A; (3) F3A and in benzene at 25°C: (4) F2B; (5) F2C; (6) F3B.

in the higher concentration range where the values of radius of gyration in good and poor solvents become almost identical.¹⁸⁻²¹ Hence the difference of the radius of gyration is not the cause for the reversal of η_{sp}^0 in concentrated solutions. Williams and co-workers¹² has explained this solvent effect in terms of polymer aggregation in poor solvents. It may be pointed out that Isono and Nagasawa¹³ have explained this phenomena that the strength of entanglement coupling in poor solvent is higher than in good solvent. However, the efficiency of entanglements is much bigger in θ solvent than in good solvent as the polymer-polymer contacts are more favored in θ solvent, and this seems to be the reason for the higher specific viscosity in poor than in good solvent.

From Figure 5 the concentrations for crossover points for F1B, F2A, and F3A have been obtained as 6.03, 10.5, and 21.1 g/dL, respectively. The same value for F2B, F2C, and F3B samples have been obtained as (from Fig. 6) as 8.71, 10.0, and 13.2 g/dL, respectively. It is presumed that the onset of entanglement has started at the crossover point concentration (to be discussed later) at which the entanglement begins to play a role in the viscosity. The variations of crossover point concentration, C_{cross} with molecular weight is shown in Figure 7. Two

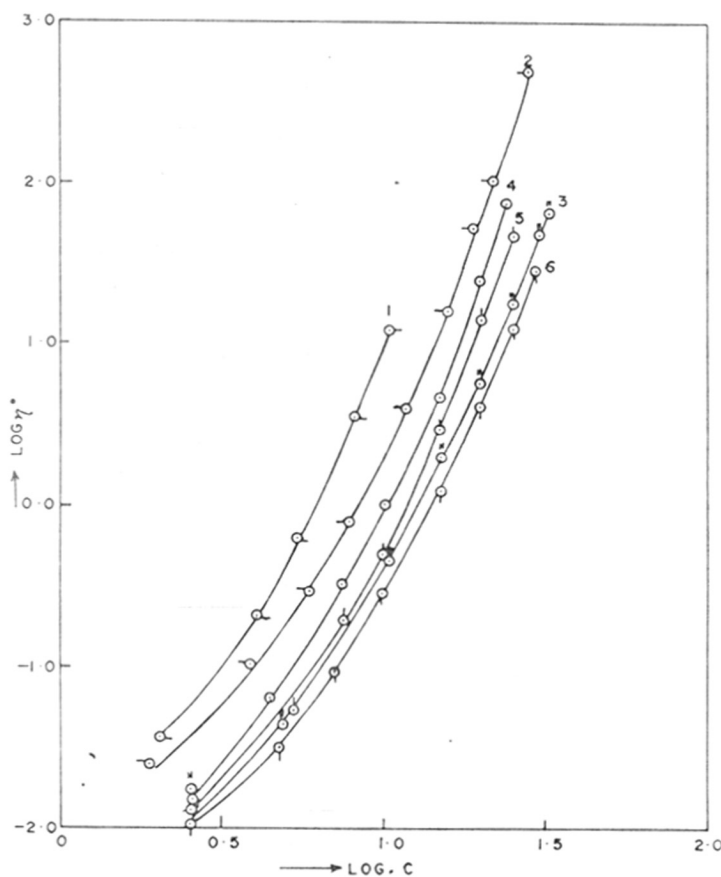


Fig. 4. Plots of $\log \eta^0$ vs. $\log C$ for polychloroprene samples in cyclohexane at 45.5°C: (1) F1B; (2) F2A; (3) F3A and in butanone at 25°C: (4) F2B; (5) F2C; (6) F3B.

separate straight lines (instead of one) almost parallel to each other were obtained with our data. From the figure it is clearly seen that the molecular weight M is proportional to -1.20 power of C_{cross} . It may be pointed out that similar to our results, Bueche and co-workers²² observed that the entanglement molecular weight M_e was proportional to the -1.20 power of the concentration in case of poly(methyl methacrylate)-diethyl phthalate system. However, the data obtained from different solvents were fitted on a single curve. It is not understood at present why our data obtained from two systems, benzene-cyclohexane and benzene-butane, are not fitted in one curve.

Superposition of the data in Figures 3 and 4 have been made so as to obtain a single composite curve for each solvent by shifting them vertically by a factor $(M/M^0)^{3.4}$. Here M^0 represents the molecular weight of sample F1B (or F2B) as a reference material. The composite curves thus obtained for benzene and cyclohexane solutions at 45.5°C and for benzene and butanone solutions at 25°C are shown in Figures 8 and 9, respectively, where K is chosen as $3.4 \log(M/M^0)$. It is interesting to note that the shift factor is found to be exactly proportional to $M^{3.4}$ in the higher concentration range, starting from the crossover point

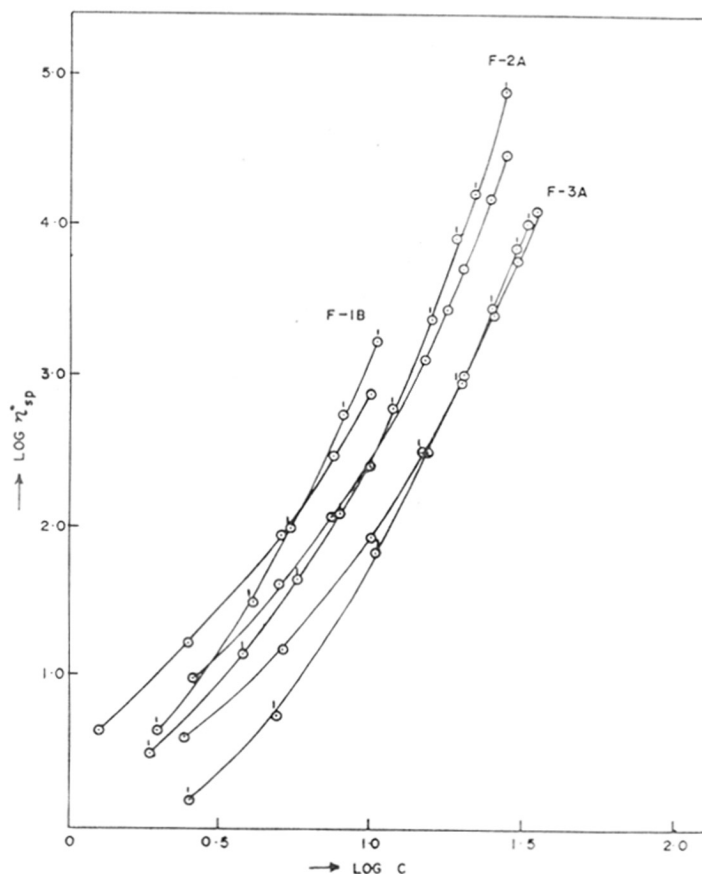


Fig. 5. Plots of $\log \eta_{sp}^0$ vs. $\log C$ for polychloroprene samples in benzene (\odot) and in cyclohexane (\ominus) at 45.5°C .

concentration. This confirmed that the relation $\eta^0 \propto M^{3.4}$ was obeyed by the present data. However, for benzene solutions the data for C_{cross} are slightly away from the composite curves. On the other hand, the shift factor is found to be approximately proportional to M in the lower concentration (below the crossover point) range. (Superposition curves for lower concentration range are not shown.)

Generally the characteristic entanglement compositions are developed from the abrupt changes in the slope in plots of $\log \eta^0$ vs. $\log C$, as well as $\log M$. If the onset point for the bulk polymer of density ρ is M^* , the estimate for the onset of entanglement in solution has been recommended by Porter and Johnson²³ as $C_{\text{ent}}M = CM_{\text{ent}} = \rho M^*$. However, this scheme totally ignores the effect of the solvents. For a number of polar and nonpolar polymers it was found that the characteristic entanglement composition, $(MC)_{\text{ent}}$ was essentially constant over a range of concentrations and molecular weights.²⁴ In the present case the (MC_{cross}) values are fairly constant over a range of concentrations and molecular

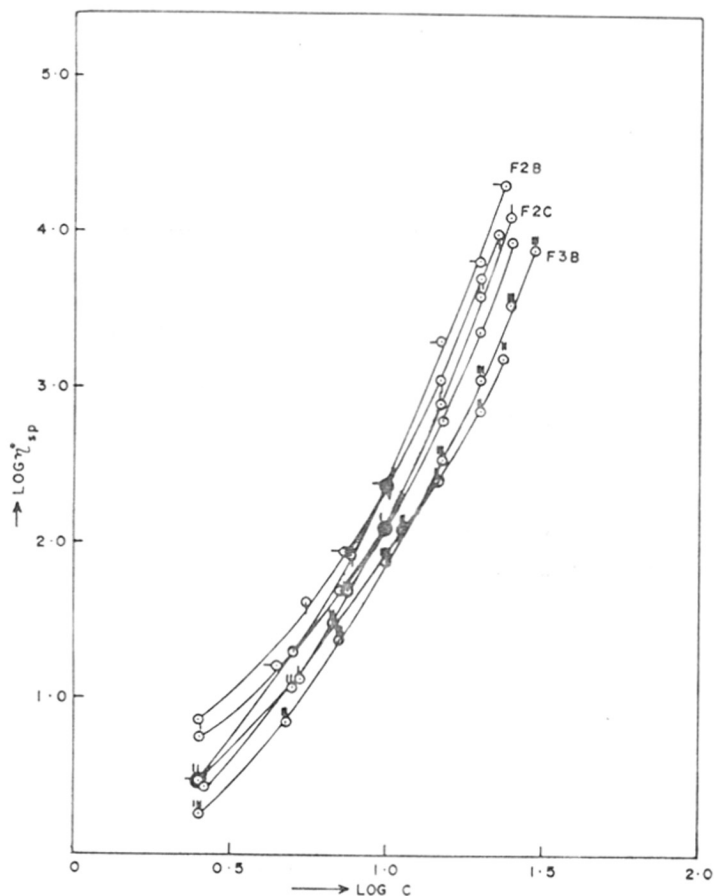


Fig. 6. Plots of $\log \eta_{sp}^0$ vs. $\log C$ for polychloroprene samples in benzene and butanone at 25°C: F2B in benzene (\odot) and in butanone (\ominus); F2C in benzene (\circ) and in butanone (\bullet); F3B in benzene (\circ) and in butanone (\bullet).

weights in each system [e. g., $(MC_{cross}) \sim 28.0 \times 10^5$ for the polychloroprene-benzene-cyclohexane system and $(MC_{cross}) \sim 14.0 \times 10^5$ for the polychloroprene-benzene-butane system], indicating that the onset of entanglement has begun at the crossover point concentration. However, the entanglement composition is not independent of the solvent system used in the present case.

Correlation of Data

Several relations have been used by various authors to correlate the viscometric data for moderately concentrated solutions. The effect of solvent and concentration on chain dimensions are reflected in viscoelastic behavior. Graessley¹⁴ recently has proposed a method for correlating viscometric properties in the semidilute region which takes into account the contraction of coil dimensions

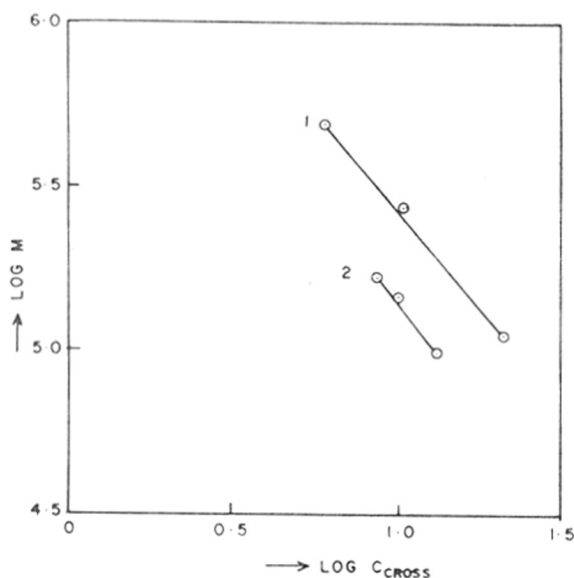


Fig. 7. Double logarithmic plots of molecular weight as a function of crossover point concentration: (1) benzene-cyclohexane; (2) benzene-butanone.

with concentration at good solvent. Since in semidilute solutions relative viscosity is a function of coil overlap (measured in a θ solvent by the product $C[\eta]_{\theta}$ at all concentrations since coil dimension do not change), the correlating variable in good solvents $C[\eta]$ should be corrected for coil contraction at each concentration. The appropriate correlating variable has been derived by Graessley¹⁴ as $0.77 (C[\eta]/0.77)^{1/2a}$, where a is the exponent of the Mark-Houwink relation. The correlating variable, however, reduces to $C[\eta]$ in the θ solvent where the exponent $a = 0.5$. The plots of relative viscosity η_r of polychloroprene samples as a function of the appropriate correlating variable are shown in Figures 10 and 11 for benzene (45.5°C) and cyclohexane solutions and benzene (25°C) and butanone solutions, respectively. The values of exponent a for polychloroprene in benzene solution at 45.5°C and 25°C have been taken as 0.64 and 0.62, respectively. For comparison, the plots of relative viscosity vs. the correlating variable $C[\eta]$ in good solvent (without correction for change of coil dimension with concentration) has been shown on the same graph. In good solvents, especially in benzene at 45.5°C, the relative viscosity increases less rapidly with $C[\eta]$ compared to that in θ solvents, and small but systematic differences appear for samples of different molecular weights. It may be pointed out that Graessley observed small but systematic differences¹⁴ similar to our results in the data⁴ of polystyrene samples of different molecular weights in toluene. The most important point that emerges from this observation is that the appropriate correction for variations in chain dimensions with concentration has positively moved the correlations for θ and good solvents closer to a common curve, but it has not been able to eliminate the difference between the data completely.

Another correlation of η^0 which is connected to $C[\eta]$ may be considered here also. It is well known that in very dilute solution the viscosity tends to the limiting behavior

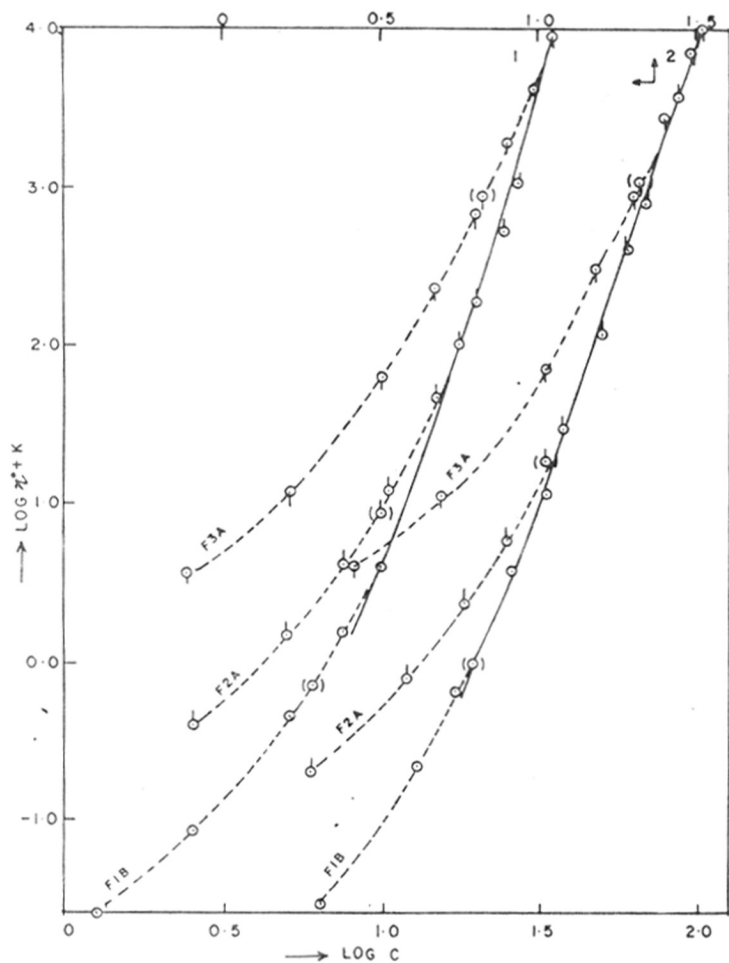


Fig. 8. Composite curves for polychloroprene samples in benzene and cyclohexane at 45.5°C: (1) benzene; (2) cyclohexane. Parentheses denote the value estimated from the crossover points. Dashed lines have been drawn with data which are away from the composite curve.

$$\eta_r^0 = \exp(C[\eta]) \quad (1)$$

and the intrinsic viscosity $[\eta]$ with the Flory-Fox equation is given as $[\eta] = \Phi \langle (S^2)^{3/2} / M$, where $\Phi \approx 2.5 \times 10^{23}$ (cgs. units) and $\langle S^2 \rangle^{1/2}$ is the root mean square radius of gyration. In terms of $[\eta]$, the overlap concentration C^* at moderately concentrated solution is given as

$$C^* = \frac{6^{3/2} \Phi}{8 N_a} \frac{1}{[\eta]} = \frac{0.77}{[\eta]} \quad (2)$$

in which N_a is the Avogadro's number.

To correlate the viscometric data for moderately concentrated solutions Simha and co-worker²⁵ have used a relation of the form (for $\eta_r^0 \gg 1$)

$$\eta_r^0 = C[\eta]P(CM^*) \quad (3)$$

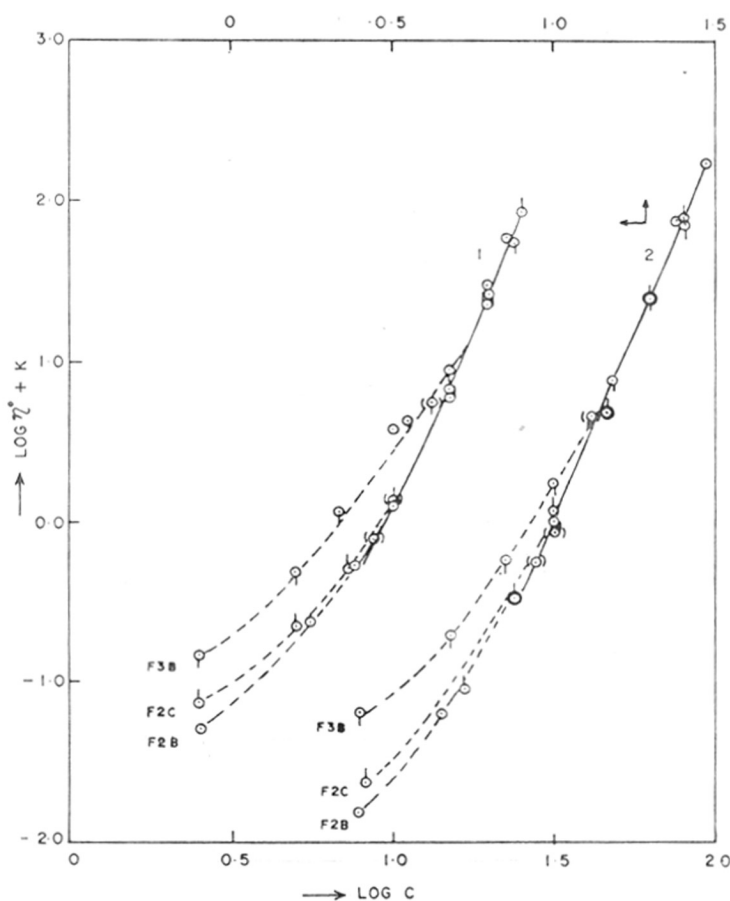


Fig. 9. Composite curves for polychloroprene samples in benzene and butanone at 25°C: (1) benzene; (2) butanone. Parentheses denote the value estimated from the crossover points. Dashed lines have been drawn with data which are away from the composite curve.

where ϵ is often equal to $d \ln[\eta]/d \ln M$. If it is obtained precisely, then eq. (2) reduces to

$$\eta_r^0 = HC[\eta] \quad (4)$$

which emphasizes the role of chain dimensions in dilute solutions (with screening length \approx root mean square radius of gyration) in the correlation of η^0 with C and M .²⁶ Here eq. (4) may be considered as a generalization of eq. (1). One variation of eq. (4) is the Martin's relation

$$\eta_r^0 = 1 + C[\eta] \exp(K'_M C[\eta])$$

or

$$\frac{\eta_{sp}^0}{C[\eta]} = \bar{\eta} = \exp K'_M C[\eta] \quad (5)$$

Dreval and co-workers²⁷ have used this Martin relation to correlate the viscosity

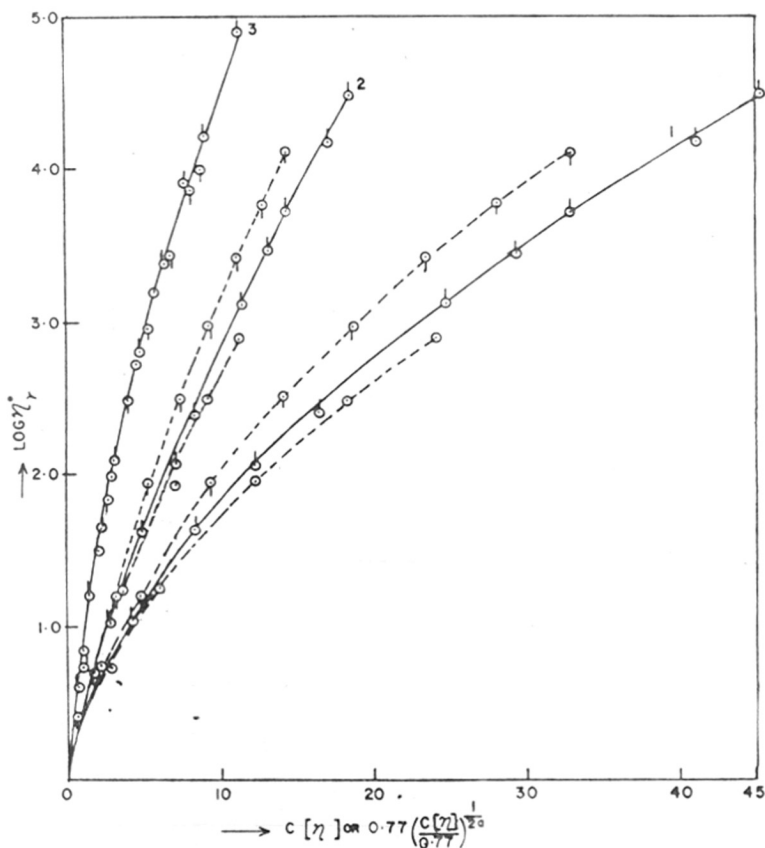


Fig. 10. Plots of $\log \eta_{sp}^0$ vs. correlating variable $C[\eta]$ or $0.77 (C[\eta]/0.77)^{1/2a}$ for polychloroprene samples in good and θ solvents at 45.5°C : (1) in benzene, not corrected for coil contraction [F1B (\odot); F2A (\odot); F3A (\odot)]; (2) in benzene, corrected for coil contraction (same symbols for F1B, F2A, and F3A); (3) in cyclohexane (same symbols for F1B, F2A, and F3A). Small but systematic differences of data for samples of different molecular weight were observed. Dashed lines show the deviations.

data in moderately concentrated solution in which a plot of $\log [\eta_{sp}^0/(C[\eta])]$ vs. $C[\eta]$ produced a single curve for samples of various molecular weights in a single good solvent over the entire concentration range. However, a similar plot of $\log [\eta_{sp}^0/(C[\eta])]$ as a function of concentration, C was proposed by Gandhi and Williams,¹² but this produced separate curves in an ordered way as a function of solvent power. The empirical representation of our data according to Dreval and co-workers²⁷ by plotting $\log [\eta_{sp}^0/(C[\eta])]$ vs. $C[\eta]$ are given in Figures 12 and 13 for good and poor solvents, respectively. As expected, the data taken in good solvents (benzene at two different temperatures are considered here as two different solvents) are fitted in two separate curves according to their solvent power (the coil dimensions vary according to their solvent power), whereas the data taken in θ solvents (butanone and cyclohexane) are fitted in a single curve as the different θ solvents are considered to have the similar solvent power, where the

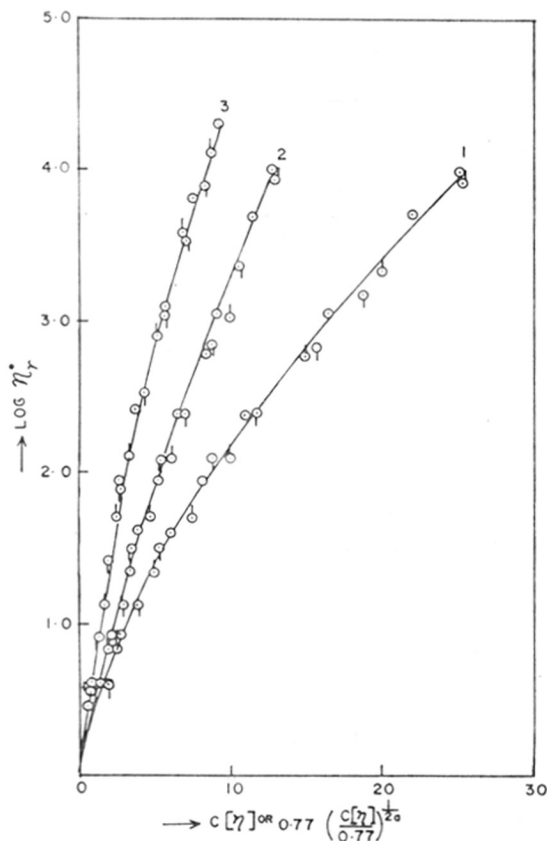


Fig. 11. Plots of $\log \eta_r^0$ vs. correlating variable $C[\eta]$ or $0.77 (C[\eta]/0.77)^{1/2}$ for polychloroprene samples in good and θ solvents at 25°C: (1) in benzene, not corrected for coil contraction [F2B (\odot); F2C (\diamond); F3B (\circ)]; (2) in benzene, corrected for coil contraction (same symbols for F2B, F2C, and F3B); (3) in butanone (same symbols for F2B, F2C, and F3B). Differences of data for samples of different molecular weights were very little (as the molecular weight of the samples were close to one another) and hence all data are shown in a single curve.

chain dimensions remain the same. The intrinsic viscosity $[\eta]_\theta$ of the polymer in two θ solvents, cyclohexane and butanone, was proportional to $M^{0.50}$.

The solvent solute interaction constant K_M obtained from the Martin equation [eq. (5)] has been used to normalize the dimensionless concentration $C[\eta]$ so as to move the correlations for θ and good solvents to a common curve. It may be pointed out that the Huggins constant K_H is theoretically equal to the Martin constant K'_M and K_M is taken as $K'_M/2.303$. The K_M was determined from the initial slope of $\log \bar{\eta}$ vs. $C[\eta]$ curves. There was a small but systemic difference of the data for three samples of different molecular weights in benzene at 45.5°C, so three different K_M values (instead of one) were determined from the curves. This scatter of data may be due to a larger difference of molecular weights among the samples. However, for samples in benzene at 25°C, only one

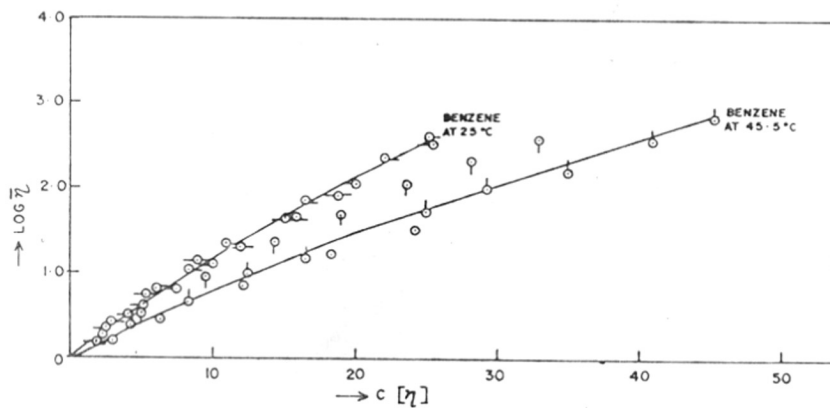


Fig. 12. Plots of $\log \bar{\eta}$ vs. $C[\eta]$ for polychloroprene samples in benzene at 45.5°C [F1B (○); F2A (⊙); F3A (⊕)] and in benzene at 25°C [F2B (○—); F2C (—○); F3B (—○—)]. Small but systematic differences of data for samples of different molecular weight especially in benzene at 45.5°C were observed.

value for K_M was obtained as the deviation of the data was very small and only a single curve was drawn with the data (Fig. 13). The values for K_M obtained at different solvents are listed in Table V. In all cases the normalization of the correlating variable $C[\eta]$ with the Martin constant K_M reduced all experimental

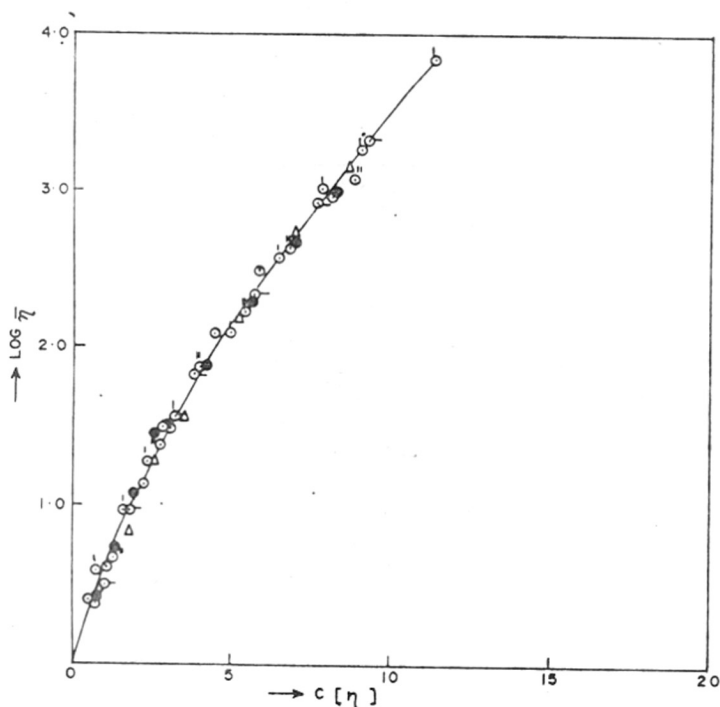


Fig. 13. Plots of $\log \bar{\eta}$ vs. $C[\eta]$ for polychloroprene samples in cyclohexane [F1B (○); F2A (⊙); F3A (⊕)] and in butanone [F2B (○—); F2C (Δ); F3B (●)]. A single curve was obtained for all the samples in two θ solvents. The scatter of the data was very little.

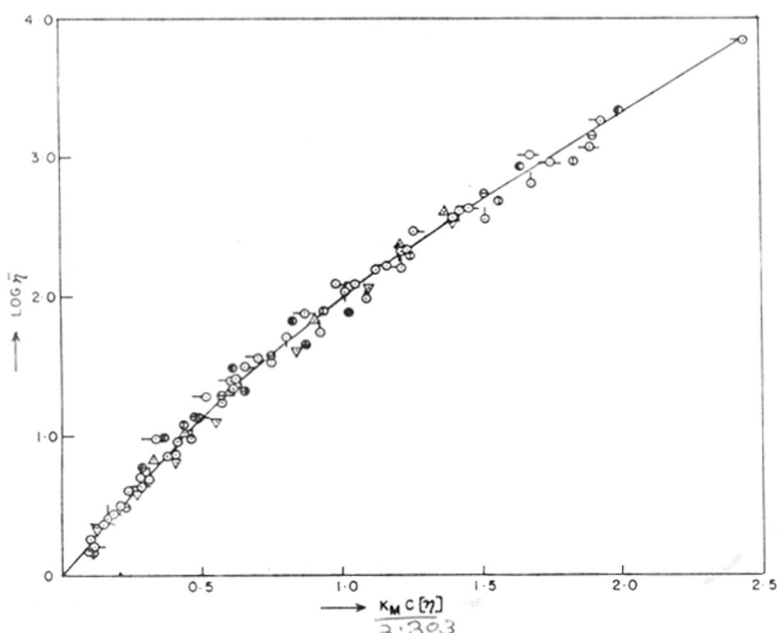


Fig. 14. Plots of $\log \bar{\eta}$ vs. $K_M C [\eta]$ for polychloroprene samples in different solvents: benzene at 45.5°C [F1B (○); F2A (—○); F3A (—○)—], cyclohexane [F1B (○—); F2A (—○); F3A (—○—)], benzene at 25°C [F2B (Δ); F2C (▽); F3B (⊕)], butanone [F2B (●); F2C (⊖); F3B (⊙)]. A single curve was obtained for all the samples in different solvents.

data for each polymer sample to the master-curve, as shown in Figure 14. The zero-shear viscosity master curve as obtained with our experimental data by plotting $\log \bar{\eta}$ vs. $K_M C [\eta]$ is valid for the entire concentration range, independent of molecular weight and nature of solvent. The introduction of the Martin constant K_M allows one to take into account effectively the flexibility of the macromolecular chain and the polymer solvent interaction. From Table V it is observed that, as the quality of the solvent deteriorates (becomes poor), the quantity K_M and consequently the viscosity of the solution becomes greater. The Martin constant K_M can be correlated with different thermodynamic properties of dilute polymer solutions, particularly with the expansion factor, α^3 of a polymer coil. The values for α^3 have been determined as the ratio of intrinsic viscosity $[\eta]$ at a given solvent to that in a θ solvent. The plots of K_M as a function of expansion factor is shown in Figure 15. The increase in expansion factor is accompanied with the decrease of K_M . The normalization of the cor-

TABLE V
Values of Martin Constant K_M and Expansion Factor α^3 for Polychloroprene-Solvent Systems

Samples	Solvent, temp (°C)	K_M^*	$\alpha^3 = [\eta]/[\eta]_\theta$
F1B	Benzene, 45.5	0.031	4.32
F2A		0.037	4.05
F3A		0.043	3.48
F2B, F2C, F3B	Benzene, 25	0.055	2.89, 2.86, 2.72
F1B, F2A, F3A	Cyclohexane, 45.5	0.216	1.0
F2B, F2C, F3B	Butanone, 25	0.216	1.0

* The reported values are for $(K_M/2.303)$ instead of K_M .

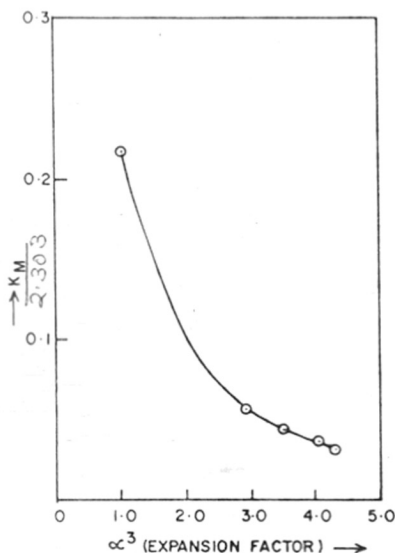


Fig. 15. Plots of K_M vs. α^3 (expansion factor).

relating variable $C[\eta]$ with K_M hence, in effect, may be to make a correction of chain dimension related to expansion factor.

In conclusion, it may be stated that the appropriate correction of the correlating variable $C[\eta]$ by the method given by Graessley for the contraction of coil dimension with concentration in good solvents no doubt improves the correlation, but it does not eliminate completely the difference between the data in the present work obtained at θ and good solvents. Further this method does not account for the increased deviations with increase of molecular weight which appeared in good solvent correlation.¹⁴ However, a few more solvent-solute systems need to be studied in detail before coming to a definite conclusion.

On the other hand, the correlation of the data by the method given by Dreval and co-workers (plot of $\log \bar{\eta}$ vs. $C[\eta]$) produced a single curve for solutions of polychloroprene samples in two different θ solvents, whereas in good solvents a separate curve for each solvent was produced. However, the normalization of the reduced concentration $C[\eta]$ by the Martin constant K_M eliminated completely all the differences between the data obtained at θ and good solvents. K_M can be correlated with the expansion factor α of a polymer coil. The normalization of this correlating variable $C[\eta]$ with K_M hence, in effect, is to make a suitable correction for chain dimension characterized by the expansion factor. This method has no doubt yielded better correlation of the data than the previous one.

References

1. S. Onogi, T. Masuda, N. Miyanago, and Y. Kimura, *J. Polym. Sci., Part A-2*, **5**, 899 (1967).
2. G. C. Berry and T. G. Fox, *Adv. Polym. Sci.*, **5**, 261 (1968).
3. P. G. de Gennes, *J. Chem. Phys.*, **55**, 572 (1971).
4. L. A. Utracki and R. Simha, *Rheol. Acta*, **12**, 455 (1973).
5. M. Doi and S. F. Edwards, *J. Chem. Soc., Faraday Trans. II*, **74**, 1789, 1802, 1818 (1978).

6. J. Klein, *Macromolecules*, **11**, 852 (1978).
7. M. Doi, *Polym. Prepr., Am. Chem. Soc., Div. Polym. Chem.*, **22**, 100 (1981).
8. D. S. Pearson, A. Mera, and W. E. Rocheforts, *Polym. Prepr., Am. Chem. Soc., Div. Polym. Chem.*, **22**, 102 (1981).
9. A. M. Jamieson and D. Telford, *Macromolecules*, **15**, 1329 (1982).
10. M. Doi, *J. Polym. Sci., Polym. Lett. Ed.*, **19**, 265 (1981).
11. M. F. Johnson, W. W. Evans, I. Jordon, and J. D. Ferry, *J. Colloid Sci.*, **7**, 498 (1952).
12. K. S. Gandhi and M. C. Williams, *J. Polym. Sci., C*, **35**, 211 (1971); *J. Appl. Polym. Sci.*, **16**, 2721 (1972).
13. Y. Isono and M. Nagasawa, *Macromolecules*, **13**, 862 (1980).
14. W. W. Graessley, *Polymer*, **21**, 258 (1980).
15. J. R. Van Wazer, J. W. Lyons, K. Y. Kim, and R. E. Colwell, *Viscosity and Flow Measurements. A Laboratory Hand Book of Rheology*, Wiley-Interscience, New York, 1963.
16. E. A. Collins, J. Bares, and F. W. Billmeyer, *Experiments in Polymer Science*, Wiley-Interscience, New York, 1973, p. 276.
17. S. H. Maron, I. M. Krieger, and A. W. Sisko, *J. Appl. Phys.*, **25**, 971 (1954).
18. J. P. Cotton, D. Decker, H. Benoit, B. Farnoux, J. Huggins, G. Jannink, R. Ober, C. Picot, and J. des Cloizeaux, *Macromolecules*, **7**, 863 (1974).
19. M. Daound, J. P. Cotton, B. Farnoux, G. Jannink, G. Sarma, H. Benoit, R. Duplessix, C. Picot, and P. G. de Gennes, *Macromolecules*, **8**, 804 (1975).
20. H. Hayashi, F. Hamada, and A. Nakajima, *Makromol. Chem.*, **178**, 827 (1977).
21. H. Hayashi, F. Hamada, and A. Nakajima, *Polymer*, **18**, 638 (1977).
22. F. Bueche, C. J. Coven, and B. J. Kinzig, *J. Chem. Phys.*, **19**, 128 (1963).
23. R. S. Porter and J. F. Johnson, *Chem. Rev.*, **66**, 1 (1966).
24. L. J. Fetters, *J. Res. Natl. Bur. Stand.*, **69A**, 33 (1965).
25. R. Simha and L. Utracki, *J. Polym. Sci., Part A-2*, **5**, 853 (1967).
26. B. L. Hager and G. C. Berry, *J. Polym. Sci., Polym. Phys. Ed.*, **20**, 911 (1982).
27. V. E. Dreval, A. Ya. Malkin, and G. C. Botvinnik, *J. Polym. Sci., Polym. Phys. Ed.*, **11**, 1055 (1973).

Received September 30, 1983

Accepted June 24, 1983